5-19-1961

Transient Sensitivity of Piezoelectric Accelerometers

William E. Baker

TRANSIENT SENSITIVITY OF PIEZOELECTRIC ACCELEROMETERS · BAKER

NAME AND ADDRESS	DATE
Milan Spanovich Box 184 Union Station	6/6/62
Ben Reznek (HARRY DIAMOND LABS.) WASHINGTON 25, D.C.	11/22/63
Donald W. Hodge 9 SUZANNE DR. PORTSMOUTH, N.H. 03801	2/26/65
Joseph S. Zelasko US Army Waterways Experiment Station Vicksburg, Mississippi	2/1/67

TRANSIENT SENSITIVITY

OF

PIEZOELECTRIC ACCELEROMETERS

By

William E. Baker

A Thesis

Submitted in Partial Fullfillment of the

Requirements for the Degree of

Master of Science in Engineering

The University of New Mexico
1961

This thesis, directed and approved by the candidate's committee, has been accepted by the Graduate Committee of the University of New Mexico in partial fulfillment of the requirements for the degree of

MASTER OF SCIENCE

E F Castetter

Dean

May 19, 1961

Date

Thesis committee

R. C. Dove

Chairman

C. T. Grace

Frederick D. Ju

This thesis, directed and approved by the candidate's committee, has been accepted by the Graduate Committee of the University of New Mexico in partial fulfillment of the requirements for the degree of [illegible]

[illegible]
Date

Thesis committee

[illegible]
Chairman

[illegible]

[illegible]

TABLE OF CONTENTS

INTRODUCTION

In the fields of experimental mechanics, design, and environmental testing of equipment, there is a continual need for the knowledge of the acceleration of a particular point, surface or body. To permit the desired information to be obtained experimentally, numerous forms of acceleration transducers have been designed, calibrated and used. Of these numerous types, the piezoelectric accelerometer has been the subject of concentrated study and use during the past ten years.

The sensing element in a piezoelectric accelerometer is a piezoelectric element. The voltage potential between the two surfaces of a piezoelectric crystal is proportional to the pressure on the crystal, and if a small mass is mounted on the crystal and the unit subjected to an acceleration, the force on the crystal will in turn be proportional to the acceleration (Newton's Second Law). This results in the voltage between the faces of the crystal being proportional to the acceleration of the mass above. Of course, the above represents a simplified description, and there are refinements made in the actual construction.

After an accelerometer of this type is made, the sensitivity must be determined in order that the acceleration may be related to voltage output. This calibration of accelerometers may be done in several ways.

One common method is to excite the accelerometer with

sinusoidal motion. The motion is usually obtained with an electrodynamic shaker, a piezoelectric shaker, or a vibrating beam. Difficulties encountered in this method of calibration are the measurement of amplitude with sufficient accuracy and obtaining true sinusoidal motion, i.e., no distortion or variation from rectilinear motion.

The reciprocity method of calibration is also used for piezoelectric accelerometers, and it also results in a sensitivity determined under steady state motion. The method requires a vibration generator, but it does have the advantage in that no mechanical quantities must be measured, only electrical quantities. Its disadvantages are that three distinct experiments must be performed, and the computations are more involved.

Another method used by manufacturers of commercial accelerometers is the comparison technique. The output of an accelerometer which has been carefully calibrated (possibly by the reciprocity method) is compared to the output of a production unit while they are experiencing the same motion, and the sensitivity of the production model found from a ratio of the voltage outputs. Again, the type of motion is sinusoidal Examples of the way two accelerometer manufacturers furnish calibration data are given in Table I page 3.

When the experimenter uses the accelerometer for determining accelerations occuring during a transient phenomena, he must make two assumptions: 1.) the accelerometer will have the same sensitivity for the transient phenomena as for the

Table I

Typical Manufacturer's Calibration Information

Endevco Accelerometer Model 2211, Serial No. 6799.

Output in Peak mv/Peak G (E_s)	13.6
Output in RMS mv/Peak G (E_c)	9.6
Accelerometer Capacity in uuf (C_p)	570
Output in Peak uu cmbs/Peak G $E_s(C_p + 100) \times 10^{-3}$	9.11
Maximum Transverse Sensitivity	3.6%

100 uuf total external capacity
for all sensitivity calibration

Frequency	20	50	100	200	400	1000	2000	4000
Sensitivity	1.0	0.0	2.0	3.0	3.0	2.0	4.0	1.0

Columbia Research Laboratories Accelerometer
Model 512, Serial No. 138.

Crystal Capacity: 200 uufd
Cable Capacity : 170 uufd
Resonant Freq. : 100 kc
Useful Range : 2 cps to 35 kc
Accel. Range : 0.15 G to 40 kG
Calibration Temp. 26°C
Temperature Range: -40° to 100°C

Weight : 5.5 gms
Housing : Stainless Steel
Mounting Stud: No. 10-32
Date Calib: 2-11-59

Measurements made at 1 G peak, into 5000 megohm resistance.

Calibration Data

Steady State

Freq.,cps :	50	100	200	300	400	500	600	700	800	1000
Sens.,mv/G:	8.9	8.9	8.5	8.6	8.9	8.7	8.2	8.2	8.4	9.0

	1200	1400	1600	1800	2000
	8.6	8.6	8.7	8.2	8.5

steady state motion for which it was calibrated, and 2.) the accelerometer will have the same sensitivity for an arbitrarily shaped pulse as it has for a sinusoidal pulse.

The thought that these two sensitivities might be different resulted from discussions with other people working in experimental mechanics and from personal experience. There seems to be general agreement that data on transient phenomena taken with piezoelectric accelerometers are usually suspected of large errors.

A study of the literature showed that several methods of calibrating accelerometers for transient phenomena have been used by other investigators. Each particular method had limitations. For example, one method resulted in a high frequency ringing of the accelerometer which necessitated the use of an electronic filter, and in addition, it only compared the output of one accelerometer to another. No effort has been made to control the waveform to determine the effect of shape on sensitivity. Most of the methods were based on the equation $V_2-V_1 = \int_{t_1}^{t_2} a\,dt$. To use this equation requires the assumption that accelerometer output be proportional to acceleration, which may or may not be valid under transient conditions.

This thesis was undertaken to accomplish the following:

1. A check of the assumption that sensitivity of piezoelectric accelerometers for steady state sinusoidal motion and transients are the same.
2. Determination of the effect of pulse shape, period,

and peak acceleration on the transient sensitivity.

3. A check of the assumption that accelerometer output is proportional to acceleration for a specified range of pulse shapes, periods, and peak accelerations.

4. Recommendation of a method of calibration of piezoelectric accelerometers for transients.

Items 1 and 2 above were done by experimentally determining the transient sensitivity of two commercially available accelerometers, and item 3 by a careful study of the calibration data.

There are an infinite number of transient acceleration pulses which might occur, and for this reason, certain limitations must be placed on those used in this investigation. Certain variables required to describe a pulse will be controlled. The variables to be controlled for the purposes of this investigation were shape, period, and peak acceleration. The shapes to be used in the test work were the half sine, sawtooth, and square wave. The range of periods and peak accelerations used was selected to cover the range most frequently encountered by investigations in the field of environmental testing, i.e., periods from 1 ms to 30 ms, and peak accelerations from 25 G to 2000 G. The range of periods has been intentionally selected to be well within those for which the assumptions of rigid body mechanics are applicable.

The accelerometers used in this investigation were the Columbia Research Laboratory accelerometer Model 512, Serial

Number 138, and Endevco Corporation accelerometer Model 2211, Serial Number 6799.

LITERATURE REVIEW

Calibration Using Sinusoidal Motion

When an accelerometer is calibrated while experiencing sinusoidal motion, the methods differ only in the method used to obtain the motion and measure the amplitude of vibration. A literature search has been made to determine the amplitude and frequency range covered using the various methods of excitation, and the degree of accuracy of calibration for these various methods. Also of interest is the peak acceleration used in the calibration methods.

Tyzzer and Hardy (1)* calibrated several accelerometers, identified only as 75 G, 200 G, and 500 G instruments, using a vibrating beam to obtain the motion. The steel free-free beams, having a 2" x 2 1/2" cross section, were excited by an electromagnetic driver, and covered the frequency range from 400 to 2000 cps. The amplitude was measured with strain gages cemented to the beam on the upper surface, and with a microscope having a calibrated reticle. The microscope was focused on a beam of light which was reflected by graphite particles cemented to the surface of the beam. Magnification of 100x was obtained this way. The strain gages were calibrated by measuring the displacement of the bar with the microscope. The strain gage instrumentation also permitted the measurement of phase angle, which was of interest since the accelerometers

---

*This notation will be used throughout to indicate references as listed in the reference section.

[illegible]

[illegible]

400 to 700 [illegible]

[illegible]

tested had internal damping.

The amplitude measurement error was stated to be $\pm 0.2 \times 10^{-3}$ cm, which corresponds to an 8% error at 2000 cps for 200 G's, the approximate maximum obtainable with this device. The frequency error of the oscillator used was $\pm 0.2\%$. The total error in calibration was not estimated, but other errors would include voltage meter error and reading error for voltage and frequency.

Zeigler (2) calibrated several piezoelectric accelerometers by obtaining the motion with a piezoelectric shaker, and measuring the vibration amplitude with a Michelson interferometer. The frequency range covered was from 250 to 7000 cps, and the amplitudes reported were up to 30 microinches at 4180 cps. This corresponds to a maximum acceleration of 54 G's. The sensitivity of one accelerometer was determined by measuring the amplitude with a microscope and an interferometer. The results agreed within 0.6% for amplitudes of 0.980×10^{-3} and 0.490×10^{-5} inches. The amplitude response curve of one accelerometer (pickup voltage vs. vibration amplitude) was determined for several frequencies, and was linear for the range covered. The overall accuracy of the work was estimated at 5%.

Yates and Davidson (3) designed a non-loading displacement transducer and vibration generator (to permit observation of signal from the transducer) for use in the calibration of vibration pickups. The range of displacements which could be measured was 0.01 inches to 100 microinches, for a band

width of 10 to 20,000 cps, and 10 microinches from 60 to 10,000 cps. These values cover an acceleration range from 2×10^{-4} G to 40,000 G. The probe produced a voltage proportional to the probe to surface separation. The signal was chopped, amplified, and read on a stable vacuum tube voltmeter. The accuracy of the displacement measurement was stated to be within 5% of full scale. Displacement readings had been compared to displacements measured using a stroboscopic illuminated microscope over the frequency range of 20 to 2000 cps, and found to agree within this tolerance. This instrument was not used to calibrate accelerometers over the range of its stated capabilities, since there are no known shakers of any type available to cover that range.

Rosenberg (4) describes an electrodynamic shaker, circa 1953, having the following specifications:

Load capacity: 5 grams

Frequency capability: 100 to 10,000 cps.

Acceleration level: 20 G.

These capabilities are representative of the range which may be covered with shakers, and they illustrate why the device designed by Yates and Davidson does not permit calibrating accelerometers over its stated range.

Another method of measuring the amplitude of vibration was devised by Sulzer, Smith, and Edleman (5). This method makes use of a stroboscope and microscope, as had been used by others. However, improvements were made. Normally this method is satisfactory only to about 800 cps. Above this, the

period of the flash becomes so long that the image becomes fuzzy. Also, the flash does not occur once for each cycle. The limitation on the frequency is removed with a specially designed circuit for the stroboscope which makes the flash duration proportional to the period, and fires the flash tube once for each cycle. The phase of the flash is changed with a toggle switch, permitting the double amplitude to be determined. It is stated that this device may be used for frequencies to 10,000 cps.

The use of the above described device for the calibration of piezoelectric vibration pickups is described in a paper by Edelman, Jones, and Smith (6). The frequencies for which these measurements apply is not specified, but it is stated that peak to peak vibratory displacement measurements were made from 0.2 cm to 6×10^{-4} cm by direct viewing. A Fizeau interferometer was used for determining amplitudes at moderate and high frequencies, and the error claimed was "considerably less than $\pm$ 5%." The frequency range covered in this work was 50 to 11,000 cps. An electromagnetic shaker was used to excite the accelerometers up to 500 cps, and above this frequency, piezoelectric shakers were used. The calibration curves for two barium titanate accelerometers were given, and for the above mentioned frequency range, the sensitivity variation was from 2.3 to 2.8 mv/G on one, and from about 3.2 to 3.6 mv/G on the other. Both were essentially linear. The authors did note that the barium titanate shakers were not consistent. That is, a frequency for which the shaker gave clean sinusoidal

motion one day, would give distorted motion on another day, or possibly it might cause the shaker to operate at one of its flexural modes. This was attributed to variation in temperature and/or history.

The stroboscopic interferometer method of amplitude measurement described in the previous reference and its use in calibration of vibration pickups is further described in reference 7. The light used in the Fizeau interferometer had a wave length of 5876 A. The shaker consisted of a stack of barium titanate rings having a 6" o.d. and 2" i.d. To determine the amplitude of vibration, the excursion of a fringe and the distance between fringes were measured with a filar micrometer. This permitted the determination of the double amplitude as some fraction of the wave length of light. Double amplitude measurements were made from 284 A at 108 cps to 651 A at 20,000 cps. Recognizing that one Angstrom unit is 10^{-8} centimeters, the G range may be computed. It was 1.33×10^{-3} G at 108 cps to 105 G at 20,000 cps. Maximum and minimum amplitudes were 808 A (3.2 microinches) at 10,000 cps and 247 A (0.98 microinches) at 2292 cps. For any frequency, the results were stated to be within $\pm$ 6%.

Manufacturers of commercial accelerometers occasionally give information on sensitivities at temperatures other than ambient, as does Endevco Corporation (8). The temperatures given cover ranges from -100°F to 500°F. For their type II crystal, the sensitivity deviation over this range was 0 to -3%. Their type I and III crystals had variations in sensitivity up to 12% for smaller ranges in temperature.

Sensitivities of several unidentified commercial accelerometers were determined in simulated space environment by Keast (9). Three accelerometers were tested at a pressure of 5×10^{-5} inches of mercury absolute for a frequency range from 20 to 70 cps, at a G level of 0.5. The motion was sinusoidal, and the amplitude was measured using a microscope with a calibrated reticle. The sensitivities for the accelerometers were down 6% to 16% from the values at atmospheric pressure, but were essentially constant for the frequency range covered.

Tests were also run on two of the above accelerometers at temperatures down to $-320^{\circ}F$. This was done by insulating an accelerometer with fiberglass and aluminum foil, immersing in liquid nitrogen, removing and mounting on a shake table, and then determining the sensitivity at a constant frequency as the unit warmed. This was done for frequencies of 30, 50 and 100 cps. A plot showed the sensitivity was independent of frequency, and that sensitivity rose gradually as temperature dropped to about $0^{\circ}F$, was approximately constant from $0^{\circ}F$ to $-200^{\circ}F$, and then dropped fairly rapidly from $-200^{\circ}F$ to $-320^{\circ}F$.

Reciprocity Method of Calibration

The methods of accelerometer calibration described in the previous section require a vibration amplitude measurement. This amplitude becomes quite small for the high frequencies, and consequently becomes quite difficult to measure accurately.

Trent (10) devised a method of calibrating electromechanical pickups based on the results of three experiments which do not require the measurement of oscillating mechanical quantities. To perform this calibration, two linear transducers are required, and one of these must be bilateral.*
Piezoelectric accelerometers are bilateral, so this method may be used for their calibration.

The first experiment which is performed is to use a vibration generator to subject the two transducers to the same motion. The voltage output of each accelerometer is measured, and the ratio of the sensitivities determined.

The second experiment consists of rigidly connecting together the mechanical sides of the transducers. In the case of piezoelectric accelerometers, the bases are clamped together. The bilateral transducer is excited with an alternating current, and the resulting voltage from the other transducer is measured.

For the third experiment, the mechanical side of each transducer is rigidly connected to opposite ends of a known mass. The bilateral transducer is again excited with an alternating current, and the resulting voltage from the other transducer measured.

Using these electrical measurements, Trent has shown that the sensitivity of a transducer on which the voltage

---

*A bilateral transducer is one which functions conveniently (tranduces) in either direction. In the case of an accelerometer, an acceleration at the mechanical side produces voltage at the other side, or a voltage at the electrical side produces an acceleration at the mechanical side.

output was measured in experiments two and three, may be determined with the following relation:

$$(S')^2 = \pm \frac{E'}{E''} \frac{j\omega M}{\left[\frac{I_2'}{E_2''} - \frac{I_1'}{E_1''}\right]^2} \qquad (1)$$

where: S' =acceleration sensitivity ratio of open circuit voltage to acceleration (directed inward at its mechanical terminal).

$\frac{E'}{E''}$ =ratio of voltage outputs of transducer being calibrated to bilateral transducer. Determined in first test.

I_1' =current driving bilateral transducer, second test.

E_1'' =voltage output of transducer being calibrated, second test.

I_2' =current driving bilateral transducer, third test.

E_2'' =voltage output of transducer being calibrated, third test.

$j\omega M$=mechanical admittance of known mass used in third test.

If phase of the sensitivity is of no importance, the magnitude only of S' may be determined by using the absolute values of E and I during the test, and dropping j. The units to be used for the quantities in the equation are meters, kilograms, seconds, volts and amperes.

Harrison, Sykes, and Marcotte (12) used the method proposed by Trent to calibrate two Massa piezoelectric accelerometers. Some of the difficulties encountered in the experimental technique include 1) the measurement of signals in the order of microvolts in circuits which are only a few inches from circuits with hundreds of volts impressed, 2) covering

the entire frequency range with one driver accelerometer, 3) obtaining a large difference in

$$\left[\frac{I'_2}{E''_2} - \frac{I'_1}{E''_1}\right]$$ with a rigid body between the accelerometers,

and 4) fastening the accelerometers rigidly to one another and to the mass.

Difficulties one and two above are related, since the low output of the accelerometers occurs at the low frequencies, and high voltages are required on the driver accelerometer to increase the G level. The result is an undesirable signal to noise ratio. To eliminate this, a larger barium titanate cylinder was used below 250 cps. This permitted an acceptable signal to noise ratios to be obtained to 100 cps.

The third difficulty is encountered since the quantities $\frac{I'_2}{E''_2}$ and $\frac{I'_1}{E''_1}$ must not be nearly the same, or large error will be introduced in the results. To obtain a large difference in these quantities requires a large mass to be used in the third experiment, and when this is done, the mass fails to act as a rigid body. Harrison, Sykes, and Marcotte considered the wave motion in the mass, and obtained a correction factor of $\cos \frac{\omega L}{c}$ to multiply E''_2 by. In this factor, L is the length of the mass, and c is the wave velocity in the mass. It is pointed out that this correction factor may not easily be determined, since c varies when the wave length approaches the same value as the diameter of the bar. These experimenters used a mass of about 0.5 kilograms and stated this

caused a 5% error at 10 kc.

The fourth difficulty was partially caused by accelerometer bases which were not flat. Correcting this shifted one accelerometer resonance from 8 kc to 12.4 kc. Nonrigid connections between the accelerometers and mass at the high frequencies also contributed to this difficulty.

The two accelerometers had a sensitivity vs. frequency curve which was essentially flat from 250 cps to 2000 cps, and then there was a gradual rise to about 7000 cycles, at which point the slope became quite large to the peak. It is stated that the calibrations are correct to 8% for the part which is flat.

The above work with the Massa accelerometers was continued by Stowe and Bort (12). They stated the accuracy of the calibration at low frequencies (below 1000 cps) had been improved thru better instrumentation and refined techniques. The error was reduced to 2%, and since this was for low frequencies, it was possible to obtain a check of the results by an independent method, i.e., measuring amplitude of vibration and frequency. The error at 10 kc was said to be 6%. At this frequency there was no way to obtain an independent check. However, Zeigler (3) used a stroboscopic interferometer method on the same type of accelerometers, and his data agreed to 6 kc.

Levy and Bouche (13) also used the reciprocity method for calibration of a variable resistance type accelerometer and a piezoelectric type. The frequency range covered for the piezoelectric transducer was 30 to 5000 cps. In this range, the sensitivity increased linearly from about

0.014 volts/G at 30 cps to 0.018 volts/G at 2000 cps. At 2000 cps, the slope of the curve became steeper. This calibration was conducted at a nominal acceleration level of 2 G's. Difficulties were essentially the same as those previously mentioned.

Transient Response Theory

Levy and Kroll (14) determined the theoretical response of a seismic mass type accelerometer to transient acceleration pulses having shapes of half sine, triangular, and square. This was done by solving the equation of motion for a seismic mass m which is suspendended in a case by spring k and dashpot c, when the case is subjected to the transient pulse y(t). This equation of motion is:

$$\frac{d^2x}{dt^2} + \frac{c}{m}\frac{dx}{dt} + \frac{k}{m}x = -\frac{d^2y}{dt^2} \tag{2}$$

To make the results of the solution to this equation more useful, it was placed in non-dimensional form, using such quantities as the critical damping coefficient c_c, pulse duration, accelerometer period, peak acceleration of applied pulse, etc.

This equation was solved numerically for ratios of c/c_c of 0, 0.4, 0.7, and 1.0, and for ratios of accelerometer period to pulse duration of 1, 1/3, and 1/5. The results were plotted to show how closely the acceleration of the seismic mass agreed with the transient acceleration applied to the case. The curves vividly show the poor agreement when c is zero (which is approximated by piezoelectric

accelerometers) and how the general trend is toward better agreement as c/c_c is increased to 0.7, and the period of the pulse is increased. It is concluded that to obtain accuracies of better than 5% of the peak acceleration, for the shapes of transients studied, the accelerometer must have a natural period less than one third the pulse duration, and damping between 0.4 and 0.7 of critical.

Rubin (15) extended the work of Levy and Kroll by considering criterion for design and selection of accelerometers for transient measurement other than fidelity of indicated pulse to applied pulse. He proposed that the criterion used be: "response spectrum of accelerometer output to be an undistorted version of the response spectrum of the transient."

This would include the requirement that the magnitude of peak accelerometer response be the same as peak value of applied pulse, and that there be an accurate reproduction of the area under the velocity time curve. An electric analog was used to determine response curve for a half sine and triangular pulse. These response curves included peak response/peak input acceleration, peak amplification of response/peak amplification of input, and response impulse/input impulse, each plotted against the response period to pulse duration ratio. Levy and Kroll's work agreed well with the first of these two curves. The third curve (not determined by Levy and Kroll) shows that if only the impulsive nature of the transient is desired, the accelerometer natural frequency need not be as high to obtain a desired accuracy as for the other two requirements.

uncertainties [illegible]
movements [illegible]
pursuit [illegible]
no better than [illegible]
literature studies, [illegible]
period less than [illegible]
between 0.4 and 0.7 [illegible]

Smith (15) [illegible]
elderly [illegible]
for transient [illegible]
pulse to applied pulse. [illegible]
the "frequency spectrum" [illegible]
undistorted [illegible]

This would [illegible]
of peak angular motion response [illegible]
of applied pulse, [illegible]
of the area under the [illegible]
timing was used to [illegible]
and triangular pulse. [illegible]
response peak input [illegible]
response/peak angle [illegible]
impulse/input impulse, [illegible]
period to pulse duration [illegible]
well as the first [illegible]
(not determined by [illegible]
impulsive nature of the [illegible]
other natural frequency [illegible]
desired accuracy of [illegible]

He states that any transient can be considered as a superposition of continuous distribution of frequency components, and that the steady state behavior of the accelerometer determines how it alters these components. For accelerometer design and selection for transient measurements application of the peak value criterion only will not necessarily result in one having ideal characteristics over the largest frequency range. An example where his requirement for accelerometer selection would be important is in the determination of response of structures to transients. An example where the peak value criterion is useful is when the item responds in a static manner to the transient.

He concludes that to meet his proposed "spectrum distortion criterion" that the accelerometer have 0.6 to 0.7 critical damping and the accelerometer period be less than 0.4 of the period of the sharpest pulse in the transient for 5% accuracy.

Calibration for Transients

Conrad and Vigness (16) determined the sensitivity of a barium titanate accelerometer for transients using impact techniques. They obtained the transients using both a ballistic pendulum and a drop tester. The accelerometer output was assumed linear with acceleration, and the sensitivity was determined from the relation $\Delta V=\int a\,dt$.

The change in velocity due to impact was measured on the ballistic pendulum in two ways. One way was by

The [illegible] that [illegible] accelerometer to a [illegible] frequency [illegible] components; and [illegible] the accelerometer [illegible] for acceleration [illegible] design [illegible] vibration [illegible] measurement applications [illegible] the peak value [illegible] noise [illegible] within the [illegible] frequency range. [illegible] his requirement for [illegible] acceleration would be important as [illegible] to transducer. [illegible] the transient.

In conclusion [illegible] to meet his proposed "[illegible] for [illegible] when the accelerometer have 0.6 to 0.7 critical damping and [illegible] period [illegible] less than 0.4 of the period of the [illegible] on the transient for 5% accuracy.

Calibration for Transients

Conrad and Vigness (15) [illegible] analyzed the sensitivity of a [illegible] accelerometer for transients [illegible] input techniques. They obtained the transients using both a [illegible] pendulum and a drop carriage. The accelerometer output was [illegible] linear with acceleration, and the sensitivity was determined from the [illegible] impact.

The [illegible] is [illegible] due to [illegible] was measured as the ballistic pendulum [illegible]. The [illegible] was by

interrupting a beam of light focused on the sensitive element of a phototube with a light grating attached to the pendulum on which the accelerometer was mounted. The signal from the phototube was recorded simultaneously with the accelerometer signal, and the change in velocity determined from the known distance between the slots in the grating and the sweep rate of the oscilloscope. Another way was to compute it from data taken with a maximum displacement indicator on the pendulum. The second way was preferred due to its simplicity, even though there were errors due to energy losses (wind, cable friction, etc.).

The change in velocity during impact on the drop tester was determined as the sum of the impact velocity and rebound velocity, and each of these was determined from the time required for a contactor to pass over a sensitized area near impact.

Considerable difficulty was encountered with high amplitude, high frequency components which obscured the rigid body motion component. On some data, this was attributed to the travelling wave in the anvil. A filter with 5 kc cutoff was used on several runs to eliminate noise. For identical drop conditions, this was found not to affect the accelerometer sensitivity, even though it lowered the peak acceleration reading by factors of 2 and 5 (on the data reported). The sensitivity was not affected since the area under the unfiltered and filtered signal was the same.

The range of pulse durations covered in this work was 0.35 ms to 2 ms. Peak accelerations to 7000 G were obtained. No consideration was given as to pulse shape or duration. It is stated that the sensitivities as determined on both machines agreed within 5%, and that the sensitivities also agreed within 5% to those obtained with sinusoidal motion.

Perls (17) used an impact method to determine an accelerometer sensitivity up to 12,000 G's. To obtain these high accelerations, the unmounted accelerometer was allowed to swing through an arc and contact an anvil. The method of computing sensitivities was essentially the same as that used by Conrad and Vigness. The differences were that the change in velocity was computed from the measured arc during fall and the measured arc during rebound. The area under the acceleration-time diagram was determined by electrical integration. The rebound arc was determined from observation at point of zero velocity.

Perls plotted accelerometer sensitivity vs. peak acceleration. There was considerable scatter. However, the best average sensitivity was the same as determined by sinusoidal excitation at ±1 G, 20 cps. Pulse durations encountered during this test were from 40 to 200 microseconds.

Other tests were run on this accelerometer (Type OBI-14) to determine its linearity at high compressive loads, which is assumed to be equivalent to high accelerations. The compressive force between the seismic mass and crystal was varied by changing the torque on the screw which held the

mass in place. The compressive force was determined from the torque measurements. At several values of compressive force, the accelerometer sensitivity was determined at ± 1 G. The results were plotted as "% of Response at 250 lb. Force" vs."Compressive Force." Knowing the seismic mass, it was possible to show that this crystal was linear to $\pm 25,000$ G, within about 1%.

Perls and Kissinger (18) continued the work of calibration at high G levels to check factors other than crystal output linearity for high compressive loads. These factors were possible accelerometer non-linearity resulting from an increased output as the pulse duration approaches the natural period of the accelerometer, and a possible mechanical failure of the transducer or cable. Since high G's are normally obtained only for very short pulses, non-linearity from the first of the above mentioned factors could show up in these tests. These tests also gave a check on the linearity and characteristics of the electronic equipment for high amplitude high frequency pulses.

Several methods were used to obtain the high G levels. The ballistic pendulum was useful in the range of pulses having accelerations from 150 to 8000 G's, and durations from 40 microseconds to 1 millisecond. The pulses were also obtained by using an air gun to fire a projectile into a small target on which the accelerometer was mounted. Duration from 25 to 800 microseconds were obtained, and the accelerations obtained were low.

shown in Fig. [illegible]. The [illegible] were [illegible] and [illegible]

also for the measurements [illegible]. Several values of [illegible]

found. The [illegible]

The results were [illegible] at [illegible] of [illegible]

in, Compressive Force [illegible]

possible to show that these curves [illegible]

within about 2%.

Static measurements (35) confirmed [illegible]

tion of high Q levels to check factors other than simple

output signal [illegible] the high temperature [illegible]

were possible nonlinearities; non-linearity [illegible]

transient output of the pulse [illegible]

period of the [illegible], and a possible [illegible]

urn of the [illegible]. Since high Q's are normally

obtained only for very short pulses, non-linearity from the

first of the above mentioned factors would show up in [illegible]

form. These tests also give a check on the linearity of

characteristics of the electronic equipment for high ampli-

tude high frequency pulses.

Several methods were used to obtain the high Q levels.

The ballistic pendulum was useful in the range of pulses

having accelerations from [illegible] to 5000 g's, and durations

of [illegible] to 1 millisecond. The pulses were [illegible]

[illegible] by using an air gun to fire a projectile [illegible]

target on which the accelerometer was mounted. [illegible]

[illegible] g's were obtained, and the [illegible]

obtained were [illegible]

Pulses were also obtained by rolling a ball down an inclined trough into an accelerometer, or an object on which an accelerometer is mounted. This method gave pulse durations from 18 microseconds to 2.5 milliseconds, and accelerations to 4000 G's.

Data from tests conducted in the above ways was reduced using the equation $\Delta V = \int a dt$, and the integration was performed electrically.

The accelerometer used in the tests was an NBS-33-14 piezoelectric type. Test results which were reported included peak G's as high as 48,000. It was stated that the accelerometer became non-linear at this point. A zero shift was encountered at a particular G level. It was believed that this was the result of a short time relief of the compressive forces on the crystal. There was a trend toward an increasing sensitivity as the pulse duration approached the natural period of the accelerometer. This began when that ratio was around 10.

The results of these tests had a $\pm$ 16% scatter. This was attributed to variations in the steepness of the front of the acceleration pulse, which, it is stated, determines the response more than the width of the pulse. Also, error was introduced by the electrical integrator. The data shown in the report also gives a clue as to another cause of error. Generally, the trace deflections were quite small, and for the shorter pulses, the shape was obscured by high amplitude, high frequency ringing.

Turnbow (19) calibrated several types of accelerometers under steady state and transient conditions for G levels to about 200. The types of accelerometers used included two barium titanate types, one using unbonded wire resistance strain gages, and one using bonded wire resistance strain gages. The unbonded wire type was a Statham Laboratories Model ASA-50-240, and the bonded wire type was designed and made for use by the author. It consisted of a loading mass on a machined tube, with four C-D-7 gages on the tube to measure its strain during tests.

The vibration generator was used only to acceleration levels up to 20 G and 400 cps. Beyond this frequency, the small amplitudes could not be measured accurately enough with the filar microscope, It was estimated that the error in sensitivities determined by this method was approximately ± 20% (±2% for frequency, ±5% for amplitude, and ±10% for voltage output).

To perform the transient calibrations, a drop tester was constructed. A carriage was constructed around a 2" diameter vertical column 64" high. A bumper at the bottom produced the desired peak accelerations.

The accelerometer sensitivities were determined by assuming that the output of the accelerometer is proportional to the acceleration, and using the relation $\Delta V = \int a dt$. The change in velocity was determined as the sum of the impact and rebound velocity. Each of these was found by using a photoelectric velocity meter. Lines a known distance apart

[illegible] several [illegible] accelerometer

under [illegible] conditions [illegible] levels to

[illegible] used [illegible] two

[illegible] types, [illegible] wire constantan

[illegible] wire [illegible]

[illegible] was a [illegible] laboratory

[illegible] wire type was designed and

made for use [illegible] It consisted of a loading mass

on a [illegible] gages on the tube to

measure the [illegible]

The [illegible] used only to acceleration

levels [illegible] Beyond this frequency, the

small amplitudes could not be measured accurately enough

[illegible] It was estimated that the error

in [illegible] by this method was approximately

[illegible] amplitude, and -10% for

voltage output.

To perform [illegible] calibrations, a drop tester

was constructed [illegible] was constructed around a 2"

diameter vertical column 6" high. A bumper at the bottom

produced the desired peak accelerations.

The [illegible] were determined by

assuming that the output of the accelerometer is proportional

to the acceleration, and using the relation [illegible] The

change in velocity [illegible] the sum of the impact

and rebound [illegible] found by using a

[illegible]

were ruled on a piece of lucite and this mounted on the carriage. A beam of light was focused on the sensitive element of a phototube, and the lines interrupted this beam of light from 0.55" to 0.05" before impact. The output of the phototube was recorded adjacent to timing marks. From this, the velocity could be computed. The required areas under the voltage-time curves were determined by enlarging the oscilloscope record and using a planimeter.

The error in the sensitivities was estimated as follows: velocity change, ± 2%; area determination, ± 5%; time calibration, ± 2%; and voltage calibration, ± 10%; for a total error of ± 20%.

The sensitivity of the unbonded wire strain gage accelerometer agreed well with the manufacturer's sensitivity, both for the steady state and transient conditions. The transient sensitivity of the bonded wire strain gage accelerometer agreed well with the theoretical value computed using gage factor, loading mass, modulus of elasticity, etc. Its output, when excited by the vibration generator, was so low no comparison could be made.

The steady state sensitivities of the barium titanate accelerometers were higher by 10% to 25% than the transient sensitivities. In addition, the sensitivities showed a tendency to decrease as the maximum acceleration increased.

The zero downward shift at the end of the pulse occured on the signal from the barium titanate accelerometers, as had been noted by other investigators (18). Since it did not

occur for the other types of accelerometers, Turnbow attributed this to some characteristic of the barium titanate sensing element (19). This zero shift was neglected in the area determination by using only the area above the initial horizontal trace. This gave better agreement with the control accelerometer on the carriage.

Tests were run over a nine month period, and the barium titanate accelerometers were stable over this time.

A commercially available ballistic pendulum for calibrating accelerometers for transients is described by Kaufman (20). The ballistic pendulum, manufactured by Gulton Industries, consists of a supporting structure, a shocking pendulum, a receiving pendulum, and a shocking pendulum release unit. A calibration curve is furnished with each unit showing peak acceleration plotted against shocking pendulum horizontal displacement for several weights of the shocking pendulum. Also furnished is a built-in standard calibration accelerometer having a specified accuracy of $\pm$ 10%.

The system is capable of producing accelerations to 500 G's, 1 millisecond long, and having an approximate half sine shape. Gulton furnished a curve to Kaufman, showing that their accelerometer A403-52 had a linear output to 500 G's.

The manufacturer states that an accelerometer may be calibrated by using their G vs. horizontal displacement curve. Kaufman states this should be supplemented by calibrating an accelerometer with a natural frequency of at least 5 kc on a centrifuge, electrodynamic shaker, or crystal shaker, and this accelerometer used as the standard for comparison. This

ment and with contact points of [illegible] elements. However diffi-
culties in [illegible] characteristics of the [illegible]
sensing element [illegible] which were neglected in the
area determination. By [illegible] the [illegible] above the initial
horizontal [illegible]. These have been corrected with the cor-
rect accelerometer on the carriage.

Tests were run over a three-month period, and the various
elements of accelerometers were tried over this time.

A commercially available ballistic pendulum for cali-
brating accelerometers for transients is described by
Kaufman (20). The ballistic pendulum, manufactured by Dalton
Industries, consists of a mounting structure, a shocking
pendulum, a receiving pendulum, and a shocking pendulum re-
lease unit. A calibration curve is furnished with each unit
showing peak acceleration plotted against shocking pendulum
horizontal displacement for several weights of the shocking
pendulum. Also furnished is a built-in standard calibration
accelerometer having a specified accuracy of ± 10%.

The system is capable of producing accelerations to
500 G's, 1 millisecond long, and having an approximate half
sine shape. [illegible] furnished a curve to Kaufman, showing
that their accelerometer [illegible] had a linear output to 300 G's.

The manufacturer states that the accelerometer may be cal-
ibrated by using their horizontal displacement curve.
Kaufman states that should be supplemented by calibrating an
accelerometer with a natural frequency of at least 5 kc on a
[illegible], electrodynamic shaker, or crystal shaker, and
this accelerometer used as the standard for comparison. This

method requires extrapolation of data, since most shakers are limited to maximum accelerations of about 50 G's.

With this type of shock excitation, the accelerometer rings. To eliminate this, Gulton furnishes a 2 kc low pass filter. Corrections must be made for the gain of the filter. Data are shown with and without the filter, and a study of the data show the zero downward shift at the end of the pulse which has been previously noted.

Kaufman states that with this error the overall accuracy of this comparison method is $\pm$ 15%, on the pessimistic side, and that normal error is $\pm$ 8%.

Brennan and Nisbet (21) approached the problem of accelerometer calibration for transients in a manner different from other investigators. A cylinder of some elastic material such as steel has strain gages mounted on it so the strain in the link may be determined. The accelerometer to be calibrated is mounted on a vehicle, and the vehicle placed against one end of the cylinder. A force which varies with time is applied to the other end of the cylinder. The accelerometer output and the strain gage output are recorded on oscilloscopes. The rigid body acceleration of the vehicle may be computed from the strain gage signal, using the strain gage factor, cylinder area and modulus of elasticity, vehicle weight, etc. The accelerometer sensitivity may then be computed from its output voltage and the vehicle acceleration. The error using this method is estimated to be

$\pm$ 5%. An electronic filter was used when the accelerometer ringing obscured the pulse shape. The band pass was set to a pass frequency which resulted in the strain gage and accelerometer signals having the same amount of ringing.

This method has one important advantage over previously used methods. There is a verification of the wave shape presented by the accelerometer, since it may be compared to the wave shape presented by the strain gages.

One assumption made in this method is that the strain gages behave under transient conditions in the same manner that they behave under steady state motion. This is the same assumption that is made for accelerometers any time they are used for shock measurement after calibration under steady state motion.

There is a frequency limitation in the force transducer due to the finite length of the strain gage. It was stated that the error becomes appreciable when the wave length becomes less than ten times the length of the strain gage. An analysis was presented to show that for a steel force link with 1/2" gage length strain gages, the error would be 0.1% for a 20" sinusoidal strain wave (10 kc). This increases to 10.7% for 2" long waves (100 kc).

They encountered a zero downward shift at the end of the accelerometer pulse. This was attributed to the time constant in the system being too short. This was corrected, and the zero shift eliminated.

No statement was made as to the G range and pulse duration which were covered with this test method.

EXPERIMENTAL METHODS FOR SENSITIVITY DETERMINATION

The transient sensitivities of the accelerometers were determined for acceleration pulses obtained with a drop tower. The accelerometers were mounted on a drop vehicle, and the vehicle arrested from free fall by cushioning designed to give the desired acceleration-time pulse. Data were taken during the tests to permit determination of the transient accelerometer sensitivity using two different methods. The reason for using two methods was to have a check on the sensitivity, and to compare the two methods. The methods are based on independent principles and measurements, and agreement under these circumstances would be conclusive evidence with regards to the transient sensitivity for that acceleration pulse.

One method is based on the equation $V_f - V_i = \int_{t_i}^{t_f} a(t)\,dt$ and the assumption that accelerometer output is proportional to acceleration. This is essentially the same approach as used previously by the authors of references 16, 17, 18, and 19.

In this equation, if $a(t)$ is an acceleration-time function for which the acceleration scale is not known, but the change in velocity for some specified time interval is known, the acceleration scale may be found by the following substitutions:

$$a = Ay$$

$$dt = Tdx$$

[illegible]

determined [illegible]

theory. [illegible]

and the [illegible]

found to [illegible]

were [illegible]

[illegible]

methods [illegible]

check [illegible]

The [illegible]

study, [illegible]

[illegible]

for the [illegible]

Our [illegible]

and the [illegible]

to [illegible]

used [illegible]

17.

In this [illegible]

tion for [illegible]

random [illegible]

the [illegible]

for some [illegible]

where a=acceleration at any time t.
A=the acceleration scale on the a(t) graph.
T=the time scale on the a(t) graph.
y=vertical ordinate of the graph.
x=horizontal ordinate of the graph.

The resulting equation is

$$V_f - V_i = AT \int_{x_i}^{x_f} y(x)\,dx \qquad (3)$$

since A and T are constants. In this equation, $\int_{x_i}^{x_f} y(x)\,dx$ is the area under the acceleration-time curve for the interval of the known velocity change. The acceleration scale is the only unknown, so it may be found. If the a(t) graph is the voltage output-time curve of an accelerometer, then the transient sensitivity has been determined for that particular pulse.

The curves recorded to apply this equation are the accelerometer output vs. time, and the vehicle position vs. time (immediately before and during impact). These data were analyzed as follows:

1. The impact velocity was determined from the initial slope of the vehicle position vs. time curve.
2. The instant of zero velocity during impact was determined from the point of zero slope on the vehicle position-time curve.
3. The accelerometer output vs. time curve was enlarged an arbitrary amount by projection, and the area under the curve to instant of zero velocity determined, using the trapezoidal rule.

4. The accelerometer sensitivity in mv/G may then be computed.

A study of this method indicates that accelerometer sensitivity is based on the impact velocity, the instant of zero velocity, and the assumption that accelerometer output is proportional to acceleration. The accuracy of the sensitivity will be dependent on accuracy of this assumption and that of the measurements made. This method does result in a sensitivity for which the laws of kinematics are satisfied.

The difference in this method and those mentioned in the references is in the change of velocity used. The total change in velocity, i.e., the sum of impact and rebound velocity, was used by the previous investigators. Here, the change in velocity for a smaller interval of time is used.

The second method of determining the transient sensitivity is based on Newton's Second Law when extended to rigid body motion. If a force which varies with time F(t) is applied to a rigid body, the acceleration of that body will vary with time in the same manner. This may be expressed as:

$$a(t) = \frac{F(t)}{\text{Mass}} \tag{4}$$

If an accelerometer is mounted on a rigid body having a known mass and a known F(t) applied, then the accelerometer

sensitivity may be determined at any time t. This method has one distinct advantage over the previous method; i.e., it was not necessary to assume the output of the accelerometer was proportional to acceleration. It was possible to check this assumption by comparing the force-time pulse to the accelerometer output-time pulse. Another way of doing this would be to compute sensitivities for several force levels during the pulse. Agreement would indicate the assumption was valid.

The curves recorded to apply this method are the accelerometer output vs. time curve and the force vs. time curve. The force transducers used were cylinders of an elastic material on which strain gages were mounted to measure the compressive strain. The strain gage signal from the appropriate electrical circuit is assumed proportional to the strain in the material; and from this, the compressive force on the cylinder may be determined. The above assumption is valid within some limit of accuracy only for force pulse durations greater than some specified lower limit. The limit depends on the degree of accuracy desired. This has been pointed out by Nisbet and Brennan (21).

When the force pulse is determined from this type of force transducer, the assumption is made that the strain gages behave for a transient load in the same way they behave for static loads. The fact that this is a valid assumption has been illustrated in several ways. Clark (22)

sensitivity may be determined at only 1 time. These assumptions are [illegible] over the previous methods. It was not necessary to measure the output of the accelerometer was proportional to acceleration. It was possible to check this assumption by comparing the force-time pulse to the accelerometer output-time pulse. Another way of doing this would be to compute sensitivities for several force levels during the pulse. Agreement would indicate the assumption was valid.

The curves recorded to apply this method was the accelerometer output vs. time curve and the force vs. time curve. The force transducers used were cylinders of an elastic material on which strain gages were mounted to measure the compressive strain. The strain gage signal from the strain plate converter circuit is assumed proportional to the strain in the material, and from this, the compressive force on the cylinder may be determined. The above assumption is valid within some limit of accuracy only for force pulse durations greater than some specified lower limit. The limit depends on the degree of accuracy desired. This has been pointed out by Himelblau and Keegan (11).

When the force pulse is determined from this type of force transducer, the assumption is made that the strain gages behave for a transient load in the same way they behave for static loads. The fact that this is a valid assumption has been illustrated in several ways. Simmons (1

was calibrating a model material for dynamic photoelasticity, and was using strain gages in the experimental work. He had determined the effective gage factor for static loading of a CR type gage on the model material and found it was lower than that given by the manufacturer. This was attributed to the stiffening effect of the paper back gage. Before proceeding with the dynamic calibration, it was necessary to determine the gage factor for dynamic loading, in the same range for which the calibration was to be done.

This was done in the following way. A long rod was struck on one end, and strain gages were used to record the initial wave in the bar, and the reflected wave. Also measured was the change in momentum of a throw-off bar at the end opposite impact. By equating this change in momemtum to the difference in area of initial wave and reflected wave (the impulse), the effective gage factor could be found. It agreed with the gage factor from the static gage factor. The pulse durations for which this check was made were around 100 microseconds.

Barton, Volterra, and Citron (23) also illustrated that strain gages respond to transients the same as to static loads. Using the Hertzian law of impact, a theoretical analysis was made to determine the stress wave in an infinitely long bar due to longitudinal impact of spheres. Then the problem was solved experimentally, using steel

was calibrated [illegible]

ticity, and [illegible]

be had [illegible]

loading of a [illegible]

it was loaded [illegible]

straightened in [illegible]

before [illegible]

necessary [illegible]

in the case [illegible]

This [illegible]

struck on one end, [illegible]

the initial [illegible]

measured was the [illegible]

the end opposite [illegible]

return to the [illegible]

flected wave [illegible]

be found. [illegible]

gage factor. [illegible]

made were [illegible]

Barton, Volterra, [illegible]

strain gage [illegible]

loads. Using the [illegible]

analysis [illegible]

infinitely long [illegible]

than the [illegible]

balls and a steel rod. The stress waves in the bar were determined from strain measurements made with type C-8 resistance strain gages. The experimental and theoretical curves were then plotted on the same graph. For the three graphs shown in the article, the agreement in peak stress, waveform, and duration was good. The pulse durations varied from 76 to 185 microseconds, and the experimental pulses were from 2 to 10 microseconds longer. The difference in the experimental and theoretical peak stresses varied about ± 5%, but this could be explained as error due to the low value of stresses occurring. The purpose of this work was not to check transient response of strain gages. However, it does accomplish this.

The transient pulses to be used in the experimental work have been previously described. The desired pulses in this range are described in Table II on page 35. Data were not obtained for the pulses of low and high impulse because of limitations in the equipment. The low impulse tests were restricted by the sensitivity of the force link, the resolution of the vehicle position transducer, and the methods of obtaining the desired pulse shape. The high impulse tests were restricted by the drop tower height, the "full scale" limit on the position transducer, and again, the methods of obtaining the desired pulse shape.

The theoretical impact velocity and maximum cushion compression were computed for the half sine pulse by assuming

[illegible]

from 70 to 150 microseconds, and that the [illegible] pulses were from [illegible] microseconds length. The [illegible] in the [illegible] is about ± 5%, but this [illegible] value of [illegible]. [illegible] not to [illegible] it does [illegible].

The standard pulses to be used in the experimental work have been previously described. The [illegible] pulses in this range are described in table II on page [illegible]. [illegible] were not obtained for the values of [illegible] and [illegible] because of limitations in the equipment. The [illegible] tests were restricted by the sensitivity of the [illegible], the resolution of the vehicle position transducer, and the methods of obtaining the desired pulse shape. The high impulse tests were restricted by the drop tower height, the "full scale" limit of the position transducer, and again the methods of obtaining the desired pulse shape.

The theoretical [illegible] velocities and [illegible] compression were [illegible] for the [illegible]

Table II. Desired pulses for Test Work

Peak G	Period					
	1 ms	2 ms	4 ms	8 ms	16 ms	
50			24.6 .031	49.2 .124	98.4 .496	Half Sine
100		24.6 .016	49.2 .062	98.4 .250	197 1.00	Half Sine
200	24.6 .008	49.2 .031	98.4 .125	197 .500		Half Sine
500	61.6 .020	123 .078	246 .312	*340 .87		Half Sine
1000	123 .039	246 .156	*340 .43			Half Sine
50			38.6 .103	77.2 .410		Sawtooth
100		38.6 .051	77.2 .206	154 .820		Sawtooth
200	38.6 .026	77.2 .103	154 .410	308 1.67		Sawtooth
500	95.2 .063	193 .257	308 1.03			Sawtooth
1000	193 .126	*340 .46				Sawtooth
50		38.6 .039	77.2 154	154 .62		Rectangular
100	38.6 .019	77.2 .077	154 .31	308 1.23		Rectangular
200	77.2 .039	154 .154	308 .62			Rectangular
500	193 .096	*340 .34				Rectangular
1000	*340 .170					Rectangular

Note: The first number in each square represents the required impact velocity, and the second number the maximum cushion compression.

An empty square means that run was beyond the capabilities of the equipment.

The * signifies a run for which the required impact velocity was greater than could be obtained with the drop tower. The maximum impact velocity was used.

the rebound velocity is equal to the impact velocity. These quantities were found for the sawtooth pulse and rectangular pulse by assuming the rebound velocity is zero.

EXPERIMENTAL APPARATUS

Drop Tower

The transient pulses were obtained on a drop tower designed by the author. The drop vehicles were guided by two wires, 4" on centers. The anvil, a 4" diameter steel cylinder 6" high, was bolted to a steel reinforced concrete block. The concrete block was used to bring the impact surface to a convenient working height. The maximum drop height was 152 inches, which permitted theoretical impact velocities of 342 inches/second. The height limit was established by the roof height of the building in which the tower was constructed.

The weight of the drop vehicles could be varied from 1.3 lbs. to 22 lbs. without materially changing the wave frequency of the vehicles. This was done to eliminate the effect of vehicle wave frequency on accelerometer sensitivity. The wave frequency was approximately 12,000 cps, and it was kept as high as possible while still maintaining adequate vehicle weight. Figure 1 describes the drop vehicles used. Included in this figure are the adapters required to mount the accelerometers on the vehicle, the vehicle guide wires, and the impact piece. Figure 2 shows the major components of the drop tower, along with other items used in the experiment work.

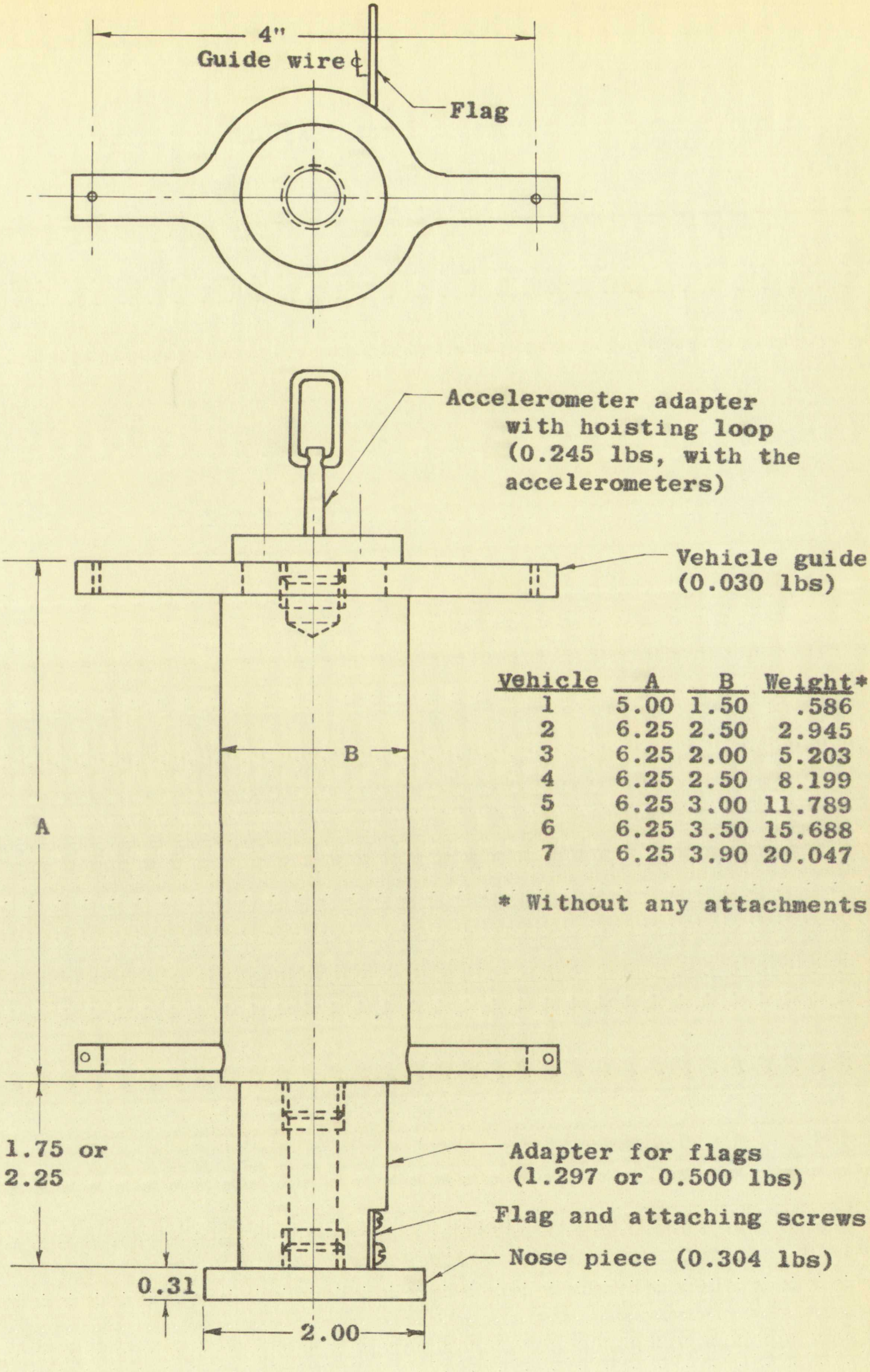

Vehicle	A	B	Weight*
1	5.00	1.50	.586
2	6.25	2.50	2.945
3	6.25	2.00	5.203
4	6.25	2.50	8.199
5	6.25	3.00	11.789
6	6.25	3.50	15.688
7	6.25	3.90	20.047

* Without any attachments

Figure 1. Drop Vehicle Description

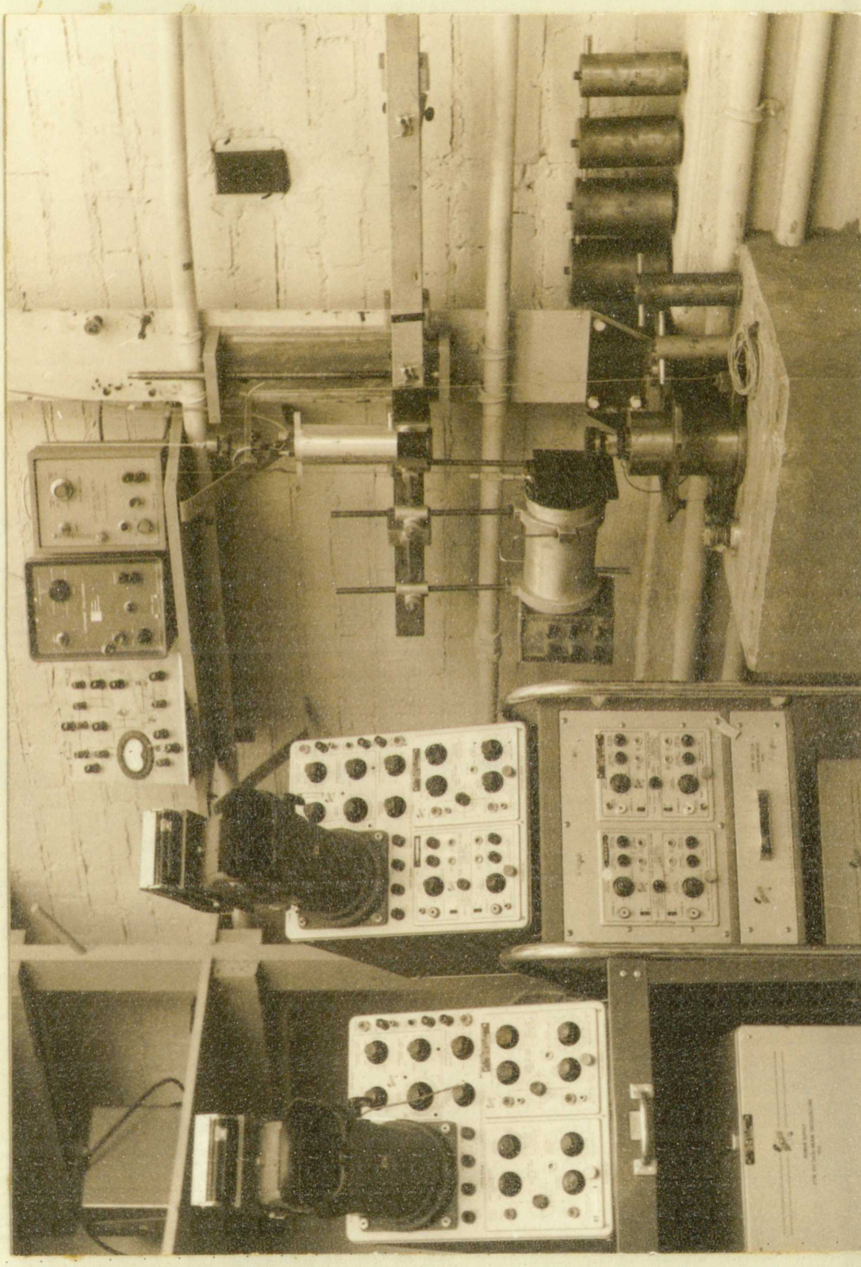

Figure 2. Overall View of Experimental Apparatus

Transducers

The acceleration transducers to be calibrated have been previously described. The transducers used for the calibration work include two force transducers and the vehicle position indicator.

Two force transducers were required to cover the range of forces to be measured. The type of force transducer used consisted of an area under compression which transmitted all of the force. The strain at this known area was measured and converted to force from the known area and modulus of elasticity of the material. If the area was selected to withstand high loads without failure, the strain at the low loads would be too low to measure accurately. Also, if the area was selected for low load measurement, the transducer would fail structurally at the high loads. Consequently, two force transducers were required.

The transducer for the low force range is shown in Figure 3. The material used was aluminum, since its low modulus of elasticity permitted the use of a large compression area to resist buckling and still obtain strains of sufficient magnitude for an acceptable signal to noise ratio. The strain was measured with four type A-14 SR-4 strain gages equally spaced around the outside diameter of the tubular section. The upper load limit was established as that which would cause 1000 microinches/inch of strain, to insure long life of the gages and the thin wall compressive member. This force transducer was used up to 2,000 lbs.

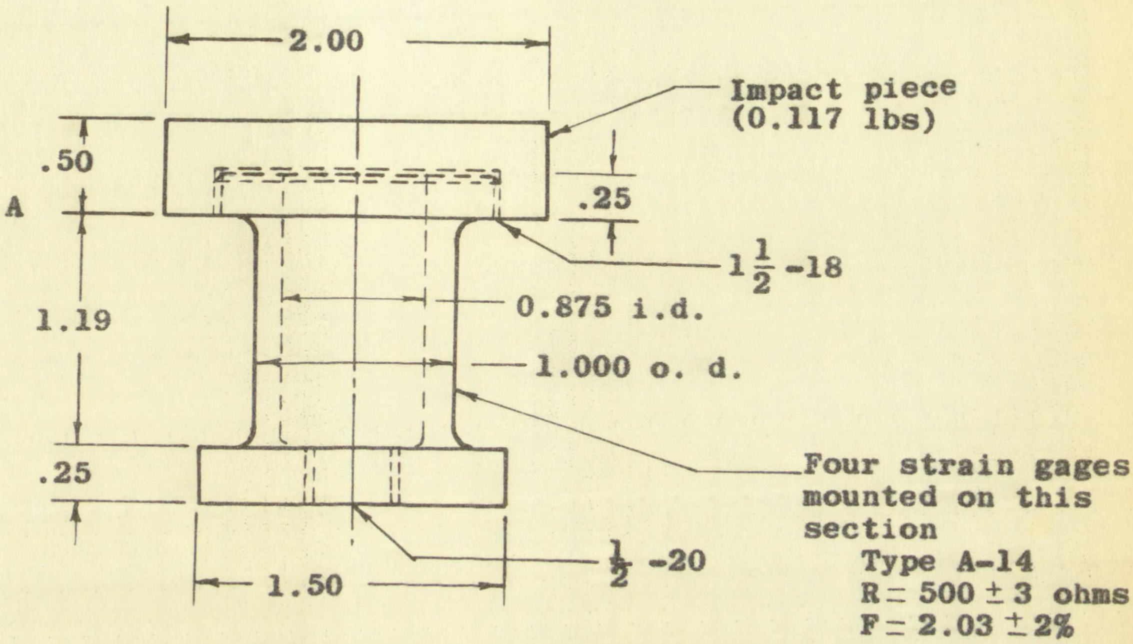

Material: 2024-T4 aluminum
Modulus of Elasticity: 10.6×10^6 psi.
Spring Constant, $k = 1.64 \times 10^6$ lb/in.
Effective Sprung Weight, $w =$ weight above $A + \frac{1}{3}$(spring weight)
$w = 0.150$ lbs

Natural Frequency of Force Link, $\omega_n = \frac{1}{2\pi}\sqrt{\frac{kg}{w}}$

$\omega_n = 10{,}300$ cps

Figure 3. Low Range Force Transducer

For loads greater than this, the high force range transducer is used. It is shown in Figure 4. Due to its larger outside diameter, it was possible to mount six type A-14 strain gages around it, and obtain more output for a given strain than for the low force transducer. It was used to measure forces from 2,000 lbs. to 36,000 lbs.

A potentiometer circuit was used to measure the change in resistance of the strain gages on the force transducers, from which the strain could be found. The circuit used is shown in Figure 5.

The vehicle position transducer was modeled after the one designed by Fitzgibbon (24). The principle used is that the output voltage of a phototube is proportional to the amount of light falling on its sensitive element. If the light is made proportional to the position of an object in between the light source and the phototube, then the output of the phototube may be used to determine the position of the object. The one designed and used for this work is shown in Figure 6.

The requirements on the light source are fairly severe. It must have an intensity great enough to give adequate signal and eliminate the effect of other light in the room. Its intensity must be constant over the distance to be measured; it must be collimated light or something approaching this, and its intensity must not vary with time. To meet the last requirement, all alternating current light bulbs were eliminated, since the variations in current

[illegible] force range transducers as shown. [illegible] Figure [illegible], the [illegible] it was possible to [illegible] 1-18 strain gages [illegible], and [illegible] higher [illegible] for a given strain than [illegible] used to measure forces from 7,000 [illegible] lbs.

A [illegible] bridge circuit was used to measure the change in resistance of the strain gages on the force transducers, from which the strain could be found. The circuit [illegible] is shown in Figure 3.

The vehicle position transducer was modeled after the one designed by [illegible] ([illegible]). The principle used is that the output voltage of a photocell is proportional to the amount of light falling on the sensitive element. If the light is made proportional to the position of [illegible] in between the light source and the photocell, then the output of the photocell may be used to determine the position of the object. The one designed and used for this work is shown in Figure 4.

The requirements on the light source are fairly severe. It must have an intensity great enough to give adequate signal and eliminate the effect of other light in the room. The intensity must be constant over the distance to be measured. It must be collimated [illegible] approaching [illegible], and the intensity must not vary with [illegible]. To meet the last requirement, [illegible] alternating current light bulbs were eliminated, since the [illegible] loses [illegible].

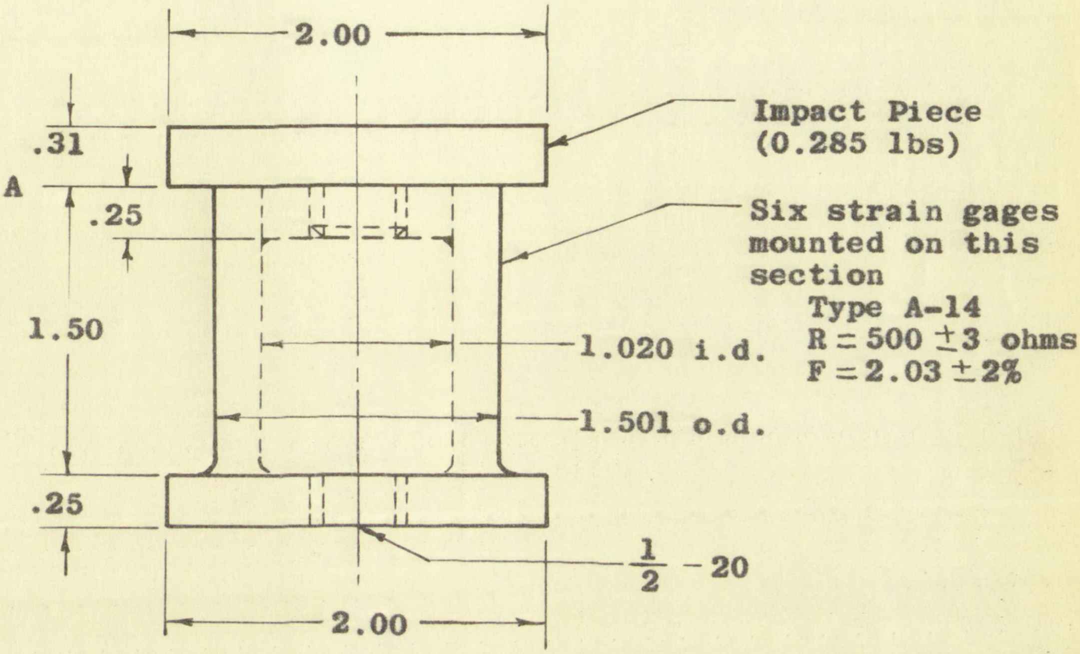

Material: Mild steel
Modulus of Elasticity: 29 x 10^6 psi.
Spring Constant, $k = 22 \times 10^6$ lb/in.
Effective Sprung Weight, $w =$ weight above $A + \frac{1}{3}$(spring weight)
$w = 0.511$ lbs

Natural Frequency of Force Link, $\omega_n = \frac{1}{2\pi}\sqrt{\frac{kg}{w}}$
$\omega_n = 20{,}500$ cps

Figure 4. High Range Force Transducer

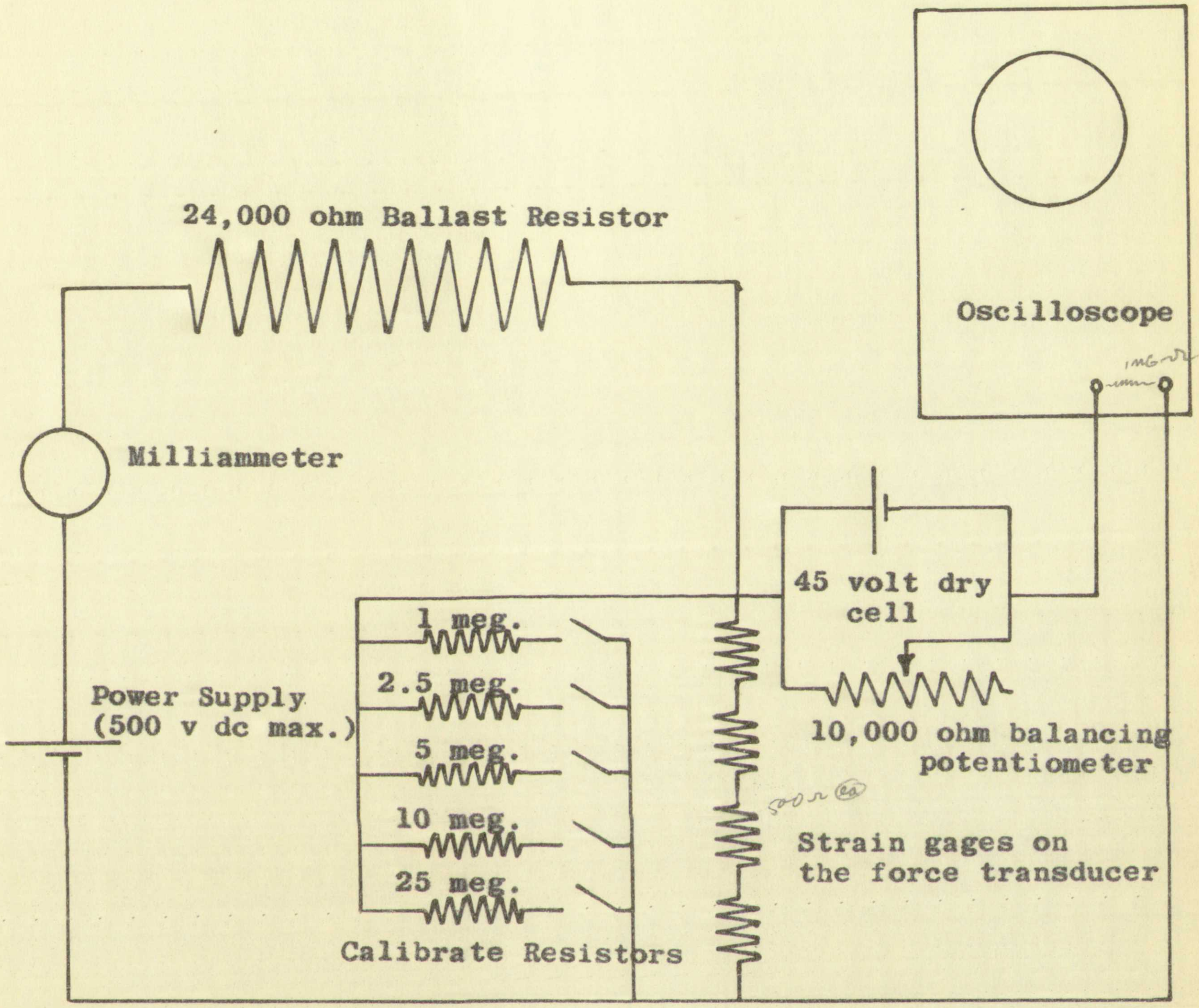

Figure 5. Circuit Used with Force Transducer

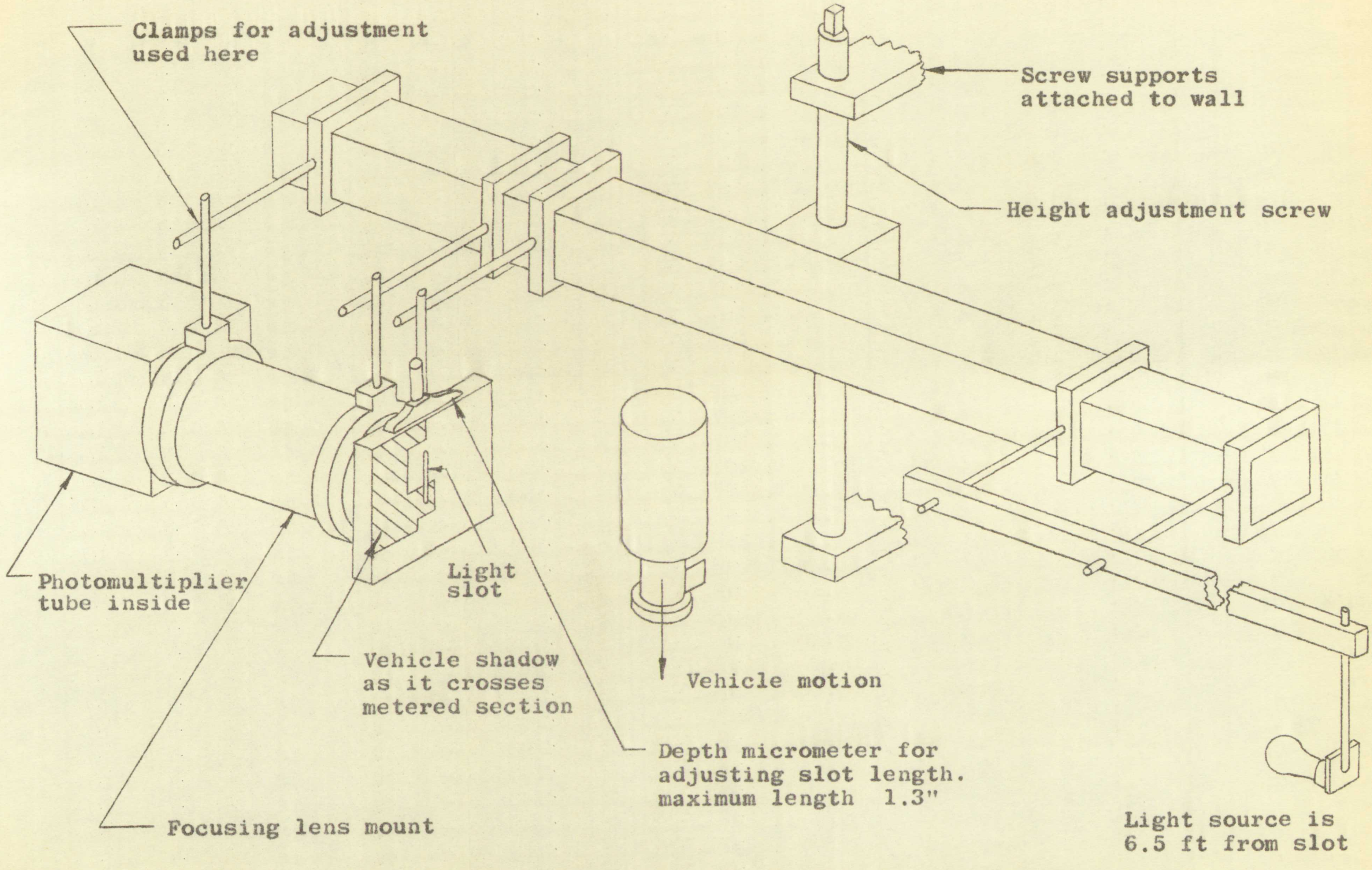

Figure 6. Vehicle Position Transducer

caused a 60 cps variation in intensity. Fitzgibbon obtained parallel light of constant intensity using a germ of wheat bulb as a point source behind a collimating lens. This method was tried, but with the available lenses, it was not possible to obtain the desired condition. The light source used was a completely exposed 60 watt, 12 volt DC mobile home light bulb, mounted about 10 feet from the vehicle path. The large distance between the light source and the slot, combined with the large size of light bulb elements, gave nearly parallel light. It was possible to obtain a constant intensity over the distance to be measured by proper positioning of the light. Even though there was a large distance between the light bulb and the phototube, the light falling on it was still sufficiently intense to give adequate signal. This was the result of the high wattage light bulb used. One advantage of this lighting system was that the light source illuminated the working area, and made it unnecessary to work in darkness.

Flags attached to the drop vehicle cut the nearly parallel rays of light before impact. The flag widths used were 1.250", 1.000", 0.750", 0.500", and 0.250". The flag widths represent the maximum displacement the vehicle may have and still be in the range of the transducer.

The slot was formed with two razor blades screwed to the mounting structure. The width of the slot was set at .031". The length was set with a depth micrometer attached to the mounting structure for that purpose. The length was made variable to obtain maximum resolution for any maximum reading desired.

The photomultiplier tube housing includes the light shield, lenses to focus the parallel light to a small area, the photomultiplier tube (positioned so the light falls on the sensitive element of the tube), and the associated circuitry. The photomultiplier tube used was RCA 931A. The circuit is shown in Figure 7.

Instrumentation

One of the problems in measuring shock pulses with a piezoelectric accelerometer is that of obtaining instruments which will not distort the signal. The instrumentation associated with shock measurement can distort the signal in several ways. These ways are discussed below, as well as the pertinent characteristics of the instrumentation used in this work.

Lazarus (25) points out that piezoelectric crystals have a high impedance (essentially capacitive), and the input impedance of the next instrument must be equally high for good low frequency response. The low frequency cut off point (3 db down) will be where the two impedances are equal, and it may be found as: $f = \frac{1}{2\pi Zc}$, where c is the crystal capacitance and Z is the instrument (usually a cathode follower) input impedance. The cathode followers used had an input impedance of 5,000 megohms resistive, shunted by 12 uufd. The CRL accelerometer had a crystal capacitance of 170 uufd, which was smaller than that of the Endevco. Using these

The photocells had been [illegible] the light [illegible] the possibility of [illegible] to a small area, the photomultiplier [illegible] lens [illegible] so the light falls on the sensitive cathode of the tube), and then [illegible] directly. The photomultiplier tube used was RCA 931A. The circuit is shown in Figure 7.

Instrumentation

One of the problems in measuring shock pulses with piezoelectric accelerometers is that of obtaining instruments which will not distort the signal. The instrumentation associated with shock measurement can distort the signal in several ways. These ways are discussed below, as well as the pertinent characteristics of the instrumentation used in this study.

[illegible] ([illegible]) points out that piezoelectric crystals have a high impedance (essentially capacitive), and the input impedance of the next instrument must be equally high for good low frequency response. The low frequency cut off point (3 db down) will be where the two impedances are equal, and it may be found as: $f = \frac{1}{2\pi RC}$, where C is the crystal capacitance and R is the instrument (usually a cathode follower) input impedance. The cathode followers used had an input impedance of 5,000 megohm resistance, shunted by 1 mmfd. The [illegible] accelerometer had a crystal capacitance of 170 mmfd which was [illegible] than that of the [illegible]. Using these

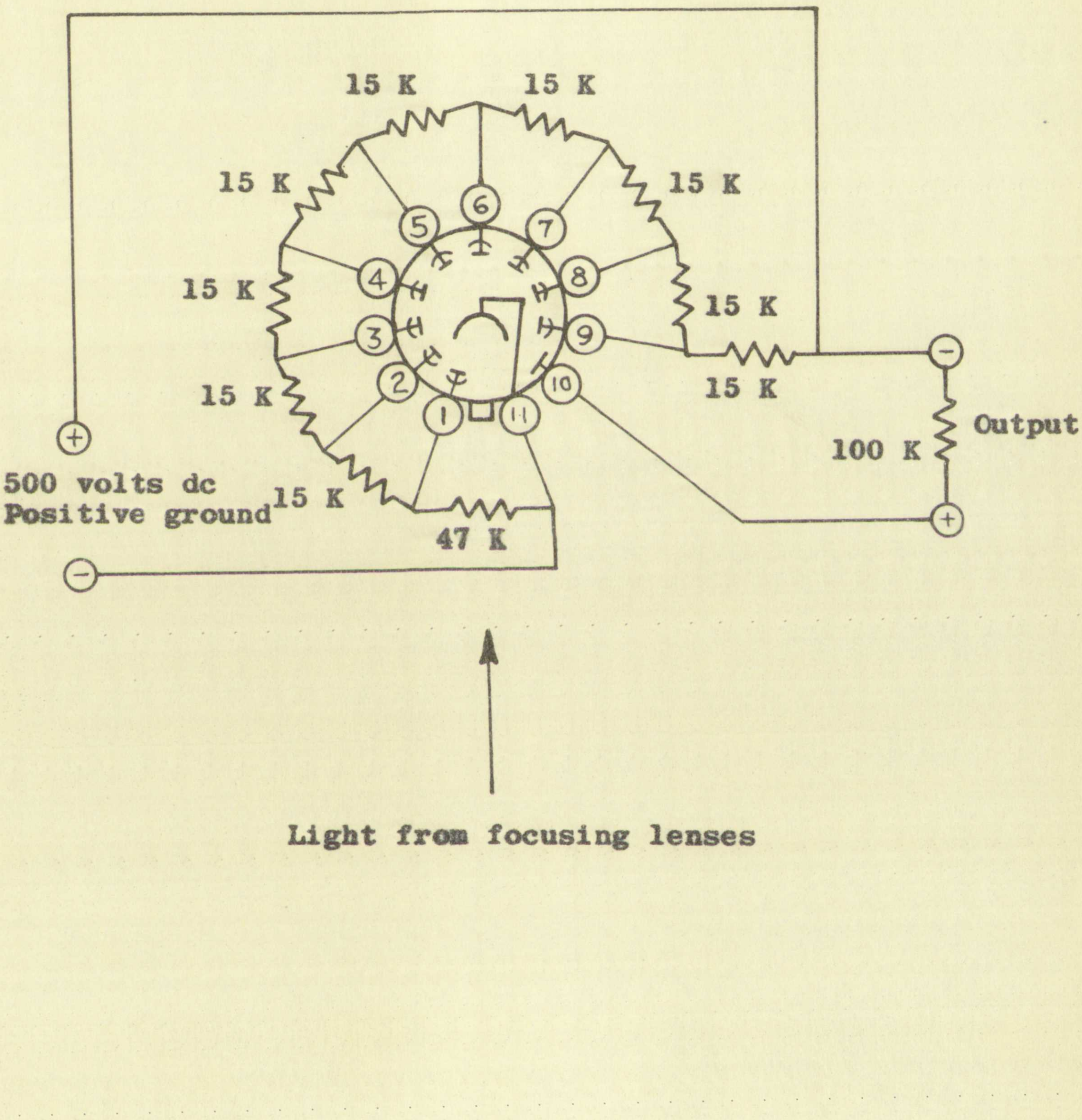

Figure 7. Circuit Diagram for Photomultiplier Tube

values, the low cut off point is 0.19 cps. This is sufficiently low.

Pulse distortion is also caused by inadequate frequency response of the recording instruments. The cathode followers used were flat from 0.02 cps to lmc. Tektronix type 551 oscilloscopes and their dual trace plug-in units were used for recording. This combination gave a frequency response which was flat from dc to 22 mc when direct coupled, and when AC coupled, it was within 3 db down to 2 cps. During the test work, the AC coupling was used.

The Endevco Instruction manual (8) states that for 2% accuracy, the instrumentation system must have a low frequency response 50 times the period of the fundamental frequency of the transient. When this deficiency exists, it will be recognized by the presence of "undershoot" or downward zero shift at the end of the recorded pulse. This result of inadequate low frequency response was also pointed out by Lazarus (25). He determined the effect of inadequate low frequency response experimentally by varying the low band pass of an electronic filter having a rejection rate of 24 db/octave. Since the rejection rate in most instrumentation is around 6 db/octave, his results were conservative.

When transient phenomena are recorded with a piezoelectric accelerometer, the main waveform is often obscured by a high frequency, high amplitude output. This is commonly referred to as ringing, and it can be caused by excitation of the accelerometer at a frequency near its natural frequency, or high frequency motion of the surface it is

mounted on (which is produced by traveling waves). This ringing considerably reduces the accuracy of data reduction. To permit the main pulse to be read, the ringing is sometimes eliminated with an electronic filter. A Spencer-Kennedy Laboratories Electronic Filter, model 302, was used in the experimental work.

There seems to be some disagreement as to the effect of filtering transducer output on accuracy when they are being used for measuring transient phenomena. Conrad and Vigness used one to eliminate the ringing, and believed the filtering did not alter the validity of the results. Kaufman (20) stated that Gulton Industries recommends the use of a filter when calibrating accelerometers on their ballistic pendulum.

However, the Endevco accelerometer manual (8) states on page 10 that "they (electronic filters) should not be used for shock work since they distort the peak acceleration values and introduce phase shift which will change the shape of the acceleration time curve by shifting different parts of the spectrum by varying amounts." Tests were run on the Spencer-Kennedy filter to determine its characteristics. The filter gain and phase shift were determined as a function of input voltage frequency using an audio oscillator. This was done with the cutoff frequency set at 3 kc, the setting used for most of the experimental work. The results of this work are shown in Figure 8, and a study of these curves substantiates the statement in reference 8.

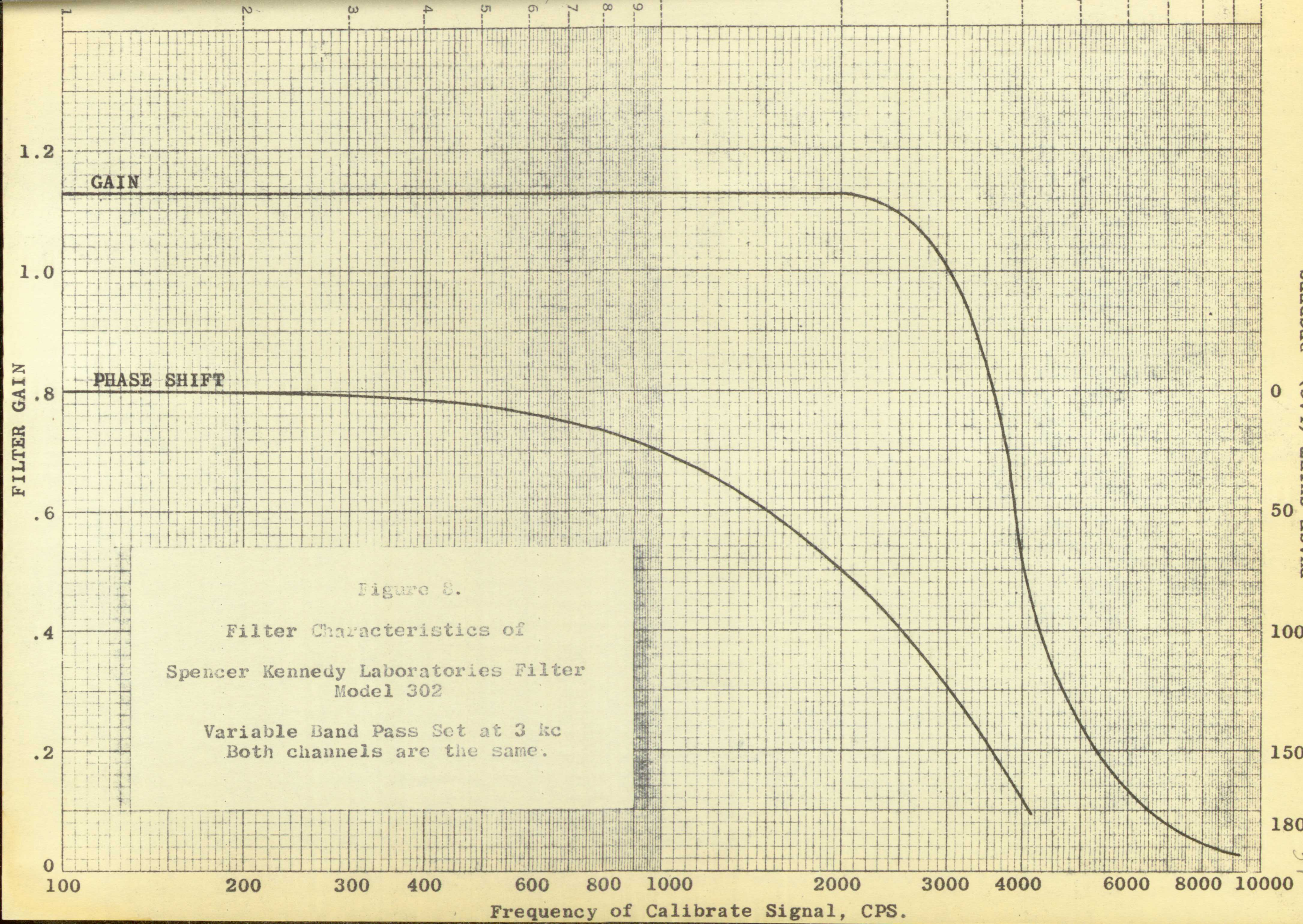

Figure 8.

Filter Characteristics of

Spencer Kennedy Laboratories Filter
Model 302

Variable Band Pass Set at 3 kc
Both channels are the same.

In the experimental work for this thesis, both the unfiltered and filtered signals of both accelerometers were recorded. The filtered signal was considered for use only if the unfiltered one showed objectionable ringing.

The instrumentation will also distort the signal if its voltage is high enough to overload the cathode follower. This may occur in shock work due to the high accelerations resulting from impact. The overload voltage of the cathode followers used is 42 volts with the multiplier in the x1 position. This was the position used during the tests. This corresponds to 3,000 G and 5,000 G, using the nominal manufacturer's sensitivity of the Endevco and CRL accelerometer, respectively.

Cushion Material

To obtain the desired shapes of transient pulses, it was necessary to select a cushion material to be placed between the force transducer and vehicle which would apply the correct force curve to the vehicle.

To obtain the half sine acceleration-time pulse, a linear spring was required. This can be illustrated with the analysis of a vehicle impacting a cushion with some known impact velocity, as shown in Figure 9.

When Newton's Second Law is applied to the freebody in Figure 9, the resulting equation of motion is

$$\frac{d^2y}{dt^2} + \frac{Kg}{w} y = 0 \qquad (5)$$

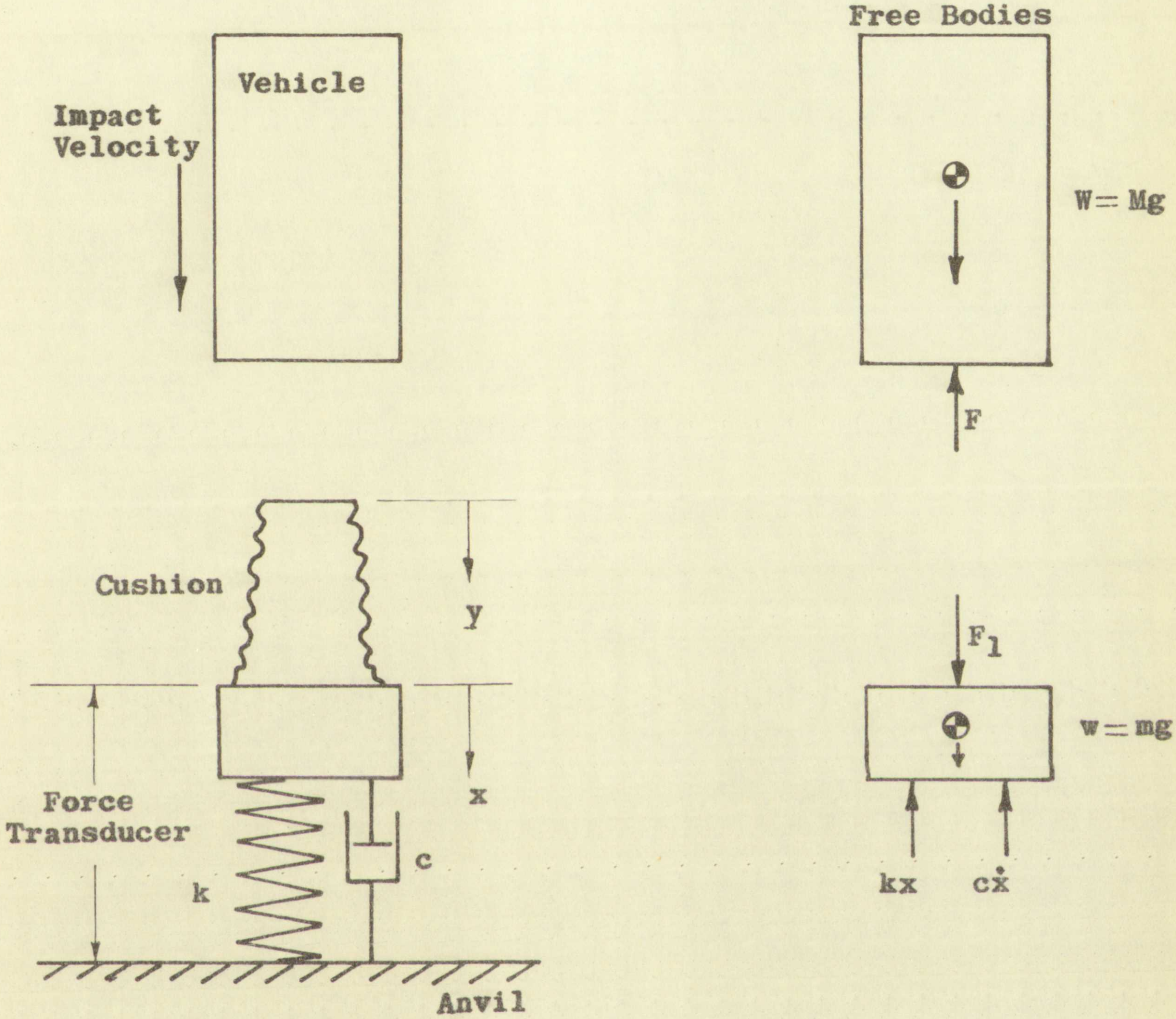

Half Sine Pulse: $F = Ky$, where K = spring modulus of cushion.

Sawtooth Pulse: $F = F_o t$, where F_o is the slope of the force-time curve.

Rectangular Pulse: F = Constant.

Figure 9. Impact Sketch and Related Free Bodies

for the time interval when the vehicle is in contact with the cushion. The solution to this equation for the specified initial conditions is

$$y = \frac{V}{\omega} \sin \omega t \tag{6}$$

where $\omega = \frac{kg}{W}$ and $\omega t \leqq \pi$. Differentiating this twice with respect to time, the resulting acceleration is

$$\ddot{y} = -V\omega \sin \omega t. \tag{7}$$

Since V and ω are constants for a given drop test, the acceleration pulse will be a half sine wave.

The peak acceleration and the pulse duration may be found from the equations

$$\ddot{y}_{max} = V\omega = V\sqrt{\frac{kg}{W}} \tag{8}$$

$$\tau = \frac{\pi}{\omega} = \pi\sqrt{\frac{W}{kg}} \tag{9}$$

Once the duration of the pulse to be obtained has been selected, the required spring modulus may be computed from equation 9. A study of this equation shows that the pulse duration is independent of impact velocity. The impact velocity may be found for the desired peak acceleration using equation 8.

The material used for the linear spring in the experimental work was neoprene. The most convenient form of neoprene to work with was the neoprene bottle stoppers commonly used in chemical laboratories. For the shorter pulses, the stoppers were too thick for the vehicle weights available, and the required "springs" were cut from neoprene sheets 1/8", 1/4", and 1/2"

thick.

To obtain the sawtooth pulse, it was necessary for the force applied to the vehicle by the cushion to vary linearly with time. It was pointed out by Morrow (26) that lead cylinders with a cone point would give a sawtooth acceleration-time pulse. The vehicle used by Morrow weighed 45 lbs. The lead pellet he used was 1" dia.. x 1" high, with a 60° cone on top. The pulses he obtained had peak G's from 200 to 300, and durations from 4 to 6 milliseconds.

The shape of the lead pellets and vehicle weights required to obtain the fourteen acceleration pulses for this work was determined by experiment and experience. The following analysis was of value in this endeavor (see Figure 9 for the definition of terms). The motion of the vehicle is defined by the equations

$$\ddot{y} = -\frac{F_o t}{M} \text{ for } t \leq \tau ,$$

$$\ddot{y} = 0, \text{ for } t > \tau . \tag{10}$$

The velocity and position equations for the vehicle may be found by integration of the first of the above equations, and evaluation of the constants of integration from the given initial conditions. The result is

$$\dot{y} = -\frac{F_o t^2}{2} + V \tag{11}$$

$$y = -\frac{F_o t^3}{3} + Vt \tag{12}$$

Once the peak acceleration and duration of the pulse to be used for a test has been selected, M may be found

[illegible]

[illegible] forces applied to the [illegible] in the [illegible]

with time, [illegible] was [illegible] (X) [illegible] left

collides with a [illegible] would give a [illegible] acceleration

when pulsed. The vehicle used [illegible] weighed [illegible] The

land pellet [illegible] high, with a 60° cone

on top. The pulses obtained had peak G's from 200 to [illegible]

and durations from [illegible] to [illegible] milliseconds.

The shape of the [illegible] and vehicle weights required to obtain the function acceleration pulses for this work was determined by experiment and experience. The following analysis was of value in this endeavor. (See Figure 9 for the definition of terms.) The motion of the vehicle is defined by the equations

[illegible]

$$\text{[illegible]} \quad \text{for } t > T \qquad (10)$$

The velocity and position equations for the vehicle may be found by integration of the first of the above equations, and evaluation of the constants of integration from the given initial conditions. The result is

$$\text{[illegible]} \qquad (11)$$

Once the [illegible] and duration of the pulse to be used [illegible] has been selected, x may be found

from equation 10. Then the impact velocity may be found from equation 11, by assuming that the vehicle velocity is zero at the maximum acceleration.

To apply a rectangular acceleration time pulse to the vehicle, the cushion must have properties which result in the acceleration being constant for the desired pulse duration. Because constant acceleration implies a constant force, it was necessary to use a cushion material which was plastic in the range of use. Figure 15 in reference 27 gives the stress-% compression curve for a 16 lb/ft.^{3} foamed aluminum, and it is reproduced here as Figure 10. A study of this figure indicates that it is essentially plastic to 50% compression, and that it is not sensitive to rate of compression. These two properties made it acceptable for use as the cushion material to give rectangular acceleration time pulses. It is marketed under the trade name of Alumafoam and is manufactured by Dynamic Metals, Inc., Houston, Texas.

An analysis similar to the one made for the sawtooth pulse may be made for the rectangular pulse. The motion of the vehicle is defined by the equations

$$\ddot{y} = -K = -\frac{\sigma A g}{W}, \text{ for } t \leq \tau,$$

$$\ddot{y} = 0, \text{ for } t > \tau. \qquad (13)$$

In the above equation, σ is the yield stress of the cushion material and A is the cushion area. The other terms have been previously described. The velocity and position equations for the vehicle may be found by integration of the

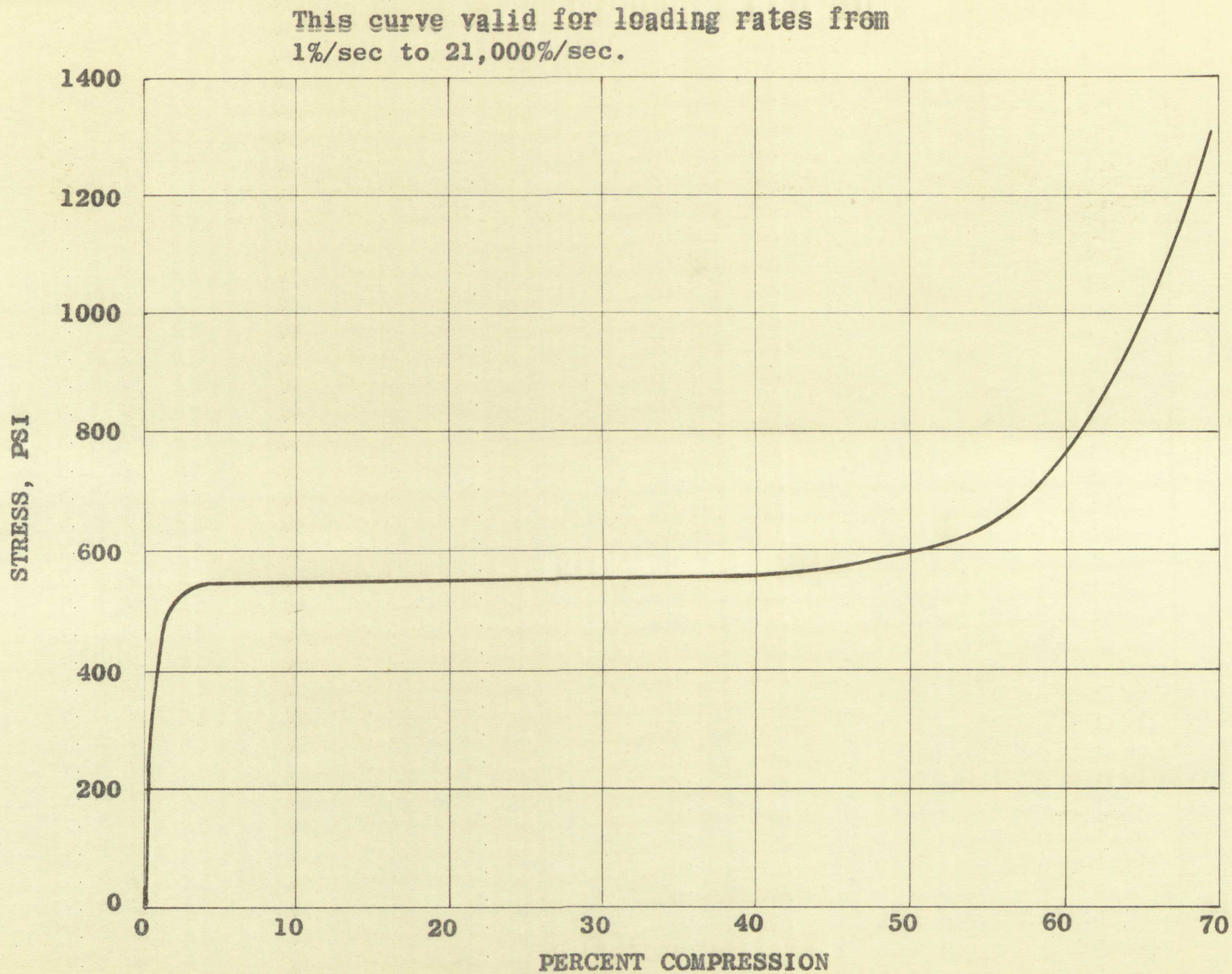

Figure 10. Typical Stress-Percent Compression Curve, For 16 lb/cubic ft. Foamed Aluminum

first of the above equations, and evaluation of the constants of integration from the given initial conditions. The result is

$$\dot{y} = -\frac{\sigma A g t}{W} + V \tag{14}$$

$$y = -\frac{\sigma A g t^2}{2W} + Vt\,. \tag{15}$$

Once the peak acceleration and duration of the pulse to be used for a test has been selected, the impact velocity may be found from equation 14 by assuming the vehicle velocity is zero at $t = \tau$.

The above equations, 5 thru 15, were used in determining the impact velocities and maximum cushion compressions given in Table II.

EXPERIMENTAL PROCEDURE

Transducer Calibration Methods

The transducers used have been described in the previous section. However, it was necessary to calibrate them before they could be used to establish sensitivity.

The force transducers were tested in a 60,000 lb. capacity Reihle Testing Machine to establish output characteristics: linearity, agreement with theoretical output, and agreement between the two transducers. For all of these tests, the potentiometer circuit described in Figure 5 was used. The circuit output was visually read on one of the oscilloscopes previously mentioned.

The linearity of the force links was determined by loading each of them to the approximate maximum load they were designed for, and recording the circuit output for both the loading and unloading. The high range force transducer was loaded to 25,000 lbs. and 30,000 lbs. The low range transducer was loaded to 2500 lbs. and 3000 lbs. The results of these tests, shown in Figure 11 and 12, indicate the transducers are linear.

It was desirable to check agreement with theoretical output and agreement between the two transducers when the loads on both were measured using the same full range scale on the testing machine. This was considered necessary, since the accuracy of the various scales on the machine were

KEY	GAIN	CALIBRATE RESISTOR	DEFLECTION
⊙	20 mv/cm	1 megohm	3.8 cm
△	10 mv/cm	5 megohm	1.5 cm

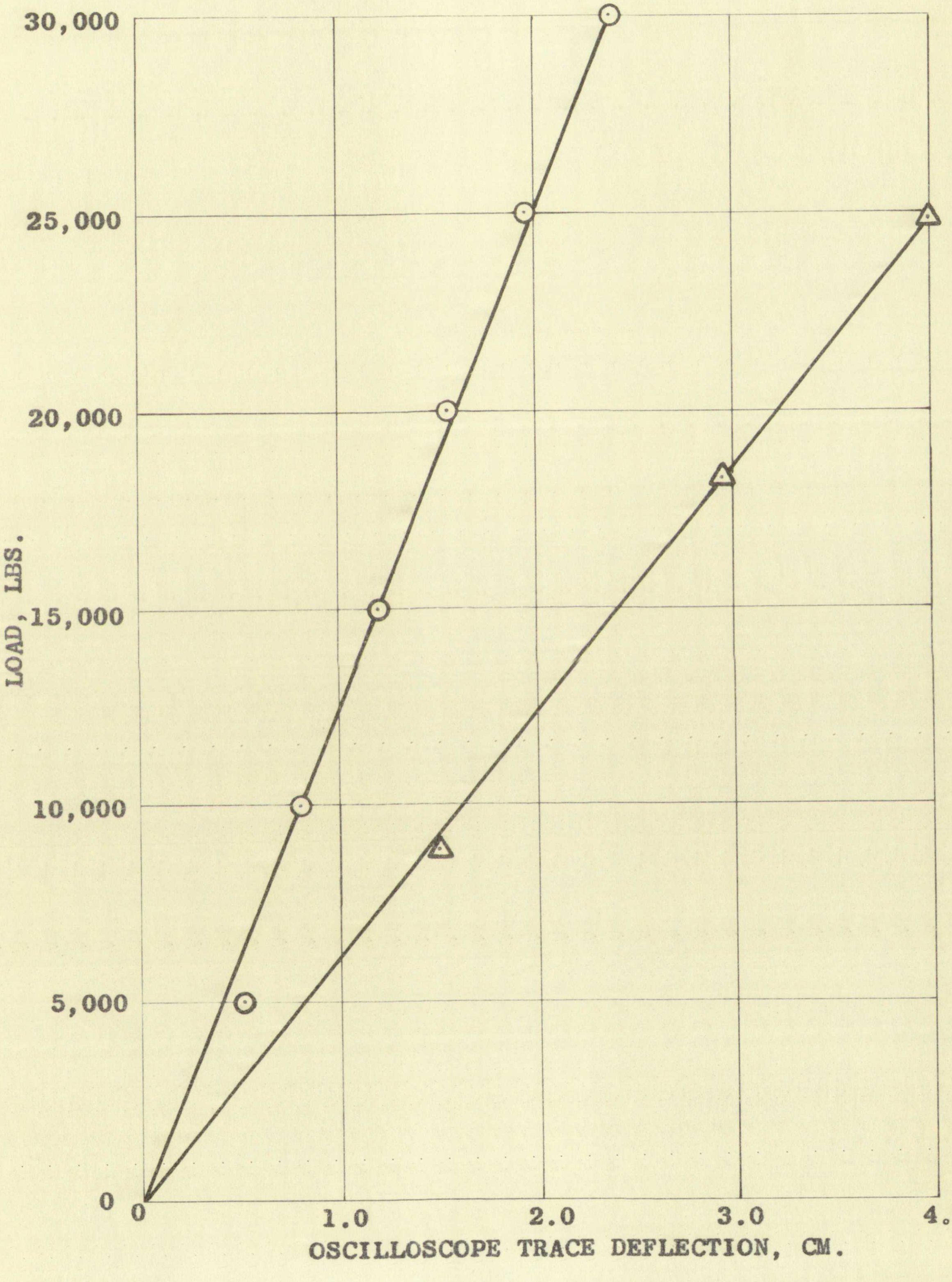

Figure 11. Calibration Curve for High Range Force Transducer

KEY	GAIN	CALIBRATE RESISTOR	DEFLECTION
⊙	20 mv/cm	500K ohm	3.5 cm
△	10 mv/cm	1 megohm	3.4 cm

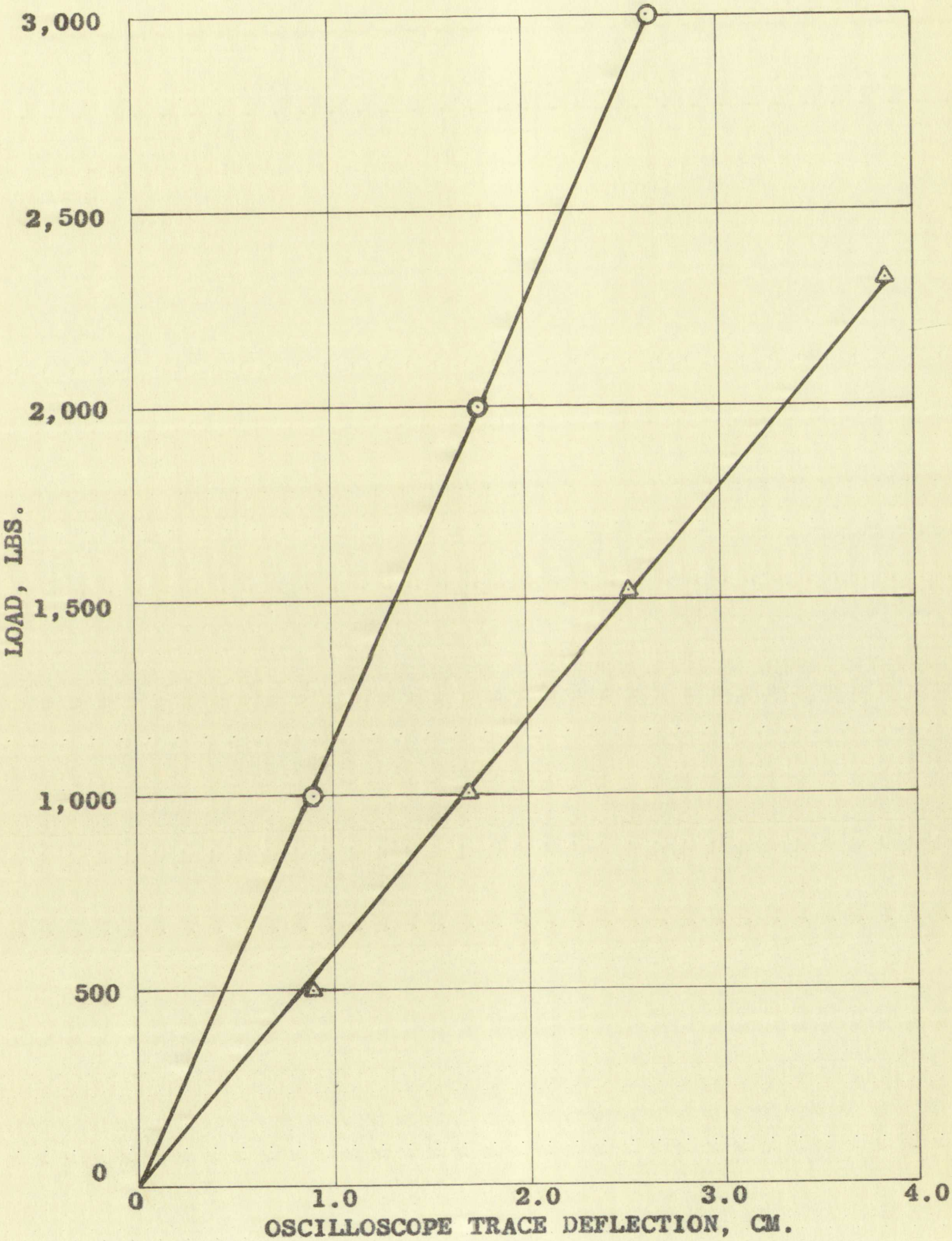

Figure 12. Calibration Curve for Low Range Force Transducer

unknown, and this procedure would eliminate this variable from the results. The actual sensitivity of the circuit in lbs/mv was computed by dividing the measured load by voltage.

The theoretical sensitivity was determined using the following quantities:

Calibrate resistance in ohms, R_c.
Compression area of force transducer in square inches, A.
Elastic modulus of force transducer in lb/in.^{2}, E.
Gage factor, F.
Strain gage resistance in ohms, R_g.
Oscilloscope gain in mv/cm, U.

The calibrate resistor was put in parallel with the strain gages, and the resulting deflection of the oscilloscope trace, y, recorded. The circuit sensitivity, S, was then computed with the following equation:

$$S\text{, lbs/mv, } = \frac{NR_g EA}{F(R_c + NR_g)yU} \tag{16}$$

The derivation of this equation is given in the appendix.

When these equations were applied, it was found that the high range force transducer had a measured sensitivity of 564 lbs/mv, and a computed sensitivity of 550 lbs/mv. The low range force transducer had a measured sensitivity of 55.6 lbs/mv and a computed sensitivity of 55.0 lbs/mv.

This agreement between measured and theoretical sensitivity for both force transducers was considered sufficiently close, and the theoretical sensitivities were used for computing accelerometer sensitivities.

The results also indicated that both force links would

give essentially the same result when used to measure the same force. The small difference in these quantities is probably due to visual reading errors.

The static test data from which all of the above results were determined is given in the appendix.

An entirely different type of calibration procedure was used for the vehicle position transducer. Its principle of operation permitted the calibration to keep to a minimum any error caused by the variation in light intensity along the light ribbon passing thru the slot.

It was found that considerable variation of light intensity along the light ribbon was caused by small variations in the position of light source or phototube. Therefore, it was necessary to check for intensity variation each day before proceeding with test work, and readjust if required. Figure 13 illustrates the method used to perform this check. The motor driven "fan" was so placed that its end passed immediately in front of the slot. If the light were of constant intensity, the amount of light passing thru the slot would initially decrease linearly with time. Once the following edge of the fan blade passed the top edge of the slot, it was exposing as much slot area as it was covering. This caused the amount of light passing thru the slot to be constant. As the leading edge of the fan passed the lower edge of the slot, the amount of light passing thru the slot then increased linearly with time.

Typical results before and after the correction of the

[illegible]
other series. The small difference in average velocities is
probably due to visual parallax errors.

The graphs and data from which all of the above results were determined are given in the Appendix.

An entirely different type of measuring procedure was used for the vehicle position transducer. Its principle of operation permitted the calibration to come to a minimum any error caused by the variations in light intensity along the light ribbon passing thru the slit.

It was found that appreciable variations of light intensity along the light ribbon were caused by small variations in the position of the lamp and lens system. Therefore it was necessary to correct the intensity variation each day before calibrations were made [illegible]. Figure III illustrates the method in its idealized form. The motor driven "fan" was so placed that its end passed immediately in front of the slit. If the light were of constant intensity, the amount of light passing thru the slit would initially decrease linearly with time. Once the following edge of the fan blade passed the top edge of the slit, it was exposing as much slit area as it was covering. This caused the amount of light passing thru the slit to be constant. As the leading edge of the fan passed the lower edge of the slit, the amount of light passing thru the slit then increased linearly with time.

Typical results before and after the correction of the

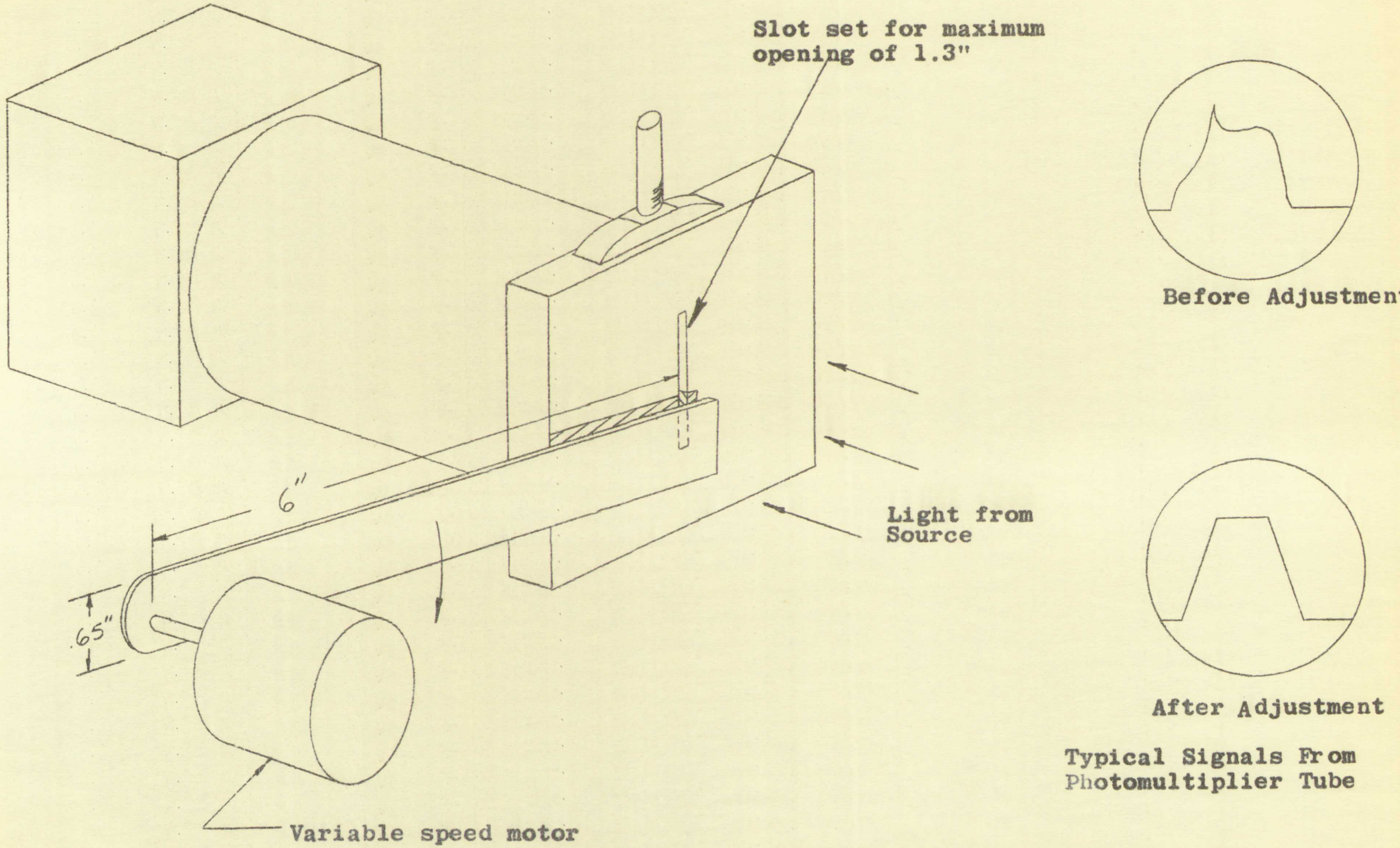

Figure 13. Method of Setting Vehicle Position Transducer

position of the light source are shown in Figure 13. Linearity requires sharp corners at the changes in slope on this curve, as well as straight lines for the three segments.

The flag width affected the accuracy of the position transducer since it was used for each run in assigning the position scale to that particular record. An attempt was made to hold the flag width to within 0.001" of nominal.

Test Procedure

The two accelerometers were assembled to the specially designed mounting adapter, and both were tightened to a torque of 60 in lbs as specified in the Endevco instruction manual. The cables were connected in the recording circuit and then taped to the mounting adapter as close to the connection as possible. Careful attention was given to the cable support, since experience had shown that distortion of low acceleration signals occur when the cables are not fastened securely. (The Endevco instruction manual also points this out). Figure 14 shows a closeup of this assembly.

The test run was selected from a chart similar to Table II. From the required impact velocity, the vehicle drop height was determined. The maximum cushion compression from the table was used in selecting the correct flag width for the vehicle position indicator.

Next, the cushion and vehicle weight to be used were selected. Two methods were used to select these items for the half sine pulse. One method involved, first, determining the spring modulus for several stoppers in a compression testing machine; and second, using these, the available vehicle weights, and equations 8 and 9, to select a combination to give the desired results. This method did not work for the shorter pulses, since the spring modulus of the stoppers were too low even for the lightest vehicle. Therefore, the lightest vehicle was used for these pulses, and

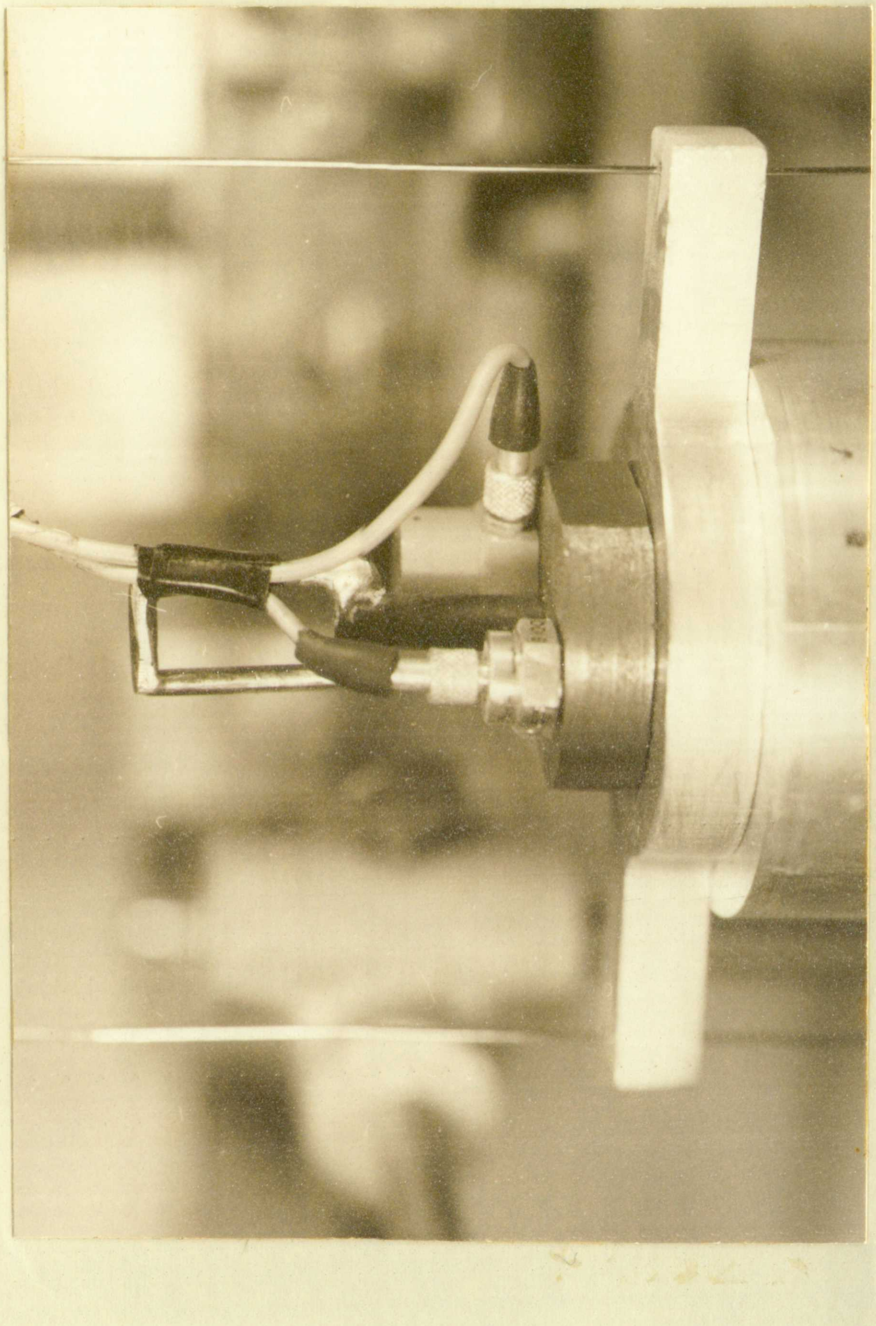

Figure 14. Accelerometers Mounted on Vehicle

the sheet neoprene was used for the cushion material. The area of the sheet neoprene was adjusted by trial and error to give the desired pulse duration.

The spring modulus of the stoppers and sheet neoprene became non-linear for % compressions greater than about 25%. Therefore it was necessary to keep the cushion thickness more than four times the expected maximum sample compression given in Table II; otherwise, the deviation between a half sine wave and the actual wave became particularly objectionable. However damping elements in the neoprene always caused some deviation.

The cushion and vehicle weight for the sawtooth pulse were also selected by trial and error. From Morrow's work it was known that a properly shaped lead pellet would give a sawtooth force pulse. Work by Anderson (28) on peak accelerations resulting from drop tests on lead cylinders was used as a guide in selecting the pellet size and vehicle weight. Also used as a guide were the required impact velocity and maximum cushion compression. Pellets were made and tests run. This procedure was repeated until the desired pulses were obtained.

Since the lead pellets were not reusable, their fabrication time became important. To keep the fabrication time at a minimum, lead cylinders were cast and required pellets made by turning the cylinders to the desired shape in a lathe. The as-cast diameters were 5/16, 7/16, 9/16, 11/16, and 25/32 inches. The length was 4".

given the [illegible]

[illegible]

[illegible]

in Table [illegible]

and the [illegible]

were [illegible]

[illegible]

[illegible]

[illegible]

[illegible]

[illegible]

as a pulse [illegible]

Also used as a [illegible]

maximum [illegible]

This procedure [illegible]

obtained.

[illegible]

[illegible]

at a maximum [illegible]

made by [illegible]

[illegible]

[illegible]

The selection of the vehicle weight and cushion size for the rectangular pulses was based upon the yield stress of the cushion material. Figure 10 shows this stress to be about 600 psi. The vehicle weight W was related to the cushion area A for the desired constant acceleration G as follows: $WG = 600A$. In using this relation, a vehicle weight was selected which resulted in a cushion area from 1.0 to 1.5 in.^{2} To stay within the plastic range of the foamed aluminum, it was necessary that the cushion thickness selected by at least twice the maximum sample compression. It may be noted that a given peak acceleration requires the same vehicle weight and cushion area. The different pulse durations are obtained by using different drop heights. For the shorter pulses, it was found necessary to precompress the sample to the yield stress or slightly past, to eliminate the elastic part of the cushion.

The foamed aluminum used was not homogeneous. There was a density variation in adjacent samples cut from the same block of material. Since the yield stress varied with density, the peak accelerations obtained were not always those desired, and this caused deviation from the desired pulse duration. However, using this method did permit pulses to be obtained which covered the desired range with suitable spacing.

The complete cushion description and vehicle weight for each of the pulses obtained is given in the appendix.

Once the vehicle weight was known, it was possible to select the proper force transducer, assemble it to the anvil, and connect the gages in the potentiometer circuit.

The vehicle was assembled to the nose piece, and the flag assembled to this unit. Then the complete assembly was weighed on a Toledo scale having a least count of 1/8 ounce. It was then assembled to the accelerometer mounting adapter in the guide wires.

The vehicle was then supported on the anvil at a height equal to the cushion thickness, by means of a metal spacer of the required thickness.

Then the height of the vehicle position indicator was set so the lower edge of the flag was about 1/16" below the lower edge of the light slot. The length of the light slot was made slightly greater than the flag width, so the oscilloscope was triggered at the correct time.

The oscilloscope was triggered by the change in signal from the phototube. The trigger level was set so it occurred after the flag had cut about 1/16" from the light ribbon at the top edge.

The oscilloscope gains, sweep rates, and trace positions were set. It was necessary to have the trace for the vehicle position indicator set coincident with one of the other traces, since the distance between its initial position and maximum deflection position represented a distance equal to the flag width, a fact used in data reduction for individual calibration of each run.

The vehicle was raised to the desired drop height, the cushion placed on the anvil, the vehicle released, and the data recorded on Polaroid film. Normally, three runs were

The [illegible] was [illegible]

was attached to the [illegible]

rotated in a [illegible]

it was then [illegible]

the outer edge.

The [illegible]

equal to the [illegible]

the required thickness.

When the [illegible]

on the inner edge of [illegible]

edge of the [illegible]. The [illegible] of the [illegible] was

slightly greater than the [illegible]

[illegible]

The [illegible] was [illegible]

from the [illegible]. The [illegible]

after the [illegible]

the top edge.

The oscilloscope [illegible]

were set. It was [illegible] the

position indicator [illegible]

since the distance between [illegible]

deflection position [illegible]

width, a [illegible]

of each [illegible]

The [illegible]

[illegible] placed on the [illegible]

data recorded [illegible]

recorded on one frame of film. After the consecutive runs had been recorded, a calibrate resistor was put in parallel with the strain gages on the force transducer, and the resulting trace deflection was recorded on the same frame as the force transducer signals. If the cushion used did not recover, its final thickness was measured to serve as a check on the vehicle position transducer.

DATA REDUCTION

Force Transducer Response

Since both force transducers were standards used in determining the accelerometer sensitivity, it was necessary to consider their transient response. It has been previously shown that strain gages behave for transients and static loads in the same way, so the average strain along the gage length is known at any instant. It was then necessary to relate this average strain signal to the force on the cushion material.

The wave propagation effects were considered in the following way and found to be negligible. The velocity of wave propagation in the force transducer materials (steel and aluminum) was approximately 16,000 fps. The minimum pulse duration considered was 0.001 seconds, which made the minimum length of the traveling wave about 16 feet. Since the length of the force transducer was less than 2", no appreciable error was introduced by assuming the strain to be the same along the reduced section of the force link.

When this assumption is made, the force transducers may then be analyzed as a spring-mass system, and the strain gage signal becomes proportional to the deflection of the "spring". The problem then becomes to relate this deflection to the transient force pulse. It is impractical to approach this problem directly because of the difficulties in expressing mathematically the experimental data. Therefore, the approach

[illegible]

[illegible]

malization [illegible]

[illegible] their [illegible]

shown [illegible]

in the same [illegible]

is known as an [illegible]

this average stress at the [illegible]

The [illegible]

following [illegible]

wave propagation [illegible]

and aluminum) was [illegible]

pulse duration [illegible]

minimum length of the [illegible]

length of the [illegible]

scale error [illegible]

same along the [illegible]

When this [illegible]

then be analyzed [illegible]

signal became [illegible]

The problem [illegible]

transient to [illegible]

problem [illegible]

[illegible]

used was to assume the desired force pulses and to determine the response of the force transducer to those transient forces. Then, using the computed deflection of the force link, and its known spring constant, it was possible to compare the force indicated by the force transducer strain signal to the applied force.

The equation of motion for the force links as derived from the freebody in Figure 9 is

$$\ddot{x} + \frac{c}{m}\dot{x} + \frac{k}{m}x = -\frac{F(t)}{m}\text{, or}$$

$$\ddot{x} + 2\zeta p x + p^2 x = -\frac{F(t)}{m}\text{, where} \tag{17}$$

ζ = the damping factor, c/C_c,

p = the natural frequency, $\sqrt{\frac{k}{m}}$.

The damping factor for the low range force transducer was computed from some of the data taken for the rectangular pulse. The constant acceleration obtained for this pulse made it easy to count the number of cycles required for the amplitude to decay 50%. From this, the damping factor could be found from the relation $\zeta = \frac{.110}{n}$, where n is the number of cycles for 50% amplitude decay (29). This was done for a series of runs, and the average damping coefficient was 0.013. The information from which the above damping factor was computed is shown in the appendix.

The high range force link was used primarily for the sawtooth pulse. This shape of pulse did not result in data which could be accurately analyzed for the damping coefficient.

[illegible] of the [illegible] were used to determine [illegible] which were [illegible] for various [illegible]. These, together with the dimensions of the cross link, and the damping constant, it was possible to compute the forces [illegible] by the [illegible] at all times to the applied force.

The equation of motion for the force field can be derived from the free body in Figure [illegible]

[illegible]

[illegible]

F = the applied force

M = the [illegible]

The [illegible] of [illegible] damping was computed from some of the data taken for the [illegible] pulse. The constant acceleration obtained for this pulse made it easy to count the number of cycles required for the amplitude to decay 50%. From this, the damping factor could be found from the equation $\zeta = \frac{.110}{n}$, where n is the number of cycles for the amplitude decay [illegible]. This was done for a series of runs, and the average damping coefficient was 0.0[illegible]. The information from which the above damping factor was computed is shown in the appendix.

The high speed model film was used primarily for the [illegible] pulses. [illegible] of pulse [illegible] results in data which would be [illegible] the damping coefficient.

However, a study of the data indicated that the damping coefficient was about the same as for the low range force link, or smaller.

Because the damping coefficient was low, it was decided to neglect it in the response computations; therefore, the second term in equation 17 drops out.

The natural frequency of the force links was computed from the information given in Figures 3 and 4, and found to be 10,300 cps, and 20,500 cps, respectively. A study of data taken with each of these units showed that each had a natural frequency of about 10,000 cps. This discrepancy in the actual and theoretical natural frequency for the high range force link is explained as being due to the flexibility of the structure upon which the force link is mounted. The natural frequency used in the response computations for the force link was 10,000 cps.

The equations of motion for the force link mass due to the half sine transient become

$$\ddot{x} + p^2 x = \frac{F_o \sin \omega t}{m}, \text{ for } t \leq \frac{\pi}{\omega}$$

$$\ddot{x} + p^2 x = 0, \text{ for } t > \frac{\pi}{\omega}. \tag{18}$$

For the boundary conditions x and $\dot{x} = 0$ at $t = 0$, the solution to the first of the above equation may be written in the form

$$kx = \frac{pF_o}{(p^2 - \omega^2)} (p \sin \omega t - \omega \sin pt), \text{ for } t \leq \frac{\pi}{\omega}. \tag{19}$$

This form is used because it relates the force exerted by the force link, kx, to the applied force, $F_o \sin \omega t$. Since the term kx is proportional to the strain gage signal, a method of comparing the strain gage signal to the applied force is obtained.

This solution has been plotted using a ratio of pulse duration to natural frequency of force link $(\frac{p}{\omega})$ of 20. This ratio represents the one which would give the greatest deviation of force link signal from applied pulse for all pulses encountered in this work. This ratio was based on the shortest pulse obtained being one millisecond, and a force link natural frequency of 10,000 cps. The plot of this solution is shown in Figure 15.

The equations of motion for the force link mass due to the sawtooth transient become

$$\left.\begin{aligned} \ddot{x} + p^2 x &= \frac{F_o t}{m}, \text{ for } t \leq \frac{19\pi}{p}, \\ \ddot{x} + p^2 x &= \frac{19\pi F_o}{mp}, \text{ for } \frac{19\pi}{p} \leq t \leq \frac{20\pi}{p}, \\ \ddot{x} + p^2 x &= 0, \text{ for } t > \frac{20\pi}{p} . \end{aligned}\right\} \quad (20)$$

Again, the pulse duration has been taken as 10 times the natural period of the force link, for the reason previously mentioned. For the boundary condition x and $\dot{x} = 0$ for t = 0 and $x = \frac{19\pi F_o}{kp}$ and $\dot{x} = \frac{2F_o}{k}$ for $t = \frac{19\pi}{p}$, the solutions to the first two equations may be written in the form

$$\left.\begin{aligned} kx &= F_o \left(t - \frac{1}{p}\sin pt\right), \text{ for } t \leq \frac{19\pi}{p}, \\ kx &= \frac{F_o}{p}(19\pi - 2 \sin pt), \text{ for} \end{aligned}\right\} \quad (21)$$

$$\left.\frac{19\pi}{p} \leq t \leq \frac{20\pi}{p}\ .\ \right]$$

A comparison of the force link response to applied transient is shown in Figure 16. The figure shows that the applied transient is not a sawtooth as normally described. This modification to the sawtooth was used, since in practice it is not possible for the force to go to zero instantaneously. To account for this in the response of the force link, the sawtooth was modified to permit the greatest deviation of response from applied transient.

A similar modification has been made to the rectangular pulse. In practice it is not possible to obtain a rectangular pulse, because there must be some finite rise time to the then constant force. For discussion purposes, the notation "rectangular pulse" will still be used. When a finite rise time is considered, the equations of motion for the mass of the force link for the rectangular pulse become

$$\ddot{x} + p^2x = \frac{F_o t}{m}\ , \text{ for } t \leq \text{rise time,}$$

$$\ddot{x} + p^2x = \frac{F_o t'}{m}\ , \text{ for rise time} \leq t \leq \text{pulse duration,} \tag{22}$$

$$\ddot{x} + p^2x = 0, \text{ for } t > \text{pulse duration.}$$

These are the same equations as those used for the sawtooth. The difference in the sawtooth pulse and the rectangular pulse is in the rise time. For the sawtooth pulse, the rise time was 95% of the pulse duration. For the rectangular pulse, it will be taken as 5% and 10%.

The solutions to equations 22 after evaluation of the

A comparison of the force time response to applied transients is shown in Figure 4[illegible]. [illegible] shows that the applied transient is not a sawtooth as generally assumed. This modification to the sawtooth was made, since it is [illegible] not possible for the force to [illegible] to account for this in the analysis of the force time network was modified to permit the prediction of system response from applied transient.

A similar modification has been made for the [illegible] pulse. In practice it is not possible to obtain a rectangular pulse because there must be some finite rise time to [illegible] constant force. The distinction [illegible] section pulses will still be used [illegible] finite rise time is considered, the equations of motion for the case of the force link for the rectangular pulse become:

$$\ddot{x} + p^2 x = \frac{F_o t}{m}, \quad \text{for } t \leq \text{rise time},$$

$$\ddot{x} + p^2 x = \frac{F_o t_r}{m}, \quad \text{for rise time} < t < \text{pulse duration},$$

$$\ddot{x} + p^2 x = 0, \quad \text{for } t > \text{pulse duration}.$$

These are the same equations as those used for the sawtooth. The difference in the sawtooth pulse and the rectangular pulse is in the rise time. For the sawtooth pulse, the rise time was [illegible] of the pulse duration. For the rectangular pulse, it will be taken as [illegible] and 10[illegible].

The solutions to equations 23 are [illegible] presented in [illegible]

constants for the boundary conditions are as follows:

$$kx = F_o \left(t - \frac{1}{p} \sin pt\right), \text{ for } t \leq \frac{\pi}{p}, \text{ and}$$
$$kx = \frac{F_o}{p}(\pi - 2 \sin pt), \text{ for } \frac{\pi}{p} \leq t \leq \frac{20\pi}{p} \tag{23}$$

for the 5% rise time pulse; and for the 10% rise time pulse,

$$kx = F_o \left(t - \frac{1}{p} \sin pt\right), \text{ for } t \leq \frac{2\pi}{p}, \text{ and}$$
$$kx = \frac{2\pi F_o}{p} \text{ for } \frac{2\pi}{p} \leq t \leq \frac{20\pi}{p}. \tag{24}$$

The above solutions are plotted in Figure 17. Two different rise times have been illustrated to show the large difference in force link response that can occur for almost identical pulses.

A study of Figures 15, 16, and 17 permits the conclusion to be drawn (regarding the force link response) that the force link is adequate for determining the transients investigated in this work. The shape of the applied transient can be determined to a high degree of accuracy by locating the mean for the oscillations occuring in the signal. The greatest deviation between the mean and the actual pulse occurs in the vicinity of maximum slope of the force pulse. At these locations the accuracy for which the shape of the pulse is known would be the lowest.

Since there is a small amount of damping in the force links, the oscillations are reduced toward the end of the pulse, and even eliminated in the longer pulses. This is indicated by a study of the graphs determined by Levy and

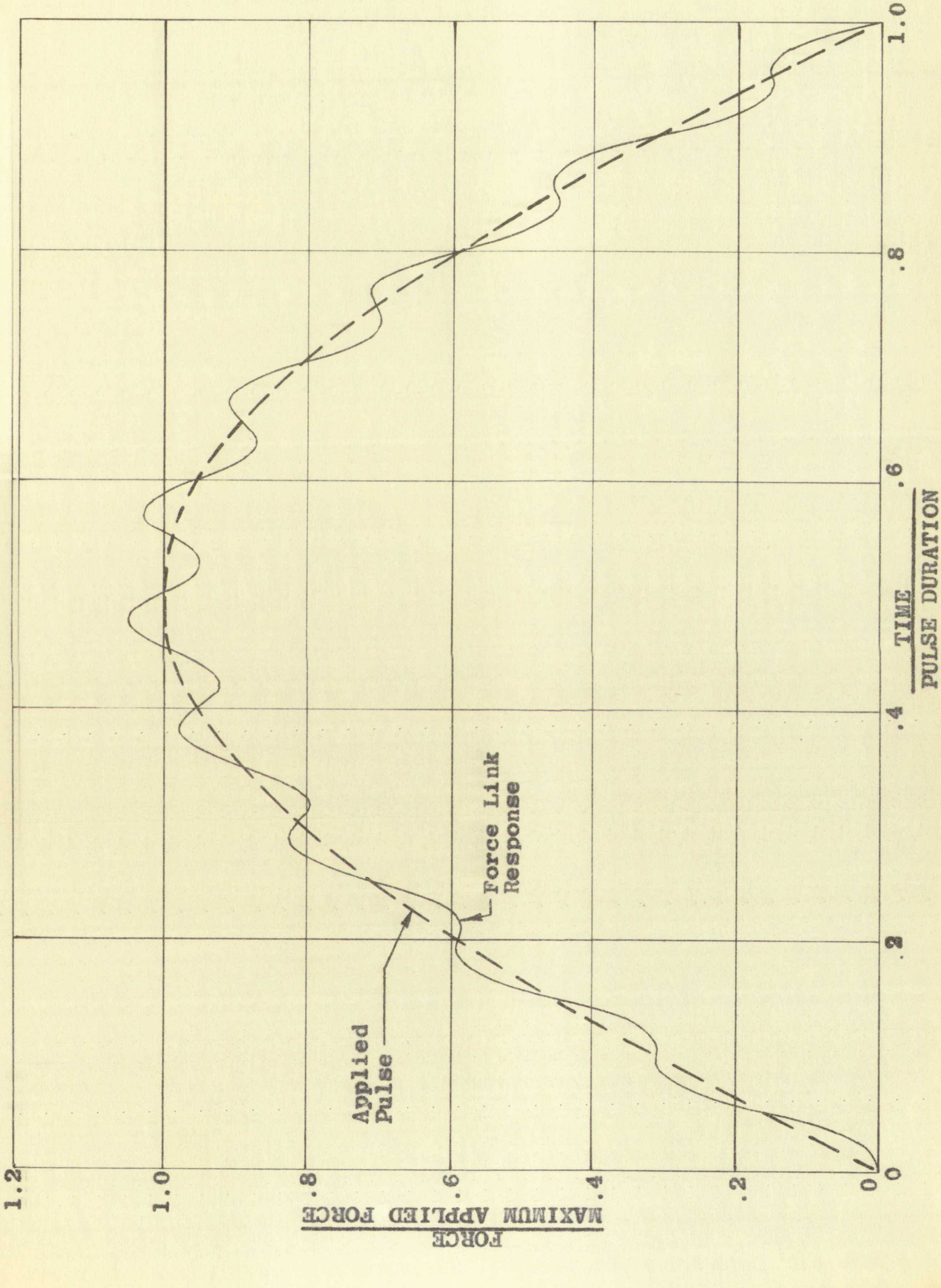

Figure 15. Force Link Response to a Half Sine Pulse. Pulse Duration of 10 Times Natural Period of Force Link.

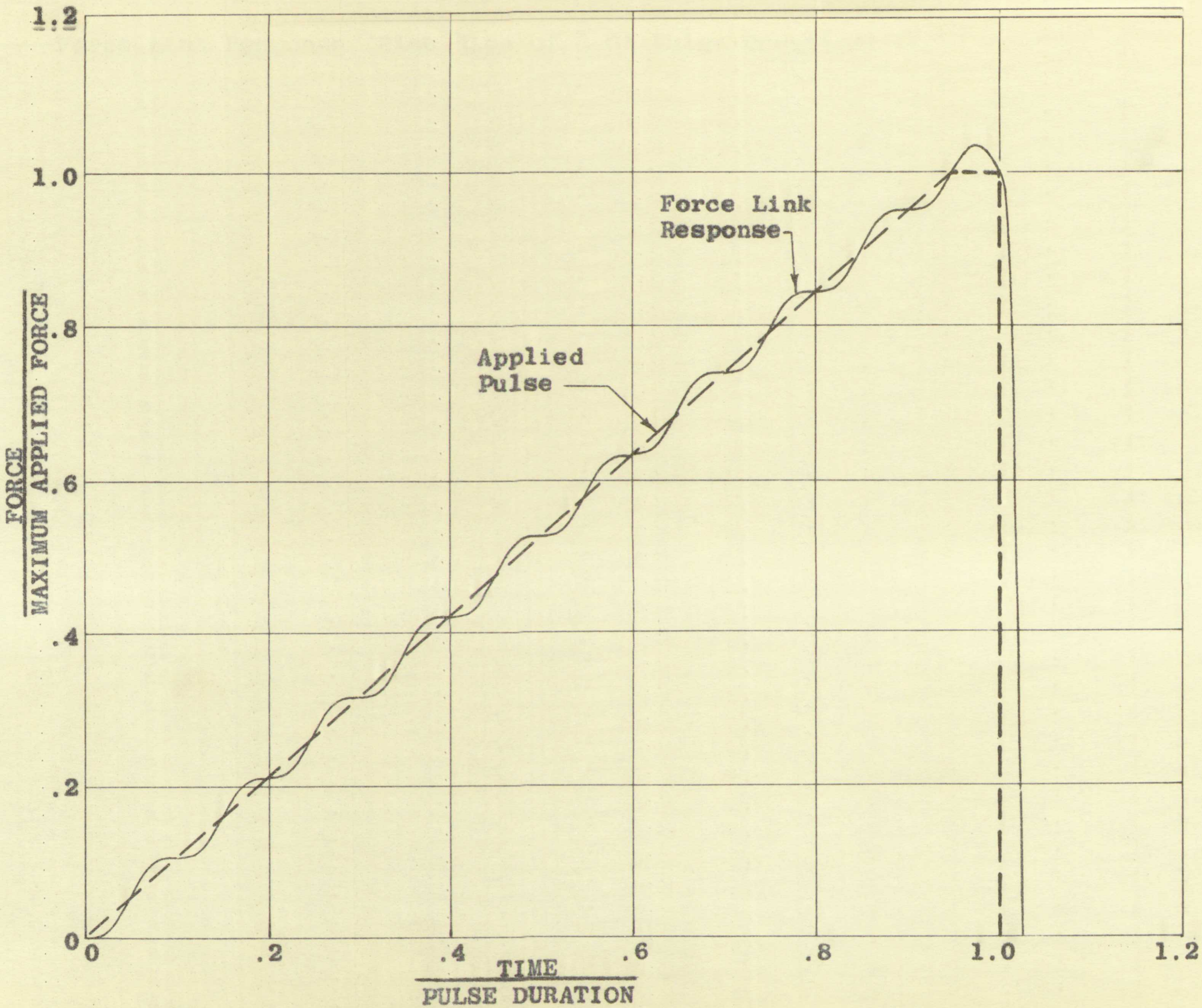

Figure 16. Force Link Response to a Sawtooth Pulse.
Pulse Duration is 10 Times the Natural Period of Force Link

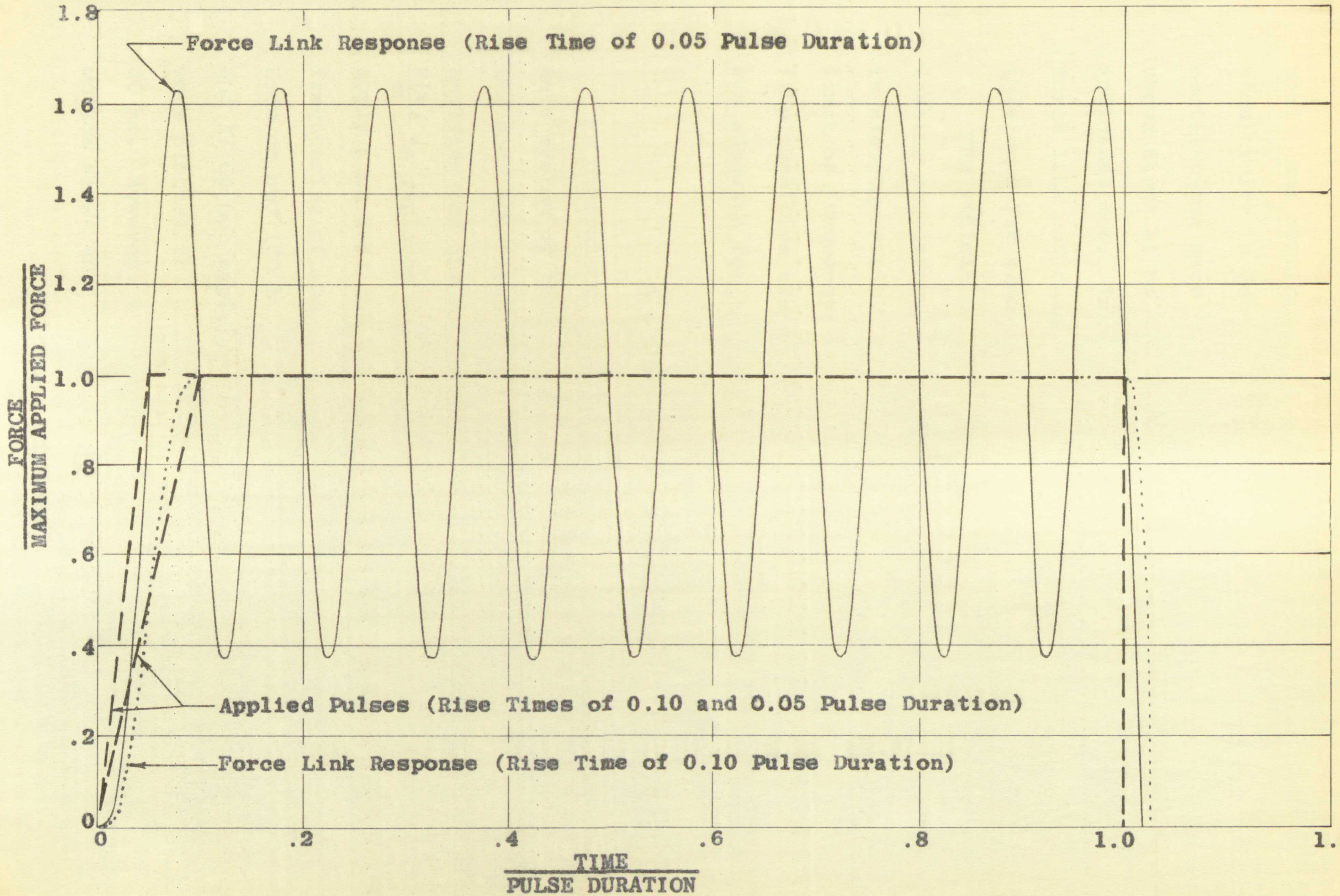

Figure 17. Force Link Response to an Approximate Rectangular Pulse. Pulse Duration is 10 Times Natural Period of Force Link.

Kroll, and confirmed by the data taken. When the accelerometer sensitivity is determined for an instant of time where the oscillations have been eliminated, the work of Levy and Knoll shows there is no difference between the applied pulse and the indicated one. In this case, no error would be introduced by force link response. It was possible to select a point of this type for almost all runs.

The vehicle position transducer was also used in establishing accelerometer sensitivities, so its frequency response is also important. Fitzgibbon (24) states that the upper limit of frequency response for the photomultiplier tube (the sensitive element of this transducer) is 10^8 cps, which was adequate for this test work.

Accelerometer Response

A piezoelectric accelerometer is composed of a spring mass system of the same form as the force link. This produces the same equations of motion (equations 18, 20, and 22) applying for the accelerometer as for the force link, if $\frac{F(t)}{m}$ is replaced by $y(t)$. Consequently the same solutions also apply when this substitution is made. However, the natural frequencies of the accelerometers tested were 70 kc for the Endevco and 100 kc for the CRL. Therefore, the Figures 15, 16, and 17 do not apply for the accelerometer response, since they were plotted for a transducer having a natural frequency of 10 kc. However, a study of the solutions to the equations of motion shows that as the ratio of natural period of transducer

[illegible]

[illegible]

applications [illegible]

shows [illegible]

[illegible]

[illegible]

this type for allowable [illegible]

The values of [illegible]

[illegible]

is also [illegible]

limits of [illegible]

the sensitive [illegible]

was adequate for [illegible] which [illegible]

A [illegible]

mass system of the [illegible]

the same equations of motion [illegible]

applying for the [illegible]

$\frac{F(t)}{m}$ is replaced [illegible]

apply when this [illegible]

frequencies of the [illegible]

[illegible]

and 17 do not apply [illegible]

were plotted [illegible]

loss. However, [illegible]

motion shows [illegible]

to period of transient is decreased, the displacement of the seismic mass is more nearly proportional to the applied transient. For this reason it was not necessary to replot the solutions for these different natural frequencies.

If it is assumed that the voltage output of the crystal in the accelerometer is proportional to the crystal compression for a transient, then the signal from the accelerometer could be found for any transient using the above method. The validation of this assumption for transients falling into a limited range of pulse durations is part of the purpose of the thesis, and is achieved by comparing the transient, as determined from the force link signal, with the accelerometer signal.

It was necessary to consider the effect of wave propagation in the vehicle on which the accelerometer was mounted, since it was not rigid. The nominal length of the assembled vehicles was 8 1/2", and the approximate wave velocity was 16,000 fps. This gave a traveling wave frequency of about 11,000 cps. For the pulses which were recorded at high sweep rates, it was possible to see this 11,000 cps wave of low amplitude superimposed on the main pulse waveform. Since this was due to the traveling wave in the vehicle, it was therefore neglected in the data reduction by using the average of the high frequency wave for the rigid body acceleration pulse for the vehicle.

[illegible] the [illegible] of [illegible] of the frequency of [illegible] [illegible] have been [illegible] of the applied signal. For this reason it was not necessary to separate the solutions for these different natural frequencies.

If it is assumed that the [illegible] at the [illegible] [illegible] proportional to the [illegible] signal [illegible], that the signal [illegible] could be found for [illegible] pulse period. The validity of this assumption for [illegible] (ref. [illegible]) limited range of pulse durations is part of the purpose of the tests, and is verified by comparing the transient, as computed from the force time signal, with the accelerometer signal.

It is necessary to consider the effect of wave [illegible] in the vehicle [illegible] [illegible] since it was not [illegible] the overall length of the assembled vehicles was [illegible] and the approximate wave velocity was 16,000 fps. This gave a predicted wave frequency of about 11,000 cps. When the pulses which were recorded at high sweep rates, it was possible to see this 11,000 cps wave of low amplitude superimposed on the main pulse waveform. Since this was due to the traveling wave in the vehicle, it was therefore neglected in the data reduction by using the average of the high frequency wave for the rigid body acceleration data for the vehicle.

Methods of Computing Sensitivity

Two methods for determining the accelerometer sensitivity have been discussed. One of these methods was based on the kinematics of the motion, and the other was based on the kinetics of the motion.

The former method was discussed in detail earlier, and equation 3 (page 30) was derived for applying this method. The result of solving this equation using the quantities defined is A, the acceleration scale in inches per sec.^{2} per inch on the drawing. This quantity may then be converted to S_c, the accelerometer sensitivity in mv/G (for the external capacitance existing for that run) using the equation:

$$S_c = \frac{386U}{AR}$$

where: R = the ratio of inches on the enlargement of the acceleration pulse to centimeters on the oscilloscope grid.
U = the gain of the oscilloscope in millivolts/centimeter.

When this equation is put in a form involving only quantities determined in the test work, the result is

$$S_c = \frac{386\ U\ T \int_{x_i}^{x_f} y(x)dx}{(V_f - V_i)\ R} \quad . \qquad (25)$$

The method for computing the sensitivity based on the

kinetics of the motion has not been previously developed, since the apparatus and the procedure had not been adequately described. The equations for this computation will now be derived. The sensitivity at any instant of time, t_1, is the voltage output from the accelerometer at that instant, divided by the acceleration in G's. This may be expressed as follows:

$$S_c = \frac{32.2 y_1 UM}{F(t_1)} = \frac{y_1 UW}{F(t_1)} \qquad (26)$$

In equation 26, y_1 is the height of the accelerometer trace in centimeters at time t_1, U is the oscilloscope gain in millivolts/centimeters, and W is the vehicle weight in pounds.

Before this equation may be solved, $F(t_1)$ must be found from the strain gage signal. It is assumed that the signal from the gages is proportional to the average strain in the gaged section. When this assumption is made, the force may be found from the following equation:

$F(t_1) = sy_2$, where s = the strain gage circuit sensitivity in lbs/cm.
y_2 = the height of the force link trace at time t_1, in cm.

In the above equation, s is found by multiplying the equation 16 by the gain of the oscilloscope, U. When this is done, and $F(t_1)$ substituted into equation 25, the equation for finding the accelerometer sensitivity using the force link data becomes

$$S_c = \frac{W y_1 UF(R_c + R_g) y}{y_2 NR_g EA} \qquad (27)$$

In equations 25 and 27, the accelerometer sensitivity found is that for the external capacitance in the accelerometer circuit for that particular run. Before this can be compared with the manufacturer's sensitivity, it must be converted to a value based on the same external capacitance as the manufacturer's sensitivity.

The Endevco Corporation specifies sensitivities of their accelerometer for 100 uufd external capacitance. The following equation from the Endevco instruction manual was used for determining the sensitivity for 100 uufd external capacitance S, when the sensitivity for some other external capacitance is known:

$$S = \frac{Sc(C_p + C_c + C_i)}{C_p + 100} \qquad (28)$$

where C_p = crystal capacitance, uufd.

C_c = the cable capacitance used, uufd.

C_i = cathode follower input capacitance, uufd.

100 = the total external capacitance which the manufacturer used when determining the sensitivity, uufd.

The CRL accelerometer has a manufacturer's sensitivity specified when used with a 170 uufd cable. To compute the sensitivities from this work on this basis, the following equation was derived:

$$S = \frac{S_c(C_p + C_c + C_i)}{C_p + 170 + C_i}\ . \qquad (29)$$

The CRL cathode followers used had a gain of 0.98. Because the instruction manual indicated that this gain was neglected for the CRL accelerometer, it was neglected for this work also. However, it was considered in computing the Endevco sensitivity.

Estimate of Error

The estimate of error for each of the methods for determining the accelerometer sensitivity was made to gain knowledge of the accuracy of the experimental work and to compare the two methods.

The estimate of error for the method using kinematic relationships may be made by putting equation 25 into a form which involves only measured quantities. To do this, $V_f - V_i$ is expressed in quantities taken as data, or measured from the recorded vehicle position indicator signal. This equation is

$$V_f - V_i = 0 - \left(\frac{\Delta Y}{\Delta X}\right)\frac{f}{Th}, \tag{30}$$

where $\frac{\Delta Y}{\Delta X}$ is the slope of the recorded signal before impact, f is the flag width, and h is the distance on the recorded trace which represents the flag width. When equation 30 is substituted into equation 25, the result is

$$S_c = \frac{386\ U\ \Delta Xh \int ydx\ T^2}{f\Delta YR} \tag{31}$$

An expression for the error in S_c is obtained by taking the derivative of the above equation. The variables (U, ΔX, h, $\int ydx$, T^2, ΔY, and R) will be represented by the capital letters A,B,C,D,E,F, and G, and the constants (386 and f) by K, or

The [illegible] in θ were [illegible] and [illegible]

the [illegible]

for the [illegible]. It was [illegible]

however, it was considered in computing the [illegible]

Sources of Error

The magnitude of error for each of the methods [illegible] mining the [illegible], [illegible] was made to gain knowledge of the accuracy of the experimental work and to compare the two methods.

The estimate of error for the [illegible] using [illegible] relationships may be made by [illegible] which [illegible]. To [illegible] is expressed in [illegible] procedure, [illegible] position [illegible] signal. This [illegible]

$$[illegible] \qquad (11)$$

where ν_1 is the [illegible] of the recorded signal before [illegible], ϵ is the line width, and h is the distance on the recorder trace which represents the line width. When equation (1) is substituted into equation (11) the result is

$$[illegible]$$

An expression for the [illegible] in R_1 [illegible] derivative of the above equation. The [illegible] will be [illegible] A,B,C,D,E,F, and G, and the [illegible]

$$S_c = \frac{KABCDE^2}{FG} \quad . \tag{32}$$

The derivative of this expression is

$$dS_c = \frac{K}{FG}\left[(dA)BCDE^2 + A(dB)CDE^2 + AB(dC)DE^2 + ABC(dD)E^2 + 2ABCDE(dE)\right] \pm KABCDE^2\left[\frac{dF}{F^2G} + \frac{dG}{G^2F}\right] \tag{33}$$

The maximum and minimum expected error in S_c may be evaluated from this expression by estimating the error in each of the measured quantities in equation 31. The quantity dA can be expressed as Aa, where a is the percent error in measurement A. Similar expressions may be written for dB, dC, dD, dE, dF, and dG, and all of these substituted into equation 33. The result is

$$dS_c = \frac{KABCDE^2}{FG}\,(a+b+c+d+2e\pm f\pm g). \tag{34}$$

This shows that the expected error for any one run may be found as the sum of the percentage errors in the measurement of quantities not squared, plus twice the percentage error of the squared quantity.

The possible error in each of the required measurements is as follows:

U, the oscilloscope gain: $\pm$ 3%
R, the scale of enlargement for the acceleration trace: $\pm$ 2%
$\int ydx$, area under the oscilloscope trace: $\pm$ 4% or $\pm$ 6%
Δ X, vertical measurement on trace: $\pm$ 1% or $\pm$ 3%
h, vertical measurement on trace, $\pm$ 1%
T, the time scale on the acceleration trace: $\pm$ 1% or $\pm$ 5%.
ΔY, horizontal measurement on trace: $\pm$ 1% or $\pm$ 2%

These estimations of the accuracy of each measurement would result in the possible error being $\pm$ 14% under good

conditions, an as great as $\pm$ 27% under poor conditions.

The above estimates of the error in each of the above terms will now be explained.

The oscilloscope gain is the accuracy stated in the instruction manual. It was not felt that the checks made on these gains resulted in any improvement.

The error in R is the human error introduced when the enlargement is made in the oscilloscope record.

In determining the area under the oscilloscope trace to zero velocity, there are two sources of error. One of these is the human error in determining the true area. This human error is introduced by interpretation of the center of the wide oscilloscope trace and use of the trapezoidal rule. The other source of error is due to the location of the point on the trace that corresponds to the instant of zero velocity. The point of zero slope on the displacement time curve is the point of zero velocity. It is estimated that this point is located within $\pm$ 2%. The percent error this causes in area is dependent on the pulse shape. It would result in a $\pm$ 2% error for the rectangular pulse, and a $\pm$ 4% error for the sawtooth. The effect on the half sine pulse is between these values.

The quantities ΔX, ΔY, and h were measured from the oscilloscope trace, and the percent error is dependent on the length measured. The values of ΔX varied from 1 to 2.5 cm. The values of ΔY varied from 1.5 to 3 cm. The values of h were always greater than 2.5 cm. An estimated maximum

reading error of 0.03 cm was used in computing the percentage error.

The error in the time scale on the acceleration trace is based on the sweep rate accuracy of the oscilloscopes. The instruction manual states that the sweep rate is accurate to $\pm$ 1%, or $\pm$ 5% if expanded sweep is used.

The estimate of error for the method using the kinetic relationships was made from equation 27. An analysis of this equation similar to that on page 88 will show the percentage error in the computed sensitivity to be the sum of the percentage error in each term of the equation. Since there are no squared quantities in equation 27, no quantity has its error doubled in the expression for sensitivity error.

The terms in equation 27 were divided into two classifications: those for which the error is fixed for a series of runs, and those for which the error might vary. The quantities for which the error is fixed, and their possible error are as follows:

Gage Factor, F: $\pm$ 2 %
Force Link Area, A: negligible
Modulus of Elasticity, E: $\pm$ 3 %
Gage Resistance, R_g: $\pm$ 0.6 %

The error in the results due to these quantities is not considered of importance, since it is fixed for one force link. Calibration of the force link under accurately known static loading could reduce it to a negligible amount.

The quantities for which the error will vary, and their contribution to the total error are as follows:

R_c, calibrate resistor: $\pm$ 1%

W, vehicle weight: negligible, to $\pm$ 1/2 %

y_1, y_2, y_3, oscilloscope trace heights: $\pm$ 1% to $\pm$ 3%

U, oscilloscope gain: $\pm$ 3%

This would result in a total variable error of $\pm$ 5% under good conditions, and $\pm$ 7 1/2% maximum.

The above estimates of error were made from the following considerations. Precision resistors were used for the calibrate resistors, and they had a specified tolerance of 1%. The scales used in weighing the vehicles read to the nearest 1/8 ounce, and the vehicle weights were from 1.4 to 21 pounds. For the error due to the oscilloscope trace heights, the reading error was estimated at 0.03 cm, and the minimum trace deflection was 1 cm, and the maximum was 4 cm.

A comparison of the two methods for determining the accelerometer sensitivity shows that the force link method would have a smaller error. This fact was substantiated by reducing some of the data and plotting. The results from the data reduced using the force link method had considerably less scatter than the results from the same data reduced using the other method.

[illegible]

4. Oscilloscope sweep - 5%

This would result in a total variation of ±6% or ±[illegible] under good conditions, and ± [illegible] [illegible] [illegible] operation.

The errors associated with the force [illegible] [illegible] [illegible] considerations. [illegible] [illegible] were used for the [illegible] [illegible] [illegible], and they had a specified tolerance of [illegible]. The [illegible] used in [illegible] the vehicle [illegible] to the [illegible] [illegible] [illegible], and the vehicle weights were from 1.5 to [illegible] pounds. For the error due to [illegible] [illegible] being [illegible], the resulting error was estimated at [illegible] cm, and the [illegible] [illegible] [illegible] was [illegible] and the [illegible] [illegible] [illegible] cm.

A comparison of the two methods for determining the accelerometer sensitivity shows that the force link method would have a smaller error. This fact was substantiated by reducing some of the data and plotting. The results from the data reduced using the force link method had considerably less scatter than the results from the same data reduced using the other method.

RESULTS

The results of the tests conducted are shown in Tables III, IV, and V, and Figures 18 thru 23. The results shown here are not those from all of the tests conducted. Numerous tests were conducted for the purpose of determining the cushion to give the desired pulse. This was particularly true for the sawtooth. Data from other tests were not satisfactory because of excessive zero shift, ringing, hum on the signals, and improper oscilloscope settings. Occasionally one of the accelerometer cables would open during the transient and make the data useless. This occurred almost exclusively on the CRL accelerometer, and was believed due to the top mount of the cable on the accelerometer case making it more difficult to secure the cable adequately.

The results shown here are from selected data free of undesirable characteristics such as those mentioned above. In addition, good agreement between the desired pulse and the one obtained was required.

To illustrate the pulses obtained for each of the desired shapes, typical data are shown in Figures 24, 25, and 26. The filtered accelerometer signal on this data is readily recognized by the abscence of ringing. The filtered signal was not used in these results. Several runs were reduced using the filtered and the unfiltered signal, but this served only to verify the statements regarding filters in the previously cited reference (8).

When the ringing was severe, additional runs were made with precautions taken to reduce the ringing. Then, y_2 was measured to the center of the envelope described by the ringing. The accuracy of results from data of this type was reduced. However, better consistency was obtained by using this procedure than by using the filtered signal.

Table III, Results for Half Sine Pulse

Run[1]	Period	Force Transducer			Endevco[4]	Sens.	Error	C R L	Sens.[4]	Error
	ms[2]	y[3]	y_1[3]	G	y_2[3]	mv/G	% [5]	y_2[3]	mv/G	% [5]
7,7-26	1.4	2.15	2.20	143	2.60	13.4	8	3.30	7.2	8
4,8-30	1.0	2.57	2.55	258	2.20	12.4	8	2.50	7.5	8
5.7-27	1.2	2.44	2.75	312	2.95	13.7	7	3.10	7.8	7
5,7-27	1.2	2.44	2.75	312	2.85	13.4	7	3.00	7.5	7
3,7-27	1.0	.93	2.55	762	3.40	13.1	9	1.85	7.6	10
4,7-27	1.0	2.40	1.85	2145	2.10	14.4	8	1.00	7.4	10
4,7-27	1.0	2.40	1.90	2200	2.10	14.1	8	1.00	7.1	10
1,7-27	2.0	3.32	2.60	109	1.90	12.9	8	2.42	6.9	7
1,7-27	2.0	3.32	2.42	101	1.85	13.5	8	2.20	6.8	8
6,7-27	2.4	2.04	2.85	389	1.78	13.5	8	1.84	7.4	8
6,7-27	2.4	2.04	2.80	382	1.70	13.3	8	1.75	7.2	8
7,7-27	2.1	1.20	3.10	719	3.26	12.3	8	1.80	7.8	9
8,7-27	2.1	3.78	2.60	956	1.62	12.5	8	2.20	7.2	7
8,7-27	2.1	3.78	2.80	1030	1.77	12.8	8	2.40	7.2	7
5,7-26	4.4	3.32	1.21	51	2.19	12.7	9	1.90	5.8	9
5,7-26	4.4	3.32	1.18	49	2.00	12.0	9	1.97	6.3	9
2,7-26	4.4	3.33	2.35	98	3.80	11.4	7	2.20	7.0	8
3,8-3	4.4	3.27	2.23	176	3.41	12.1	7	2.20	7.3	8
2,8-3	4.0	1.60	3.17	514	2.50	12.1	8	1.70	7.8	9
2,8-3	4.0	1.60	3.12	505	2.50	12.3	8	1.70	7.9	9
4,7-26	3.5	3.28	1.87	793	2.80	10.4	8	1.75	6.9	8
4,7-26	3.5	3.28	1.64	695	2.40	10.2	8	1.51	6.8	9
9,7-27	8.8	3.35	3.64	56	2.57	13.6	7	2.50	7.0	7
9,7-27	8.8	3.35	3.29	50	2.42	14.1	7	2.30	7.1	7
10,7-27	8.0	2.20	2.98	139	2.40	12.8	8	2.50	7.0	8
10,7-27	8.0	2.20	2.80	130	2.35	13.3	8	2.30	7.1	8
11,7-27	8.8	.85	1.51	182	1.69	13.7	11	1.42	6.1	12
11,7-27	8.8	.85	1.43	172	1.60	13.7	11	1.38	6.3	12
12,7-27	8.8	.85	3.25	319	2.88	13.3	9	1.88	9.2	10
12,7-27	8.8	.85	3.10	304	2.82	13.7	10	1.79	9.2	10
3,9-8	16.0	3.55	2.94	24	2.13	13.0	7	1.33	8.6	8
3,9-8	16.0	3.55	2.89	23	2.03	12.7	7	1.25	8.2	8
1,8-1	16.4	2.22	3.29	42	2.00	13.8	8	2.03	7.5	8
2,9-8	16.4	2.98	2.53	49	2.17	13.0	8	2.60	8.2	7
1,9-8	15.2	2.90	2.35	116	1.98	13.6	8	3.33	8.8	7
1,7-28	15.2	3.28	2.75	120	2.27	13.9	7	3.51	9.2	7
4,9-8	35.0	3.36	2.66	14	1.29	13.4	8	1.51	8.3	8
4,9-8	35.0	3.36	2.84	15	1.30	13.2	8	1.63	8.4	8

[1] The run number is a means of identifying the results with the data used in obtaining them. Where runs have the same number, they were recorded on the same frame of film.

[2] The period is the time from contact to maximum acceleration.

[3] These symbols are defined on page 84.

[4] The sensitivities shown are those determined for that run, and apply when the accelerometer is used with the same external capacitance for which the manufacturer's sensitivity is specified.

[5] The percent error specified here represents the maximum expected error for that run.

Table IV. Results for Sawtooth Pulse

Run[1]	Period	Force Transducer			Endevco			C R L		
	ms[2]	y[3]	y_1[3]	G	y_2[3]	Sens.[4] mv/G	Error %[5]	y_2[3]	Sens.[4] mv/G	Error %[5]
5,8-11	1.0	2.05	3.05	194	1.70	12.7	8	1.65	6.5	8
1,8-23	1.0	2.60	1.30	553	2.46	12.9	9	2.40	6.7	9
2,8-23	1.0	2.60	1.40	595	2.62	12.8	8	2.82	7.3	8
4,8-31	.9	3.00	2.80	1030	1.95	13.7	8	2.28	6.8	7
4,8-31	1.0	3.00	2.44	899	1.68	13.6	8	2.04	7.0	8
7,8-15	1.0	1.60	2.02	1400	2.60	13.5	9	1.40	7.7	9
1,8-31	1.0	1.50	1.90	1400	2.65	13.7	9	1.39	7.6	10
4,8-11	1.9	2.00	3.24	102	2.00	14.2	8	2.59	7.8	8
3,8-11	1.8	2.04	2.99	185	1.71	13.4	8	1.82	7.6	8
3,8-11	2.0	2.75	1.82	177	1.72	14.2	8	1.72	7.5	8
2,8-15	2.2	3.00	1.52	339	1.52	13.0	8	1.62	7.3	8
3,8-18	1.6	3.20	2.40	505	2.38	13.7	7	2.48	7.5	7
1,8-15	2.0	2.38	2.14	602	1.15	13.8	9	1.49	7.6	9
5,8-17	1.8	2.40	2.50	696	1.30	13.6	9	1.69	7.4	8
4,8-12	3.6	2.88	1.18	53	2.29	12.7	9	2.13	6.2	9
2,9-6	3.6	2.92	1.04	46	2.10	13.3	9	2.21	7.4	9
1,8-5	3.0	1.95	3.00	120	2.34	14.2	8	1.20	7.6	9
1,8-5	3.4	1.95	2.83	113	2.23	14.3	8	2.70	7.3	8
2,8-5	3.0	2.40	2.90	235	2.28	14.1	8	2.40	7.8	8
2,8-5	3.5	2.40	2.71	220	2.03	13.4	8	2.10	7.3	8
2,8-10	4.5	2.00	2.90	340	1.62	13.8	8	1.68	7.6	8
5,8-12	4.0	2.09	2.30	337	1.60	13.9	9	1.74	8.0	8
1,9-7	8.0	2.62	1.50	45	2.07	13.5	9	2.12	7.3	9
3,8-19	8.2	1.90	2.02	80	1.55	14.2	9	2.12	8.1	8
4,8-19	7.9	1.88	2.10	84	1.63	14.2	9	2.20	8.0	8
2,8-19	7.0	2.79	2.76	186	1.82	14.2	8	1.85	7.7	8

[1] The run number is a means of identifying the results with the data used in obtaining them. Where runs have the same number, they were recorded on the same frame of film.

[2] The period is the time from contact to maximum acceleration.

[3] These symbols are defined on page 84.

[4] The sensitivities shown are those determined for that run, and apply when the accelerometer is used with the same external capacitance for which the manufacturer's sensitivity is specified.

[5] The percent error specified here represents the maximum expected error for that run.

Table V. Results for Rectangular Pulse

Run[1]	Period	Force Transducer			Endevco[4]			C R L[4]		
	ms[2]	y^3	$y_1{}^3$	G	$y_2{}^3$	Sens. mv/G	Error % [5]	$y_2{}^3$	Sens. mv/G	Error % [5]
3,8-2	1.0	3.28	1.44	138	3.13	14.1	8	1.84	8.2	9
3,8-2	.9	3.28	1.39	134	3.03	14.1	8	1.78	7.8	9
6,8-4	1.0	3.44	1.82	268	2.39	13.0	8	1.21	6.9	9
6,8-4	1.2	3.44	1.53	225	1.99	12.9	8	1.01	6.9	10
4,8-3	1.2	2.72	2.82	538	2.78	12.9	7	1.50	6.5	8
4,8-3	1.2	2.72	2.89	550	3.02	13.7	7	1.45	6.2	8
7,8-3	1.0	2.98	2.77	1205	2.19	13.3	7	--	--	--
2,8-2	2.3	1.52	2.65	53	2.81	13.2	8	1.90	8.4	9
2,8-2	1.9	1.52	3.15	63	3.50	13.9	8	--	--	--
4,8-2	2.2	1.07	1.99	117	--	--	--	1.60	8.0	10
4,8-2	1.9	1.07	2.05	121	2.60	13.4	9	1.76	8.5	10
5,8-4	2.0	3.50	1.58	228	2.04	13.0	8	1.05	7.1	10
5,8-4	1.8	3.50	1.79	259	2.30	12.9	8	1.10	6.2	9
5,8-3	1.8	2.70	2.65	509	2.40	13.7	8	1.29	7.8	10
5,8-3	2.0	2.70	2.65	509	2.30	13.1	8	1.20	7.2	10
5,8-1	3.8	1.57	3.25	63	3.00	14.0	8	--	--	--
1,8-2	3.8	1.52	3.21	60	3.21	13.2	8	2.32	9.0	8
5,8-2	3.6	1.07	1.82	107	2.40	13.9	10	1.38	7.5	11
5,8-2	4.2	1.07	1.80	106	2.50	14.7	10	3.40	7.5	9
8,8-3	5.0	2.43	1.08	225	2.04	13.2	10	1.00	6.8	11
3,8-4	3.2	3.50	2.02	294	2.85	12.9	7	1.35	7.0	9
4,8-1	8.2	1.55	3.29	61	2.73	13.2	8	--	--	--
7,8-1	9.0	1.56	2.65	49	2.65	13.6	8	2.04	9.8	9
6,8-2	8.6	1.08	2.13	110	2.10	13.8	10	1.24	8.7	11
7,8-4	7.0	2.11	2.30	122	2.30	13.7	8	--	--	--

[1] The run number is a means of identifying the results with the data used in obtaining them. Where runs have the same number, they were recorded on the same frame of film.

[2] The period is the time from contact to end of constant acceleration.

[3] These symbols are defined on page 84.

[4] The sensitivities shown are those determined for that run, and apply when the accelerometer is used with the same external capacitance for which the manufacturer's sensitivity is specified.

[5] The percent error specified here represents the maximum expected error for that run.

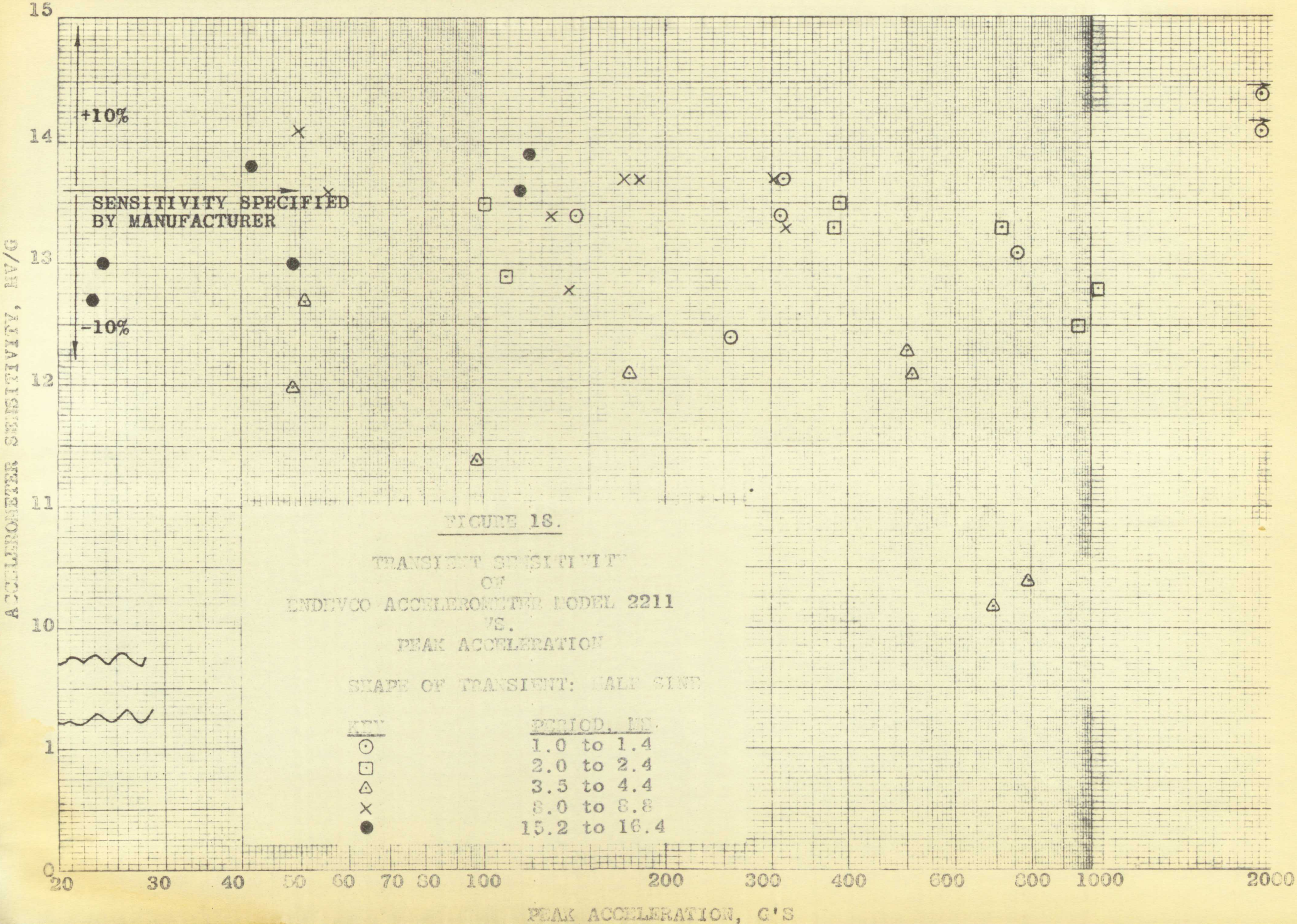

FIGURE 18.

TRANSIENT SENSITIVITY
OF
ENDEVCO ACCELEROMETER MODEL 2211
VS.
PEAK ACCELERATION

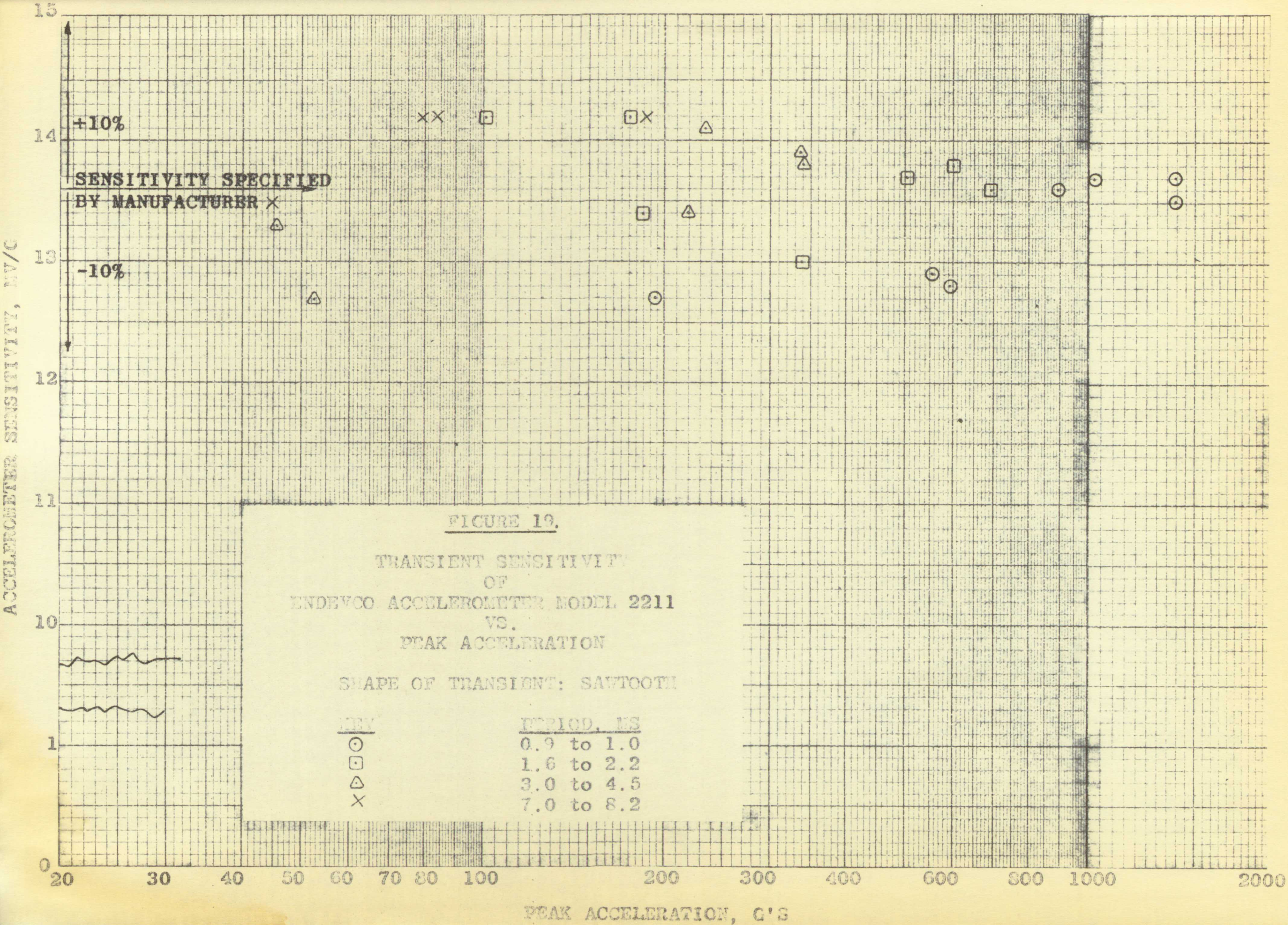

FIGURE 19.

TRANSIENT SENSITIVITY
OF
ENDEVCO ACCELEROMETER MODEL 2211
VS.
PEAK ACCELERATION

SHAPE OF TRANSIENT: SAWTOOTH

KEY	PERIOD, MS
⊙	0.9 to 1.0
⊡	1.6 to 2.2
△	3.0 to 4.5
×	7.0 to 8.2

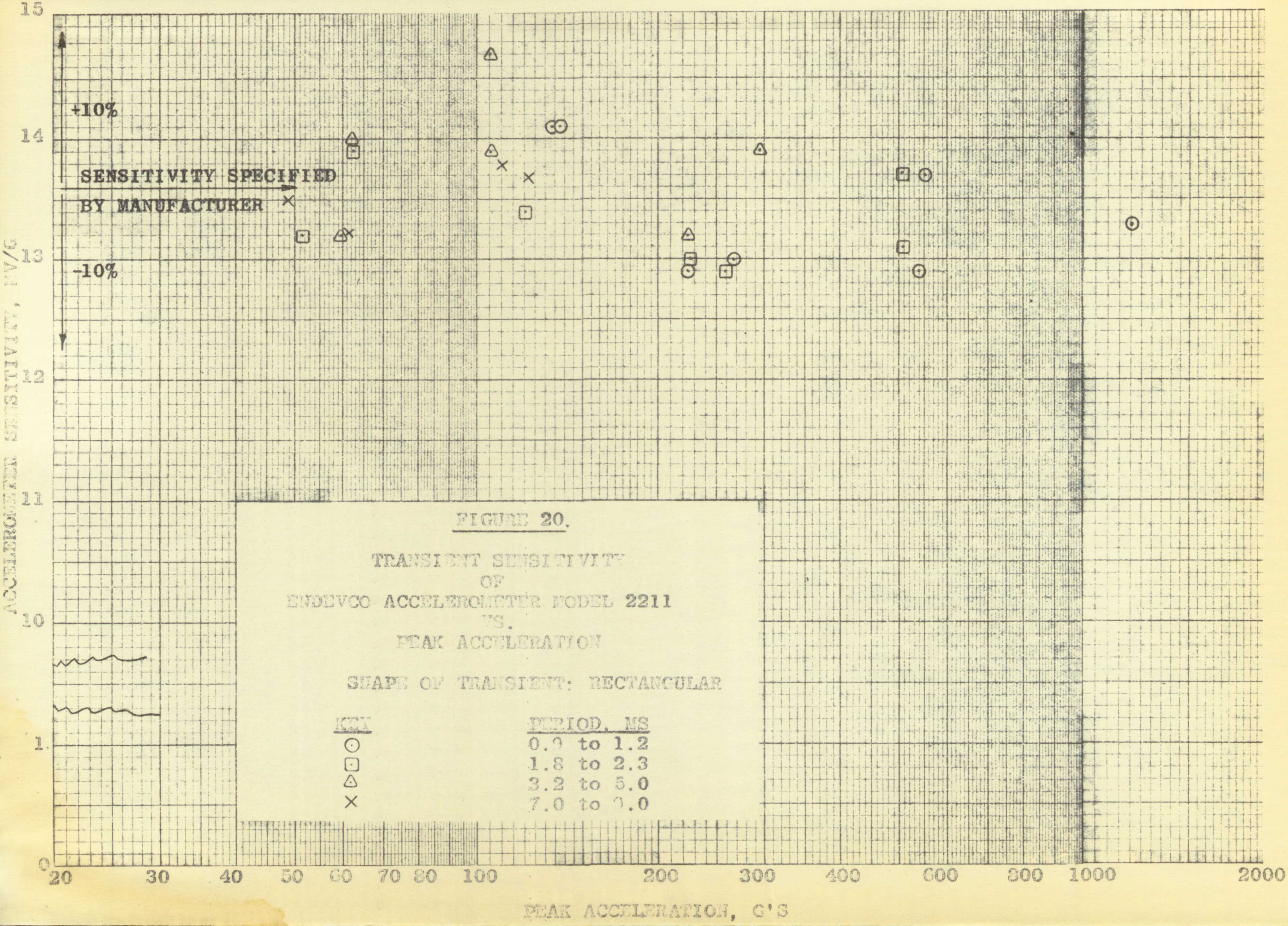

FIGURE 20.

TRANSIENT SENSITIVITY
OF
ENDEVCO ACCELEROMETER MODEL 2211
VS.
PEAK ACCELERATION

SHAPE OF TRANSIENT: RECTANGULAR

KEY	PERIOD, MS
⊙	0.9 to 1.2
⊡	1.8 to 2.3
△	3.2 to 5.0
×	7.0 to 9.0

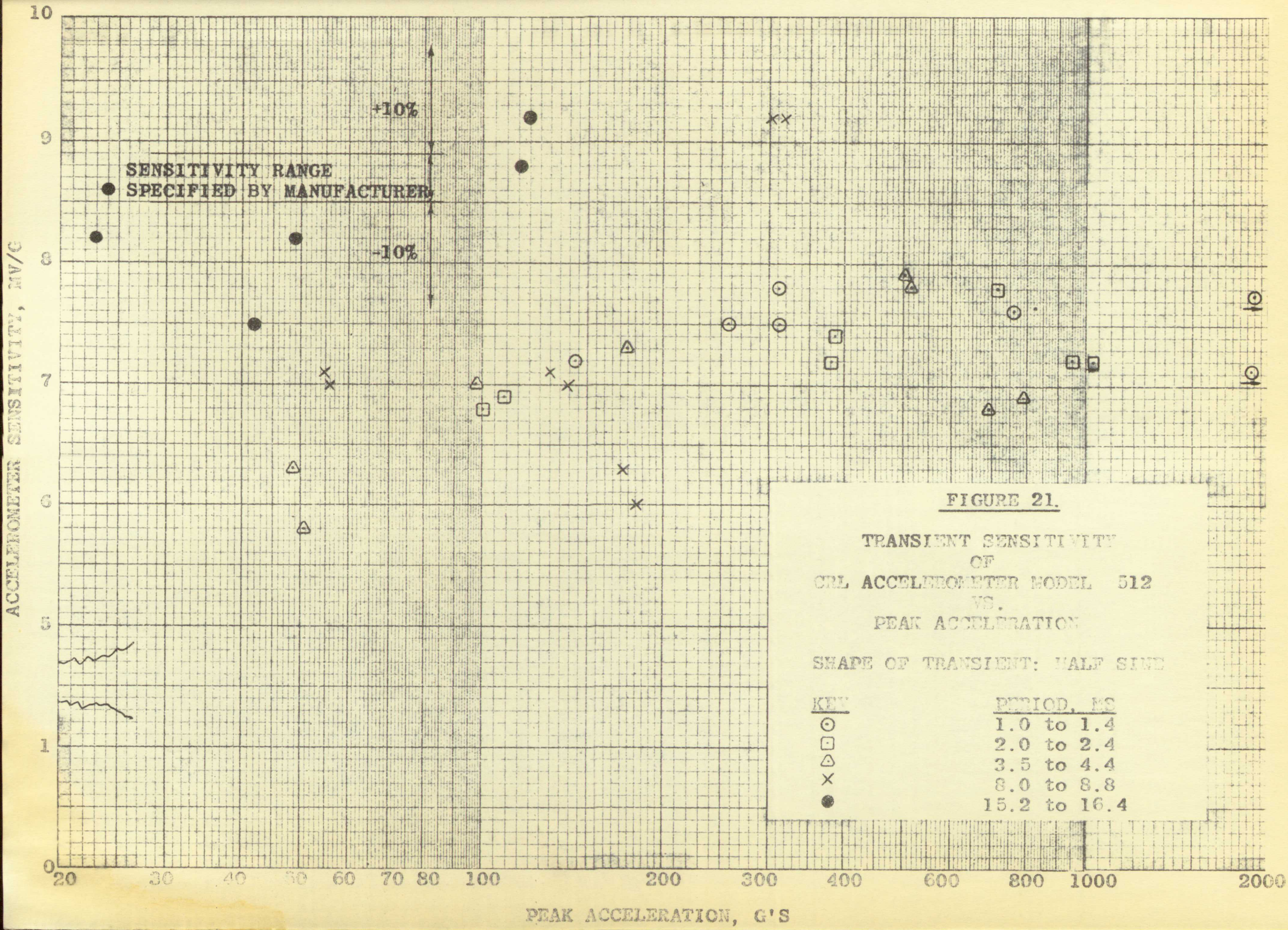

FIGURE 21.

TRANSIENT SENSITIVITY OF CRL ACCELEROMETER MODEL 512 VS. PEAK ACCELERATION

SHAPE OF TRANSIENT: HALF SINE

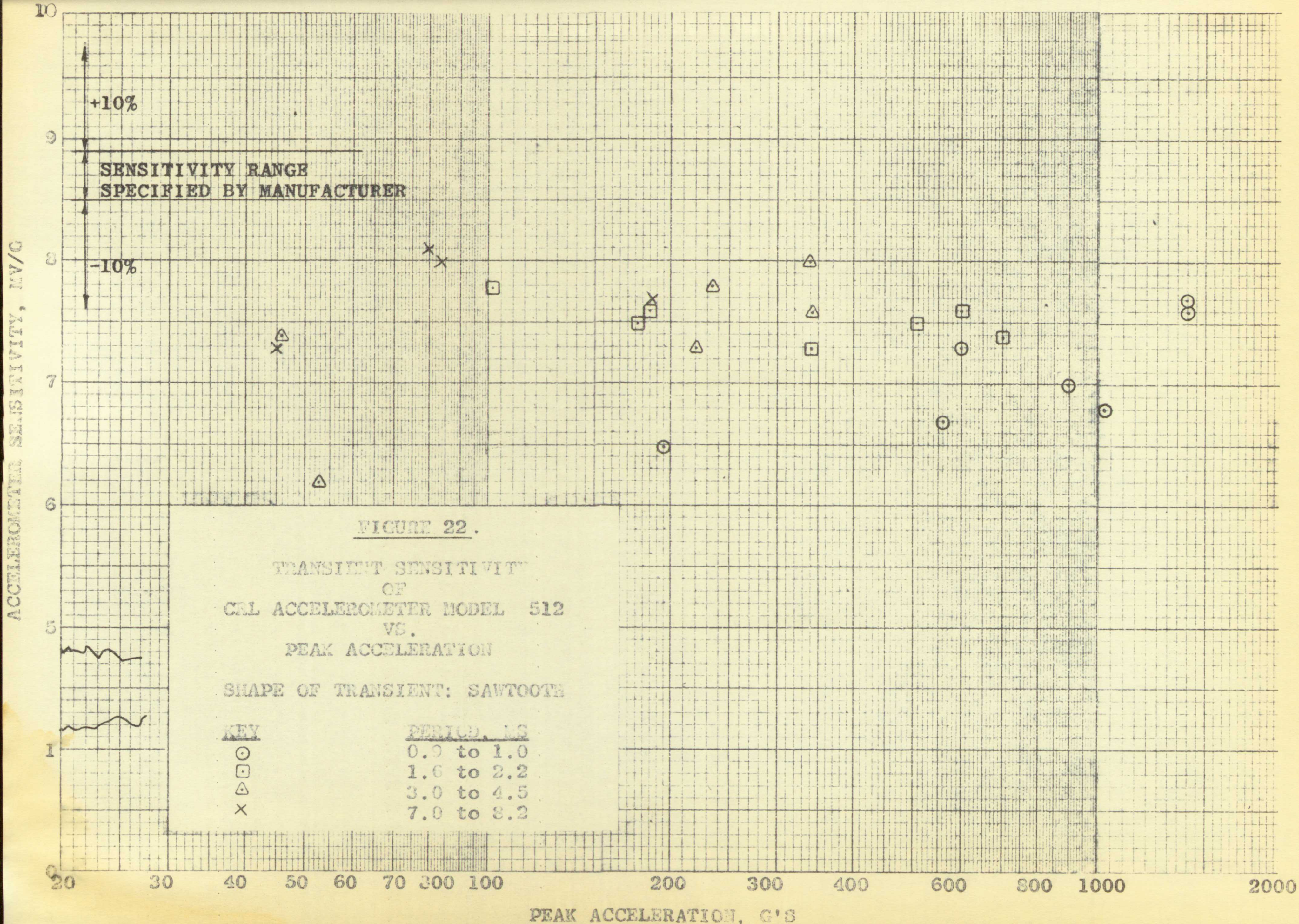

FIGURE 22.

TRANSIENT SENSITIVITY
OF
CRL ACCELEROMETER MODEL 512
VS.
PEAK ACCELERATION

SHAPE OF TRANSIENT: SAWTOOTH

KEY	PERIOD, MS
⊙	0.9 to 1.0
⊡	1.6 to 2.2
△	3.0 to 4.5
×	7.0 to 8.2

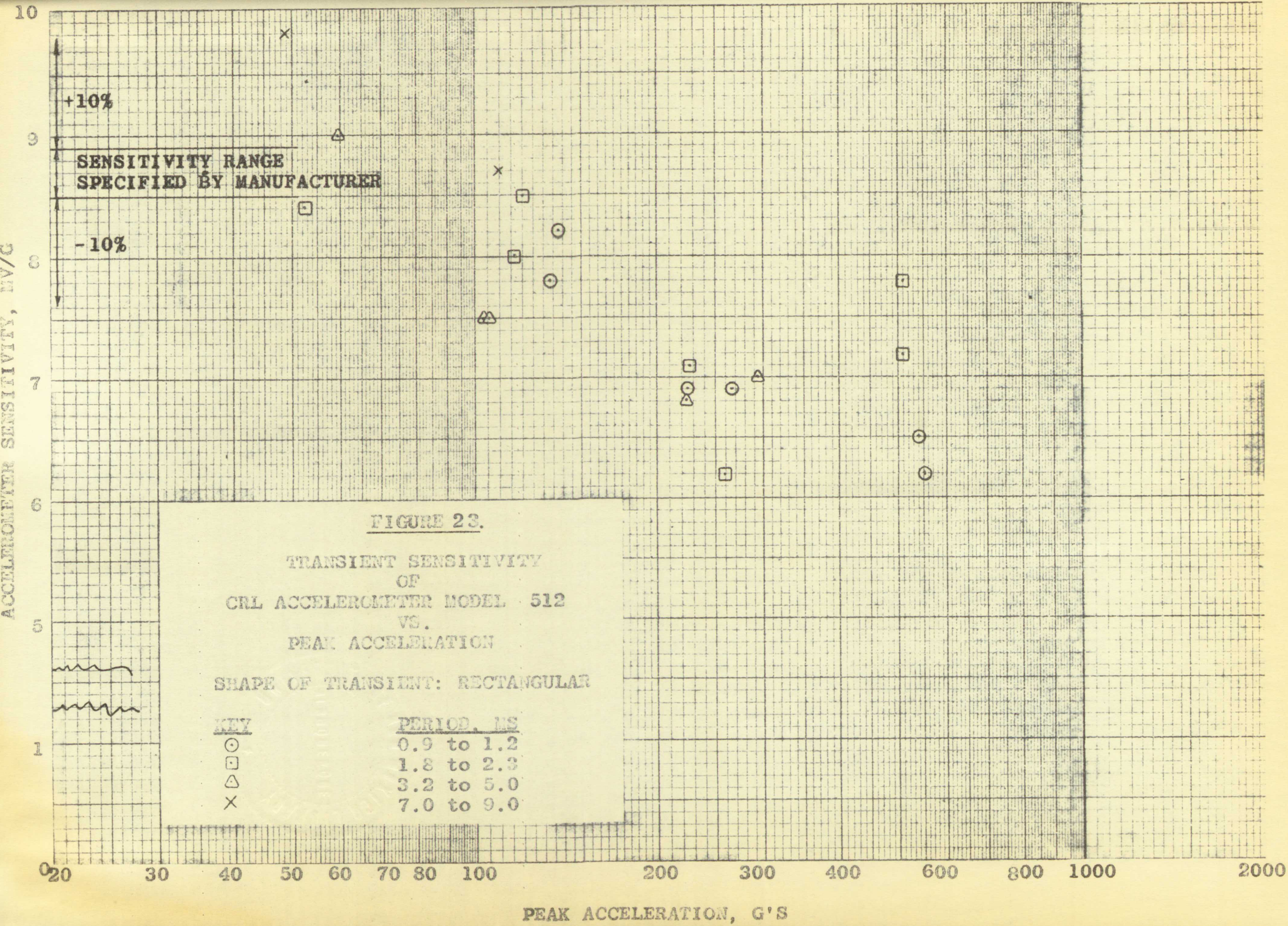

FIGURE 23.

TRANSIENT SENSITIVITY
OF
CRL ACCELEROMETER MODEL 512
VS.
PEAK ACCELERATION

SHAPE OF TRANSIENT: RECTANGULAR

KEY	PERIOD, MS
⊙	0.9 to 1.2
⊡	1.8 to 2.3
△	3.2 to 5.0
×	7.0 to 9.0

TEST DATA

Run 9, 7-27-60 Pulse half sine , 8 ms, 50 G

Drop height 5.0 in. Theo. impact vel. 62 ips

Vehicle weight 3.750 lbs. Flag width 0.25 in.

Endevco 2211	CRL 512
Tektronic 551, no. 001570	Tektronic 551, no. 756
Cathode follower Brown	Cathode follower Gray
Cable capacitance 386 uuf	Cable capacitance 385 uuf
Sweep rate 2 msec/cm	Sweep rate 2 msec/cm
Gain 2u 200 3F 200 mv/cm	Gain 1u 100 2F 100 mv/cm

Filter cutoff frequency 5000 cps

Force Link (On oscilloscope with CRL)

Material alum. Calibrate resistance 10 meg ohms

Oscilloscope gain 1 mv/cm

Note: The numbers in the "Gain" blank represent the trace number counting downward. The filtered and unfiltered signals are represented by u and F respectively. Trace 1 on oscilloscope 001570 is the vehicle position indicator.
The sweep is from left to right in the pictures.

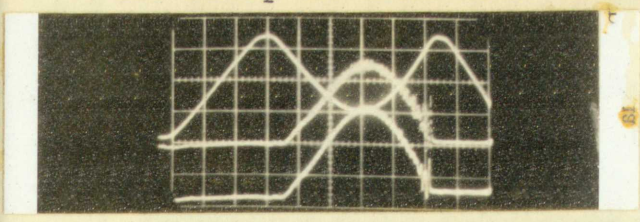

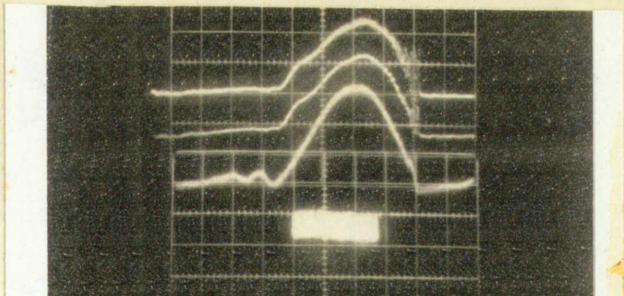

Figure 24. Typical Data for the Half Sine Pulse

TEST DATA

Run 1, 8-23-60 Desired pulse sawtooth, 1 ms 500 G

Drop height 13.5 in. Theo. impact vel. 102 ips

Vehicle weight 1.473 lbs. Flag width .25 In.

Endevco 2211	CRL 512
Tektronic 551, no. 001570	Tektronic 551, no. 756
Cathode follower Brown	Cathode follower Gray
Cable capacitance 373 uuf	Cable capacitance 374 uuf
Sweep rate 0.4 msec/cm	Sweep rate 0.4 msec/cm
Gain 2u 2000 3F 2000 mv/cm	Gain 2u 1000 1F 1000 mv/cm

Filter cutoff frequency 3000 cps

Force Link (On oscilloscope with CRL)

Material steel Calibrate resistance 25 meg ohms

Oscilloscope gain max

Note: The numbers in the "Gain" blank represent the trace number counting downward. The filtered and unfiltered signals are represented by u and F respectively. Trace 1 on oscilloscope 001570 is the vehicle position indicator.

The sweep is from left to right in the pictures

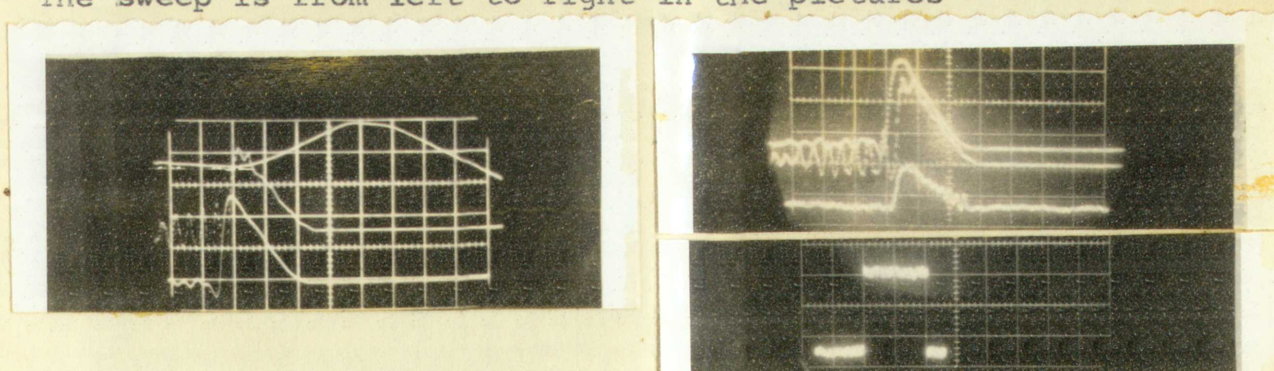

Figure 25. Typical Data for the Sawtooth Pulse

TEST DATA

Run 4,8-26-60 Pulse Rect., 2 ms, 100 G

Drop height $7\frac{13}{16}$ in. Theo. impact vel. 80.4 ips

Vehicle weight 6.091 lbs. Flag width .25 in.

Endevco 2211	CRL 512
Tektronic 551, no. 001570	Tektronic 551, no. 756
Cathode follower Brown	Cathode follower Gray
Cable capacitance 235 uuf	Cable capacitance 235 uuf
Sweep rate 0.4 msec/cm	Sweep rate 0.4 meec/cm
Gain 2u 500 3F 500 mv/cm	Gain 1u 500 2F 500 mv/cm

Filter cutoff frequency 3000 cps

Force Link (On oscilloscope with CRL)

Material Alum. Calibrate resistance 5 meg chms

Oscilloscope gain 5 mv/cm

Note: The numbers in the "Gain" blank represent the trace number counting downward. The filtered and unfiltered signals are represented by u and F respectively. Trace 1 on oscilloscope 001570 is the vehicle position indicator.
The sweep is from left to right in the pictures.

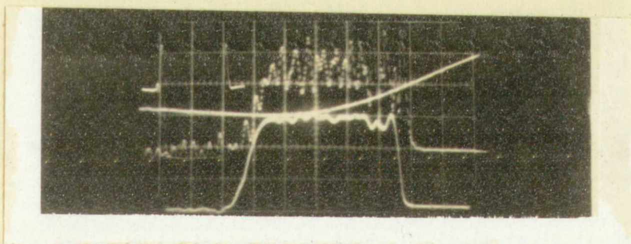

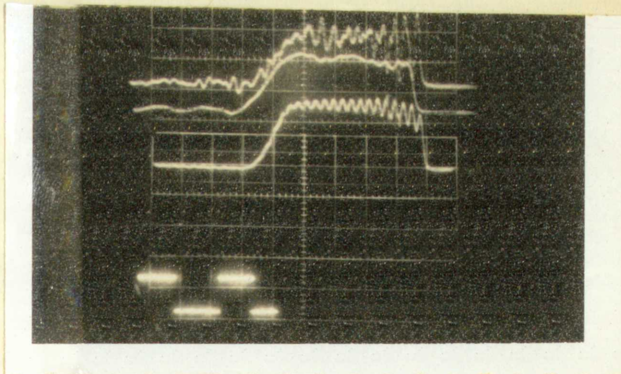

Figure 26. Typical Data for the Rectangular Pulse

CONCLUSIONS

A study of Figures 18 thru 23 shows that the shape and period of the transient have no effect on the sensitivity for the range covered in this work. Or, if they do, the effect is less than the inherent experimental error. The sensitivity curves for the CRL accelerometer indicate a decreasing sensitivity for increasing peak acceleration for the rectangular pulse only. No similar trend appeared for the other shapes for the CRL accelerometer, or for any shape for the Endevco accelerometer. Therefore, this decreasing sensitivity for the CRL accelerometer is believed due to something other than a change in sensitivity due to pulse shape. It is possibly due to a small amount of cable freedom near the accelerometer.

The effect of pulse duration can not be established with certainty, due to difficulty encountered in the experimental work. It was found impossible (with the existing equipment) to cover the complete range of G's (50 to 2000) for a specified period and shape. This was the case since the high G pulses have a tendency to be of short duration, and the low G pulses of long duration. A certain amount of overlapping could be obtained for all shapes and periods, but when this was obtained, no trend was indicated. However, it is not believed that this difficulty in covering the intended calibration range is significant because the same thing occurs when accelerometers are used in practice. That is, neither high G long pulses or low G short pulses are obtained. This may also

be stated as follows: the range of peak G and pulse duration obtained in this experimental work will be essentially the same as the accelerometer will encounter in practice. Consequently, the range covered is adequate.

The sensitivity curves also show that the manufacturer's sensitivity determined during sinusoidal motion agrees with the sensitivity as determined here for transient motion for one of the accelerometers, and does not agree for the other accelerometer. The agreement (within the limits of experimental error) occurred for the Endevco accelerometer. For the CRL accelerometer, the transient sensitivity was about 15% lower than the manufacturer's sensitivity for sinusoidal motion. The two accelerometers were calibrated by the manufacturer immediately before this series of tests was conducted.

The average maximum expected error in the results of this work was nine or ten percent. There were some results from both accelerometers which did not agree with the others within this limit, indicating that when a piezoelectric accelerometer is used, there will be occasional runs which will have errors greater than those normally expected. In order to eliminate these odd results, several runs must be made. This characteristic of the accelerometers was not attributed to the force link response because this would cause the sensitivities of both accelerometers to be odd for the same run, however, this did not occur. The odd results of each accelerometer occurred independently of the odd results for the other accelerometer.

[illegible]

techniques for these types of work will be essentially the same as those which are commonly in practice. Con- sequently, the sample obtained is adequate.

The calibration curves also show that the sensitivity of a piezoelectric accelerometer during successive tests agrees with the sensitivity as determined with the standard during the use of the accelerometers, and that they agree for the other accelerometers. The agreement (within the limits of experimental error) obtained for the Endevco accelerometers. For the CEC accelerometers, the measured sensitivity was about 10% lower than the manufacturer's sensitivity that was supplied and that the two accelerometers were calibrated by the manufacturer immediately before this series of tests was conducted.

The average maximum relative error in the results of this work was nine or ten percent. There were some results from both accelerometers which did not agree with the others within this limit, indicating that when a piezoelectric accel- erometer is used, there will be occasional runs which will have errors greater than those normally expected. In order to eliminate these odd results, several runs must be made. This characteristic of the accelerometers was not attributed to the force link response because this would cause the sens- itivities of both accelerometers to be odd for the same run. However, this did not occur. The odd results of each accel- erometer were odd independently of the odd results for the other accelerometer.

RECOMMENDATIONS

When piezoelectric accelerometers are to be used to measure transient motion, their sensitivity should be determined for shocks similar in peak G and period to the ones they are to measure. This is particularly true when the manufacturer's sensitivity has been determined for sinusoidal motion of the accelerometer only, since the sinusoidal motion used in calibration is limited to peak accelerations considerably lower than those encountered in shock work. The results of this work show that there may be a significant difference in the manufacturer's sensitivity for sinusoidal motion and the transient sensitivity.

If the shocks to be recorded are of the type resulting from impact obtained from tests on a drop tower, a convenient, accurate, and easily applied method is the one used in this work. The force transducers should be designed to have a natural period less than one tenth the period of the pulses to be measured. The force transducer should be calibrated in a testing machine of known accuracy to eliminate the variable error previously discussed. Lead pellets should be used as the cushion material, since lead results in accelerometer signals which are almost completely free of the high frequency ringing frequently obtained during impact. This increases the accuracy due

to the reduction of the error in interpreting the data. The close grouping of the experimental sensitivity around the manufacturer's sensitivity in Figure 19 illustrates this. The sensitivity should be determined over the range of peak accelerations expected in the test work for which the accelerometer is to be used. This requirement is easily satisfied if the same drop tower is used for the calibration and test work. It would also be desirable to use the same instrumentation for the test work that was used for the calibration in order to eliminate the effect of the instrumentation on the results.

If low accelerations are to be measured with piezoelectric accelerometers, considerable care must be exercised in securing the cable near its attachment to the accelerometer. Deformation of the accelerometer case due to cable motion during the pulse distorts the pulse, since the resulting crystal deformation is no longer proportional to the acceleration of the seismic mass. For high acceleration pulses, this effect is insignificant since the signal caused by cable movement is small relative to the signal due to the transient.

It should be recognized that the results from data taken of transient phenomena with piezoelectric accelerometers cannot be expected to have a greater accuracy than $\pm$ 10%. If only a few runs are made, and proper precautions are taken, the accuracy may be even less.

The above mentioned figure is applicable only if the pulse duration is significantly greater than the natural period of the accelerometer, say 50 times or more. If the exceptionally short pulses that normally occur with exceptionally high G's are to be measured, additional error will result. When these pulses are measured, the pulse duration may easily become less than 10 times the natural period of the accelerometer. When this occurs, the crystal compression is not proportional to acceleration. Because of the low natural frequency of the force link, the method used here cannot be applied to pulses this short.

Additional work might include computing response for various shapes of pulses applied to undamped accelerometers when the pulse duration is small relative to the natural period of the accelerometer; and checking the assumption made in these computations, i.e., that the voltage output of the accelerometer is proportional to the crystal compression. This assumption might be checked by using a traveling wave in a long rod to apply the pulse to the accelerometer, and by determining the pulse from strain gages mounted on the rod.

REFERENCES

(1) Tyzzer, F G., and Hardy, H. C., Accelerometer Calibration Technique, Journal of the Accoustical Society of America, Vol. 22, 454-7, 1950

(2) Ziegler, C. A., Electromechanical Pickup Calibration by the Interferometer Method, Journal of the Accoustical Society of America, Vol 25, 135-7, 1953.

(3) Yates, W. A. and Davidson, M , Wide Range Calibrator for Vibration Pickups, Electronics, Vol 26, part 2, 183, September 1953

(4) Rosenberg, J. D., A Flat Vibration Generator for Accelerometer Calibration, National Bureau of Standards Report No. 2624, 85-9, 1953

(5) Sulzer, P. G., Smith, E. R., and Edelman, S., High-Speed Stroboscope for Accelerometer Calibration, Review of Scientific Instruments, Vol. 25, 837-8, 1954

(6) Edelman, S., Jones, E., and Smith, E. R., Some Developments in Vibration Measurement, Journal of the Accoustical Society of America, Vol 27, 728-34, 1955

(7) Smith, E. R , Edelman, S., Jones, E., and Schmidt, V. A., Journal of the Accoustical Society of America, Vol. 30 part 2, 867-70, 1958.

(8) Endevco Series 2200 Accelerometers Manual, Endevco Corporation, Pasadena, California, 5-6, 1959.

(9) Keast, D. M., Calibration of Accelerometers in a Simulated Space Environment, Journal of the Accoustical Society of America, Vol. 31, part 1, 584-7, 1959.

(10) Trent, H. M., The Absolute Calibration of Electro-mechanical Pickups, Journal of Applied Mechanics, ASME Transactions, Vol. 70, 49-52, 1948.

(11) Harrison, H., Sykes, A. O., and Marcotte, P. G., The Reciprocity Calibration of Piezoelectric Accelerometers, Journal of the Accoustical Society of America, Vol. 24, 384-9, 1952.

(12) Stowe, E. J., and Bort, R. L., Calibration of Accelerometers to 10 Kilocycles by the Reciprocity Method, National Bureau of Standards Report No. 2624, 109-113, 1953.

(13) Levy, S., and Bouche, R. R., Calibration of Vibration Pickups by the Reciprocity Method, Journal of Research of the National Bureau of Standards, Vol. 57, No. 4, 227-243, 1956.

(14) Levy, S., and Kroll, W. D., Response of Accelerometers to Transient Accelerations, Journal of Research of the National Bureau of Standards, Vol. 45, 303-309, 1948.

(15) Rubin, S., Design of Accelerometers for Transient Measurements, Journal of Applied Mechanics, Vol.25, 509-13, 1958.

(16) Conrad, R.W., and Vigness, I., Calibration of Accelerometers by Impact Techniques, Proceedings of the Instrument Society of America, Vol. 8, 166-170, 1953.

(17) Perls, T.A., Tests of Accelerometer Linearity at High Accelerations, National Bureau of Standards Report No. 2624, 133-138, 1953.

(18) Perls, T.A., and Kissinger, C.W., High G Accelerometer Calibrations by Impact Methods with Ballistic Pendulum, Air Gun, and Inclined Trough, Proceedings of the Instrument Society of America, Vol. 9, part 5, 1954.

(19) Turnbow, J.W., Calibration of Accelerometers under Steady State and Transient Conditions, Proceedings of the Instrument Society of America, Vol. 9, part 5, 1954.

(20) Kaufman, A.B., Accelerometer Calibration by Ballistic Pendulum, Instruments and Automation, Vol. 29, part 2, 1322-1327, 1956.

(21) Brennan, J.N., and Nisbet, J.S., Direct Method of Accelerometer Calibration, Journal of the Acoustical Society of America, Vol. 30, 41-46, 1958.

(15) [illegible]

[illegible], Journal of [illegible]

[illegible]

(16) [illegible], and [illegible], [illegible] Calibration of [illegible]

[illegible]

of the [illegible]

(17) [illegible], Tests of [illegible]

High [illegible], [illegible] Report of [illegible]

Report No. [illegible]

(18) [illegible], and [illegible], [illegible] Accelerometer

Calibration by [illegible] with [illegible]

[illegible]

Proceedings of the [illegible] Society of [illegible]

[illegible]

(19) [illegible], Calibration of [illegible]

Sound, Fields and Transient Conditions, Proceedings

of the International Society of [illegible], Vol. [illegible]

[illegible]

(20) [illegible], Accelerometer Calibration by [illegible]

[illegible], Instruments and Automation, Vol. [illegible]

[illegible]

(21) [illegible], and [illegible], Direct Method of

Accelerometer Calibration, Journal of the Acoustical

Society of America, Vol. [illegible]

(22) A. B. J. Clark, Static and Dynamic Calibration of a Photoelastic Model Material, CR-39, Proceedings of the Society for Experimental Stress Analysis, Vol. XIV No. 1, 195-204, 1956.

(23) Barton, C. S., Volterra, E. G., Citron, S. J., On Elastic Impacts of Spheres on Long Rods, Proceedings of the Third U. S. National Congress of Applied Mechanics.

(24) Fitzgibbon, D. P., Displacement Measurements During High Velocity Impacts, Stress-Strain Characteristics of Materials at High Strain Rates, Part 1, University of Texas Structural Mechanics Research Laboratory, Austin, Texas, 1958.

(25) Lazarus, M., Shock Testing Instrumentation, Environmental Quarterly, 1960.

(26) Morrow, C. T., Sawtooth as a Component Test, Journal of the Accoustical Society of America, Vol. 28, 959-965, 1958.

(27) The Effect of Loading Rate on Mechanical Properties, Annual Report of 30 June 1960, Engineering Experiment Station, Department of Mechanical Engineering, University of New Mexico, Albuquerque, New Mexico.

(28) Anderson, C. A., personal note to author, June 1960.

(29) Thompson, W. T., Mechanical Vibrations, Second Edition, Prentice-Hall, Inc., p. 57, New Jersey, 1948.

ACKNOWLEDGMENTS

Appreciation must be expressed for the assistance and time given by Professor R. C. Dove of the Mechanical Engineering Department, and to Los Alamos Scientific Laboratory for supporting this work.

Thanks must be given Lee Wojack and Jack Kibbe for their help in constructing the drop tower; also to D. W. Brewer, Research Engineer at the University of New Mexico, for designing and assembling the vehicle position indicator and recording circuitry, and for his help in obtaining the data.

APPENDIX

EQUIPMENT LIST

1. Columbia Research Laboratories Accelerometer, model 512, serial number 138.

2. Columbia Research Laboratories cathode follower, model 4000, serial number 0354.

3. Tektronic oscilloscope, model 551, serial number 756.
   Plug ins: Type CA, serial number 008640.
   Type 53/54 D, serial number D 7079.

(The above three items were always used together as a unit, as were the three items listed immediately below.)

4. Endevco accelerometer model 2211, serial number 6799.

5. Columbia Research Laboratories cathode follower, model 4000, no serial number.

6. Tektronic oscilloscope, model 551, serial number 001570.
   Plug ins: Type D, serial number 009063.
   Type 53/54 c, serial number 9343.

7. Spencer-Kennedy Laboratories Electronic Filter, model 302, LASL S/N 1506.

8. Hewlett Packard power supply, model 712B, serial number 1771.

9. Polaroid oscilloscope cameras (two).

POTENTIOMETER CIRCUIT SENSITIVITY

In the potentiometer circuit of figure 6, page 44, the instantaneous current, I_i, flowing thru the ballast resistor and the gage will be

$$I_i = \frac{E}{NR_g + R_b}, \tag{1}$$

if it is assumed that the oscilloscope impedance is infinite. Since their impedance is 2 megohms resistive, the assumption is valid for practical purposes. In this equation, E is the regulated voltage from the power supply, R_g is the individual gage resistance, N is the number of gages in series, and R_b is the ballast resistance.

The voltage drop across the gages is found from the equation

$$E_g = \frac{ENR_g}{NR_g + R_b} \tag{2}$$

When the material on which the gages are mounted is unstrained, this is the voltage which the bucking circuit voltage must balance if high signal amplification is to be used. When the material on which the gages are mounted is strained , the gage resistance changes. The rate of change of E_g with respect to R_g may be found by taking the derivative. The result of this is

$$\frac{dE_g}{dR_g} = \frac{R_b EN}{(NR_g + R_b)^2} \tag{3}$$

The gage factor, F, is defined as $\frac{\Delta R_g}{\epsilon R_g}$, where ϵ is the

strain in the material on which the gages are bonded. When this is substituted into equation three (for a finite change in gage resistance), the result is the circuit sensitivity in volts/inch per inch of strain, found with the following equation:

$$\frac{\Delta E_g}{\Delta \epsilon} = \frac{N R_g R_b E F}{(NR_g + R_b)^2} \qquad (4)$$

The supply voltage and ballast resistance are eliminated from this equation by using a calibrate resistance, which is put in parallel with the gages during calibration. A large calibrate resistance is used so the change in resistance will be small - of the same order of magnitude as that due to strain. The change in resistance will be

$$R_g = \left[NR_g - \frac{N R_g R_c}{NR_g + R_c} \right] \frac{1}{N} \qquad (5)$$

$$= \frac{N R_g^2}{NR_g + R_c} ,$$

where R_c is the calibrate resistance. The circuit output from this change in resistance may be found using equation 3, and is

$$\Delta E_g = \frac{R_b E n}{(NR_g + R_b)^2} \times \frac{N R_g^2}{NR_g + R_c} = U \times y \qquad (6)$$

In the above equation, U is the oscilloscope gain in millivolts/ centimeter, and y is the deflection of the oscilloscope trace when the calibrate resistance is put in parallel with the gages.

Equation 6 may be solved for E, and this value substituted into equation 4. The result is

$$\frac{\Delta E_g}{\Delta \epsilon} \quad \frac{U\,y\,(NR_g + R_c)\,F}{NR_g} \qquad (7)$$

This may be converted to the circuit sensitivity, S_c, in lbs/millivolt by defining strain in the force transducer as $\epsilon = \frac{F}{E\,A}$, substituting this into equation 7, and taking the reciprocal. Equation 16 on page 62 is the result.

DATA FROM STATIC TESTS ON FORCE TRANSDUCERS

Equipment

Reihle 60,000 lb capacity testing machine, serial number R-47379.

Tektronic oscilloscope, model 551, serial number 003640.

High Range Force Transducer

Run 1. Full scale reading on testing machine: 60,000 lb.
Oscilloscope gain: 20 mv/cm.
Calibrate: Resistance - 1 megohm
Trace deflection - 3.8 cm

Load, lbs.	Trace Deflection, cm.
0	0
5,000	0.5
10,000	0.8
15,000	1.2
20,000	1.55
25,000	1.95
30,000	2.40

Run 2. Full scale reading on testing machine: 30,000 lb.
Oscilloscope gain: 10 mv/cm.
Calibrate: Resistance - 5 megohms
Trace deflection - 1.5 cm

Load, lbs.	Trace Deflection, cm.
0	0
8,850	1.5
18,250	2.95
24,850	4.00

Run 3. Full scale reading on testing machine: 6,000 lb.
Oscilloscope gain: 2 mv/cm
Calibrate: Resistance - 10 Megohms
Trace deflection - 3.7 cm.

Load, lbs.	Trace Deflection, cm.
0	0
1,860	1.7
3,930	3.5
0	0
3,950	3.4
0	0
3.860	3.5

Low Range Force Transducer

Run 1. Full scale reading on testing machine: 6,000 lb.
Oscilloscope gain: 20 mv/cm
Calibrate: Resistance - 500 k ohms
Trace deflection - 3.5 cm.

Load, lbs.	Trace deflection, cm.
0	0
1,000	0.9
2,000	1.75
3,040	2.70

Run 2. Full scale reading on testing machine: 3,000 lb.
Oscilloscope gain: 10 mv/cm
Calibrate: Resistance - 1 megohm
Trace deflection - 3.4 cm.

Load, lbs.	Trace deflection, cm.
0	0
510	0.9
940	1.7
1,510	2.65
2,320	4.00

DAMPING FACTOR OF LOW RANGE FORCE TRANSDUCER

Run	Desired Pulse[1]	N[2]	δ[3]	c/C_c
7,8-3	1-1000	5	0.140	0.022
5,8-2	2-500	8	0.087	0.014
5,8-4	2-200	9	0.077	0.012
4,8-4	2-200	7	0.099	0.016
4,8-4(2)	2-200	9	0.077	0.012
4,8-2	2-200	5	0.087	0.014

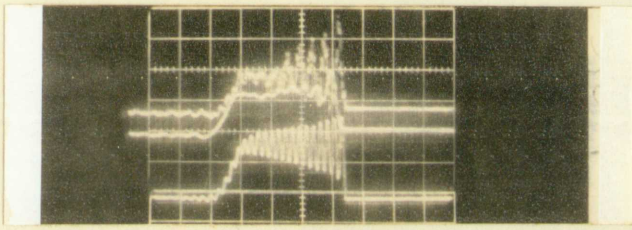

Example of data from which above information was taken

[1] The first number in the desired pulse represents the pulse duration, and the second number represents the peak acceleration in G's. The pulse shape from which all of the above data was taken was rectangular.

[2] This is the number of cycles required for a 50% amplitude decay.

[3] This is the logarithmic decrement of the damped vibration.

VEHICLE WEIGHTS AND CUSHION MATERIAL DESCRIPTION

Desired Pulse	Vehicle Weight, lbs.	Cushion Description
1-200	1.380	1.5 in^2 of 1/4 in neoprene
1-500	1.380	" " " " " "
1-1000	1.380	" " " " " "
1-2000	1.380	" " " " " "
2-100	1.380	0.4 in^2 of 1/4 in neoprene
2-200	1.380	#13 neoprene stopper
2-500	1.380	#13 neoprene stopper
2-1000	1.380	#12 neoprene stopper
4-50	1.380	" " "
4-100	1.380	" " "
4-200	1.481	" " "
4-500	1.481	" " "
4-1000	1.481	" " "
8-50	3.754	#9 neoprene stopper
8-100	3.754	#9 neoprene stopper
8-200	3.754	2 #11 neoprene stoppers, stacked
8-350	4.596	2 #11 neoprene stoppers, stacked
16-25	13.438	2 #12 neoprene stoppers, stacked
16-50	13.438	2 #11 neoprene stoppers, stacked
16-100	13.438	2 #11 neoprene stoppers, stacked
30-25	21.707	2 #11 and 2 #12 neoprene stoppers, all stacked

Rectangular (Cushion material was Foamalum.)

Desired Pulse	Vehicle Weight, lbs.	Cushion Description
1-100	6.091	1.4 in^2 x 0.2 in high
1-200	3.788	1.8 " " 0.2 " "
1-500	1.481	1.3 " " 0.5 " "
1-1000	1.481	2.6 " " 0.5 " "
2-50	12.680	1.3 " " 0.2 " "
2-100	6.091	1.4 " " 0.2 " "
2-200	3.788	1.8 " " 0.5 " "
2-500	1.481	1.3 " " 0.8 " "
4-50	12.570	1.3 " " 0.5 " "
4-100	6.091	1.4 " " 0.8 " "
4-200	3.788	1.8 " " 1.5 " "
8-50	13.430	1.5 " " 1.5 " "
8-100	6.871	1.7 " " 2.5 " "

Sawtooth (Cushion material was lead. See sketch on following page for explanation.)

Desired Pulse	Vehicle Weight, lbs.	Cushion Description
1-200	1.477	.447 x .230 x 8°
1-500	1.477	.619 x .437 x .494 x 10°x20°
1-1000	1.473	.748 x .508 x 25°
1-2000	1.473	.617 x .491 x 20°
2-100	6.098	.559 x .237 x 15°
2-200	6.098	.489 x .257 x 20°
2-500	6.098	.744 x .250 x .493 x 70°x20°
2-1000	6.098	.748 x .370 x .741 x 80°x20°
4-50	12.681	.375 x .090 x .240 x 60°x20°
4-100	20.934	.750 x .500 x 30°
4-200	20.934	.750 x .500 x 30°
4-500	13.442	.709 x .250 x 1.254 x 80°x40°
8-50	20.943	.371 x .220 x .750 x 80° x40°
8-100	21.708	See sketch on following page
8-200	21.708	" " " " "

Lead Cushion Descriptions Having Three Numbers

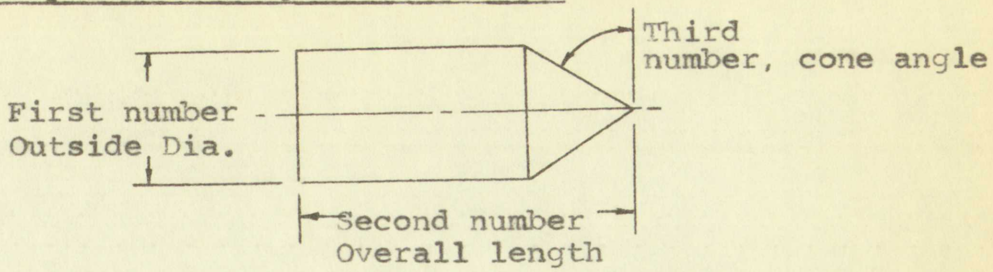

Lead Cushion Description Having Five Numbers

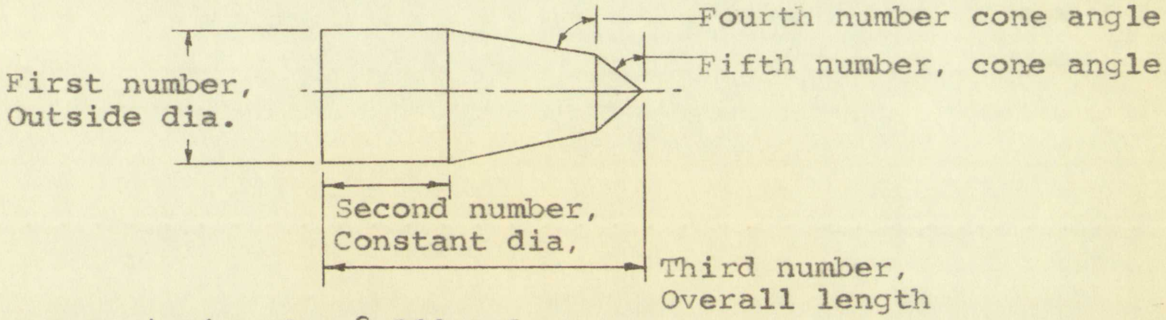

Cushion Description for 8-100 Pulse

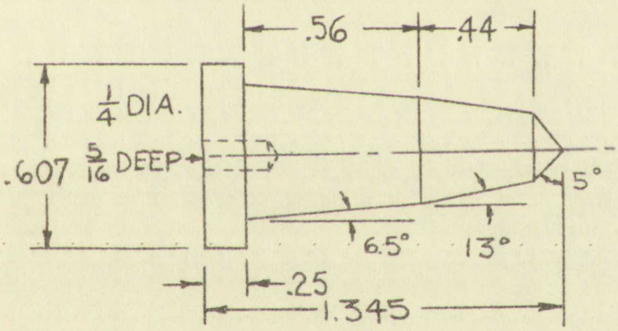

Cushion Description for 8-200 Pulse

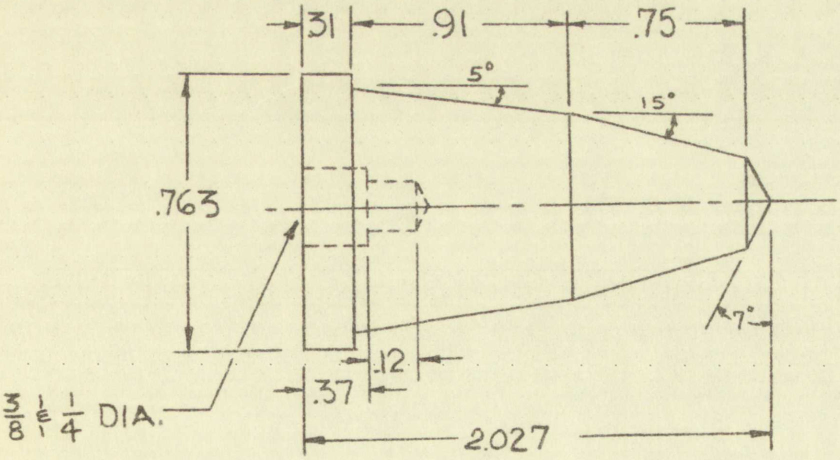

All dimensions in inches